

NASA Contractor Report 3290

N82-71027

Advanced Composite Elevator for Boeing 727 Aircraft

Volume I - Technical Summary

D. V. Chovil, S. T. Harvey, J. E. McCarty,
O. E. Desper, E. S. Jamison, and H. Syder

CONTRACT NAS1-14952

NOVEMBER 1981

NASA

NASA Contractor Report 3290

**Advanced Composite Elevator
for Boeing 727 Aircraft**
Volume I - Technical Summary

D. V. Chovil, S. T. Harvey, J. E. McCarty,
O. E. Desper, E. S. Jamison, and H. Syder
Boeing Commercial Airplane Company
Seattle, Washington

Prepared for
Langley Research Center
under Contract NAS1-14952

NASA

National Aeronautics
and Space Administration

**Scientific and Technical
Information Branch**

1981

FOREWORD

This technical summary report was prepared by the Boeing Commercial Airplane Company, Renton, Washington, under contract NAS1-14952. It covers work performed between 24 May 1977 and 31 December 1979. The program was sponsored by the National Aeronautics and Space Administration, Langley Research Center (NASA-LARC). Dr. H. A. Leybold was the NASA project manager. The Boeing program manager was S. T. Harvey. Details of this work are provided in Volume 2 of this report (ref. 1).

The following Boeing personnel were principal contributors to the program:

Design

W. C. Brown
G. N. Roe
C. R. Zehnder

Structural Analysis

G. G. Holland
R. W. Johnson
J. E. McCarty
R. D. Wilson

Weight and Balance Analysis

R. E. Baum
J. T. Parsons

Production Manager

W. D. Grant

Manufacturing Technology

D. M. Cantrell
M. C. Garvey
E. S. Jamison
V. S. Thompson

Technical Operations Manager

L. D. Pritchett

Business Management

D. V. Chovil
D. A. Foster
S. M. Lytle
M. R. Wiebe

CONTENTS

	Page
1.0 SUMMARY	1
2.0 INTRODUCTION	3
3.0 TECHNICAL APPROACH	5
3.1 Design	5
3.1.1 Structural Concepts	5
3.1.2 Material Selection	6
3.1.3 Strain Distribution and Design Values	7
3.2 Test	8
3.2.1 Ancillary Tests	8
3.2.2 Full-Scale Ground Test	12
3.2.3 Ground Vibration Test	13
3.3 Manufacturing Development	14
3.3.1 Detail Tooling	14
3.3.2 Kitting, Layup, and Bagging	14
3.3.3 Cure Cycle	14
3.3.4 Nondestructive Inspection	15
3.3.5 Problems and Solutions	16
3.4 Fabrication and Assembly	16
3.4.1 Part Fabrication	16
3.4.2 Problems and Solutions	17
3.4.3 Joining Methods	17
3.4.4 Assembly Tools	18
3.4.5 Assembly Techniques	18
3.5 Repair Techniques	20
3.6 Weight	20
3.7 Flight Tests	20
3.8 FAA Certification	20
4.0 COST ANALYSIS	23
4.1 Production Costs	23
4.1.1 Production Environment	23
4.1.2 Total Costs	23
4.2 Composite Material Usage Factors	24
4.3 Cost Comparisons	24

	Page
5.0 CONCLUDING REMARKS	27
6.0 REFERENCES	29
7.0 ABBREVIATIONS AND SYMBOLS	31

FIGURES

No.		Page
1	First Advanced Composite Elevator Installed on a Commercial Aircraft	33
2	Program Technical Approach	34
3	727 Elevator General Arrangement	35
4	Preliminary Composite Elevator Configurations	36
5	727 Composite Elevator Structural Arrangement	37
6	Lightning Protection System	38
7	Corrosion Protection--Typical Graphite-Epoxy/Aluminum Interface	39
8	Elevator and Stabilizer Hinge Concept	40
9	Elevator/Stabilizer Finite Element Model	40
10	Ultimate Front-Spar Chord Strains for Load Case 125	41
11	Ultimate Rear-Spar Chord Strains for Load Case 125	41
12	Ultimate Skin Panel Strains, Load Case 125	42
13	Ultimate Skin Panel Strains, Load Case 125	43
14	Ultimate Actuator Rib Strains for Load Case 125	44
15	Front-Spar Chord Strains, Thermal Load Case $\Delta T = 81^{\circ}\text{C}$ (145°F), at $T = -59^{\circ}\text{C}$ (-75°F)	44
16	Skin Panel Strains, Thermal Load Case $\Delta T = 81^{\circ}\text{C}$ (145°F), at $T = -59^{\circ}\text{C}$ (-75°F)	45
17	Ancillary Test Program	46
18	Material Coupon Test Plan (Test 1)	47
19	Basic Laminate Properties Test Plan (Boeing Funded)	48
20	Effect of Moisture, Temperature, and W/D on Tension Strains of $\pm 45/0/90$ -deg Fabric Laminate Coupons	49
21	Structural Elements Test Plan (Test 4)	50
22	Effect of Moisture and Temperature on Fastener Bearing Stress	51
23	Effect of W/D on Tension Failure Strain Values for Open and Filled Holes	51
24	Elevator Subcomponent Test Plan	52
25	Cover Panel Padup Specimen Geometry (Test 8)	54
26	Spar Web Shear Test Setup (Test 9)	55
27	Honeycomb Skin Compression Panel Stability Test Setup (Test 10)	56
28	Honeycomb Skin Panel Shear Stability Test Setup (Test 10)	57
29	Panel Edge Shear and Bending Test Specimen Geometry (Test 12)	58
30	Actuator Support Rib Test (Test 14)	59
31	Front-Spar Actuator Fitting Splice Test Schematic (Test 11)	60
32	Front-Spar Actuator Fitting Splice Test Specimen Failure	61
33	Front-Spar Actuator Fitting Specimen, Measured Vertical Deflections	62
34	Elevator Outboard Test Setup (Test 17)	63
35	Elevator Outboard Box Section Test--Torsion Windup Test and Prediction Comparison	64
36	Elevator-Box Sonic Test Setup (Test 15)	65
37	Production Hardware Verification Test Coupons	66
38	Graphite-Epoxy Elevator Lightning Test Article	66
39	Honeycomb Repair Test Results	67
40	Environmental Test Plan	68
41	Elevator Ground Test Setup	69
42	727 Composite Test Elevator Hinge Locations	70

No.		Page
43	Lower Skin Panel Outer Face Strain Comparisons—Predicted Versus Test	71
44	Spar and Rib Strain Comparisons—Predicted Versus Test	71
45	Elevator Rotation Comparison for Load Case 128	72
46	Interaction Curve Bearing Stress Versus Tension Bypass Strain	72
47	Front Spar and Layup Mandrel	73
48	Rear Spar and Layup Mandrel	73
49	Skin Panel and Layup Mandrel	74
50	Rib-Station 117.37 and Layup Mandrel	74
51	Inboard Closure Rib and Layup Mandrel	75
52	Outboard Closure Rib and Layup Mandrel	75
53	BAC 5562 Bagging Procedure (No-Bleed Material)	76
54	BAC 5562 Cure Cycle (No-Bleed Material)	77
55	Typical Advanced Composite Fabrication Process	78
56	Elevator System Actual Weight and Balance Data (Elevator Surface, Control Tab, and Balance Panels)	79
57	Flight Flutter Altitude and Speed Test Conditions	80
58	Total Recurring and Nonrecurring Production Costs by Major Element (5-1/2 Shipsets)	80
59	Total Recurring and Nonrecurring Component Production Labor Hours (5-1/2 Shipsets)	81
60	Total Recurring and Nonrecurring Production Labor by Major Element (5-1/2 Shipsets)	81
61	Fabrication and Assembly Recurring Costs, Percentage of Labor Hours (5-1/2 Shipsets)	82
62	727 Composite Elevator—Graphite Components Recurring Costs (5-1/2 Shipsets)	82
63	Relative Elevator Cost Comparison (for Initial 200 Shipsets)	83

TABLES

No.		Page
1	Concept Comparison	84
2	Design Ultimate Loads	84
3	Major Structural Items (Ultimate Design Value Strains).....	85
4	Comparison of Ground Vibration Test and Analysis Natural Frequencies	85
5	Material Form and Finishing Cost Study	86
6	Weight Comparison [kg (lb)/Airplane]	86
7	Metal Elevator Versus Composite Elevator Cost Comparison Assumptions	86

1.0 SUMMARY

This report is the technical summary for the Advanced Composite Elevator program for the Boeing 727 commercial transport. It covers all work performed on the program from May 1977 through December 1979.

Program objectives were to design and produce an advanced composite elevator that would meet the same functional criteria as those for the existing metal elevator. Preliminary design activity consisted of developing and analyzing alternative design concepts and selecting the final elevator configuration. This included trade studies in which durability, inspectability, producibility, repairability, and customer acceptance were evaluated. Preliminary development efforts consisted of evaluating and selecting material, identifying structural development test requirements, and defining full-scale ground and flight test requirements necessary to obtain Federal Aviation Administration (FAA) certification.

After selection of the best elevator configuration, detail design was begun and included basic configuration design improvements resulting from manufacturing verification hardware, the test program, weight analysis, and structural analysis. Detail and assembly tools were designed and fabricated to support a full-scope production program, rather than a limited run. The producibility development programs were used to verify tooling approaches, fabrication processes, and inspection methods for the production mode. Quality parts were fabricated and assembled with a minimum rejection rate, using existing inspection methods.

Basic program goals were: (a) make extensive and effective use of advanced composite material; (b) obtain a minimum weight reduction of the composite elevator over the metal elevator by 20% (27% was achieved); and (c) demonstrate cost-competitive status with a metal elevator. All program technical goals were realized when the design met or exceeded all established design requirements, criteria, and objectives with an FAA certification in December 1979. Actual cost experience showed that composite structure is not competitive with metal. However, we believe that by applying innovative manufacturing methods and engineering designs, composite structures can become competitive.

Component elevator manufacture was performed in a semiproduction environment by production people of an average skill level for the shop. Hand methods were used in cutting and layup of broadgoods, ply-by-ply inspection, and training. The limited production quantity of five-and-one-half shipsets did not warrant facilitization and automation that would be used in quantity production; therefore, a cost-competitive status with metal could not be demonstrated by the actual program cost. However, it is our judgment that using automated manufacturing methods and the expected reduction in relative material cost differences would achieve cost parity in real terms.

The five shipsets produced on the program have FAA certification and are in service on commercial aircraft.

2.0 INTRODUCTION

The use of advanced composite materials to reduce weight of commercial transport aircraft is one of the many areas being investigated by NASA and industry under the Aircraft Energy Efficiency (ACEE) program. The overall objective of the ACEE program is to improve the energy efficiency of air transportation and to conserve petroleum fuel. A segment of the ACEE program (design, production, and testing of a composite structure for a commercial aircraft) was established to accelerate the application of composite structures in new aircraft design.

This report is a technical summary of the successful development and manufacture of an advanced composite elevator for the Boeing 727 commercial transport. Detailed data are provided in Reference 1. The elevators designed and produced under this program met all design requirements and program goals without any sacrifice to structural integrity of the elevator. Five-and-one-half shipsets were fabricated and assembled. The first full shipset produced was installed on a Boeing-owned 727 and flight tested. The composite elevator has been certified by the Federal Aviation Administration (FAA) and all five composite shipments are in service on commercial aircraft. Figure 1 shows the first advanced composite elevator to be installed on a commercial transport.

The 727 Advanced Composite Elevator program goals were:

- The elevator should make extensive and effective use of advanced composite materials.
- The elevator should weigh at least 20% less than the current metal elevator.
- The elevator should be cost competitive with a metal elevator.

The program requirements for the advanced composite elevator were:

- The elevator must meet the same functional and structural criteria as those of the existing metal elevator.
- The elevator must be interchangeable with the existing metal elevator.
- The elevator aerodynamic effectiveness must not be altered; the stiffness must match that of the metal elevator.
- The elevator strength, durability, and inspectability must equal or exceed those of the metal elevator.
- The elevator must provide protection against lightning effects and static discharges in a service environment.

Use of trade names or names of manufacturers in this report does not constitute an official endorsement of such products or manufacturers, either express or implied, by the National Aeronautics and Space Administration.

3.0 TECHNICAL APPROACH

Program development and design activities concentrated on providing a composite elevator design and preparing a technical plan to develop an advanced composite elevator that would meet the stiffness and interchangeability criteria of the existing Model 727 metal elevator. Figure 2 illustrates the technical approach used to successfully accomplish the program.

Preliminary design consisted of developing and analyzing alternative design concepts, followed by selecting the elevator configuration. This included trade studies in which durability, inspectability, producibility, repairability, and customer acceptance were evaluated (see sec. 4.1).

Preliminary development included material evaluation and selection, identification of ancillary structural development test requirements (encompassed all testing except ground and flight tests of the full-scale component), manufacture of verification hardware, and definition of the full-scale ground and flight test requirements necessary to obtain Federal Aviation Administration (FAA) certification.

The detail design of the composite elevator reflected design improvements resulting from verification hardware, the ancillary test program, and weight and structural analysis. Ground and flight testing activities completed the program. Production-quality fabrication and assembly tools were designed and fabricated to support a production program, rather than a development program. The producibility development programs were used to verify tooling approaches, fabrication processes, and inspection methods for the production mode and to identify costs associated with the short production runs.

3.1 DESIGN

Program design activities focused on providing a lightweight, producible elevator design that would meet the same criteria as those for the existing metal (baseline) elevator shown in Figure 3. Major design areas evaluated were materials and their selection, configuration, and environmental protection systems. These are discussed in the following subsections.

3.1.1 Structural Concepts

Four advanced composite elevator concepts (fig. 4) were considered. Results of an analysis of these concepts are summarized in Table 1. The selected concept used skin panels that were stabilized by Nomex honeycomb core and a minimum number of ribs. The structural arrangement is shown in Figure 5, which also defines the portions constructed of advanced composites.

Lightning—The selected lightning protection system consists of aluminum diverter strips separated from the graphite-epoxy surfaces by a two-ply fiberglass dielectric layer; this concept is shown in Figure 6. The aluminum diverter strips are electrically bonded to the aluminum nose skins to provide an electrical path in the aluminum stabilizer box. A test panel was constructed and tested to substantiate this system. There was no visible damage, nor was any damage revealed by subsequent nondestructive inspection.

Corrosion—The corrosion protection system was designed to isolate graphite-epoxy surfaces from the aluminum structure, which would minimize the cathodic area (graphite) available for electrochemical reaction. Several systems that included the use of

fiberglass, Tedlar, paint, and polysulfide sealant were investigated in a Boeing-funded study. Assemblies incorporating these systems were subjected to salt spray and compared to systems using conventional anodized and primed aluminum parts; see Vol. 2 (ref. 1) for details of these tests. The corrosion protection system selected for the advanced composite elevator was equivalent to that of the existing baseline metal elevator (fig. 7).

Thermal Expansion—It was necessary to modify hinges and fittings to accommodate the relative motion between the aluminum stabilizer and the advanced composite elevator caused by thermal expansion. Figure 8 shows the modified hinge. The thermal analysis is discussed in Section 3.1.3.

3.1.2 Material Selection

Before this contract was started, Boeing-funded development efforts were devoted to selecting and evaluating material. This selection and evaluation included testing and manufacturing considerations as well as material history and current industry usage. The graphite fiber/epoxy resin systems investigated are listed below. Their suppliers are in parentheses after each system.

- System (supplier)
 - T300/5208 (Narmco)
 - T300/934 (Fiberite)
 - AS/3501-5A (Hercules)
 - T300/F263 (Hexcel)

Each system was ordered and tested in the following forms:

- Preplied tape, 0.0089 mm (3.5 mil), two plies
- Unidirectional tape, 0.0132 mm (5.2 mil)
- Plain-weave fabric prepreg, 0.0178 mm (7.0 mil)

Ordering of prepreg forms complied with the general requirements of a Boeing materials specification, and tolerances for prepreg and cured laminate physical properties were specified. Testing included:

- Resin
 - Differential scanning calorimetry
 - Liquid chromatography
 - Thermal gravimetric analysis
- Prepreg
 - Resin content (percentage of weight)
 - Volatile content (percentage of volume)
 - Resin gel time (minutes)
 - Resin flow (percentage of weight)
 - Graphite weight (per yard)

- Laminate properties
 - Fiber volume
 - Density (thickness/ply, void content)
 - Weight
 - Tensile/modulus
 - Short beam shear
- Sandwich properties
 - Flatwise tension
 - Porosity
 - Peel
 - Weight

Manufacturing producibility was evaluated by fabricating a test panel from each candidate material that represented the typical layup complexity of the actual structure. Drape, tack, work time, and degree of difficulty in layup were determined for each material system and form. The Quality Control organization performed receiving inspection tests on all materials used in the evaluation, in addition to a thorough comparison of suppliers' certified test data and the Boeing test results. The test results agreed with the suppliers' certified test data and the Boeing test results.

Materials selection consisted of analyzing and comparing these tests plus such additional factors such as:

- Available industry data base
- Demonstrated resin durability in different environments
- Supplier production experience
- Supplier production capacity and control
- Supplier ability to provide all materials forms
- Supplier cooperation for process audit

The Narmco 5208 resin system was selected because it best satisfied a majority of the selection criteria established by the Boeing Commercial Airplane Company.

3.1.3 Strain Distributions and Design Values

3.1.3.1 Strain Distribution

A finite-element model was developed for the 727 graphite-epoxy elevator. The elevator model was mounted on a stabilizer finite-element model to ensure that strains induced in the elevator by the stabilizer-deflected shape were accounted for within the elevator model; the stabilizer and elevator finite-element model definition is shown in Figure 9. The stabilizer was modeled with a large grid, using structural elements that produced representative bending and torsion stiffness. The elevator was modeled with a finer grid to produce a more comprehensive strain distribution.

The hinge attachment points were modeled to produce the required rotational and translational freedoms. The hinge supporting structure at station 17.20 (see fig. 9) was modeled to provide a lateral restraint.

The external load cases that were used for the ultimate strength analysis are listed in Table 2. In addition to these flight load cases, two uniform temperature thermal conditions of 82 and -59°C (180 and -75°F) were analyzed.

Ultimate strain levels for load case (LC) 125 for the front and rear spars, upper and lower skin panels, and actuator rib are presented in Figures 10 through 14. Typical thermal strains are presented for the front spar in Figure 15 and for one of the skin panels in Figure 16. The final strains at the ultimate flight load and thermal conditions were obtained by algebraically adding the ultimate flight load strains to 1.5 times the thermal analysis strains.

3.1.3.2 Design Values

The design values used for the final strength analysis were based on coupon or structural element test data from the ancillary test program. Average test values were reduced to the probability and confidence levels of MIL-HDBK-5B "B" basis; namely, that 90% of the population will be higher with a confidence of 95%. These reduction factors conservatively accounted for material strength variations, test specimen geometry variations, and test condition variations.

Material strength correction factors for each test condition were based on process control test results collected from the ancillary test specimens and analyzed to establish the strength variations. A material factor was used to correct each test point to the mean of the process panel population and a second factor was used to correct the mean value to the required confidence level. A variation magnification factor was determined that accounted for variations in test specimen geometry and test conditions. Coefficients of variation for every unique test condition and specimen geometry were calculated. A distribution analysis of these coefficients of variation was performed. From this distribution, the maximum variance with less than a 5% probability of exceedance was determined to be 9.0%. The variance magnification factor then was computed as:

$$V_{MF} = 1 - K_{B_{\infty}} \nu_{MAX}$$

where K_B is the "B" basis factor for an infinite sample. The ν_{MAX} is the maximum variance.

Reduction factors were obtained by multiplying the three correction factors, and the final design values were obtained by multiplying the average test values by the reduction factors. The reduction factors calculated by this procedure varied from 0.70 to 0.86. Based on this procedure, the design value strains for the most critical environmental conditions for the major structural items are summarized in Table 3.

3.2 TEST

The testing program consisted of: ancillary tests (sec. 3.2.1), full-scale ground tests (sec. 3.2.2), and ground vibration tests (sec. 3.2.3).

3.2.1 Ancillary Tests

The ancillary test program (fig. 17) included coupon, element, and subcomponent-sized specimens. This test plan was structured to provide the following data:

- Material design values, including environmental effects for FAA certification
- Strength and fatigue performance of specific design details
- Verification of final design details
- Verification of torsional stiffness
- Real-time exposure environmental effects (moisture and temperature)
- Strength and fatigue performance of repairs

Moisture conditioning of all coupons, structural elements, and subcomponents was accomplished by placing the parts in an environmental chamber at 60°C (140°F) and 100% relative humidity (RH) until 1.1% moisture level was obtained.

Coupon Tests—The material coupon test plan (Test 1) is shown in Figure 18. Basic laminate strength tests funded by Boeing are defined in Figure 19. Data from these tests were used to establish design values for certification. In all cases, the failure strains were calculated from the failure load and the laminate modulus, and all plotted data points are average values. Test results, showing the effect of temperature and moisture on ultimate tension strains for the open-hole coupons, are shown in Figure 20. Similar plots were obtained for the other specimen configurations defined in the test plans (figs. 18 and 19).

Structural Element Tests—The structural elements test plan (Test 4) is shown in Figure 21. These tests were used to show the effects of fastener spacing, edge margin, moisture, and temperature on fastener bearing stresses. Fastener bearing failure stresses were calculated using the fastener nominal diameter. Figure 22 is a typical plot of results. Figure 23 compares the results of an open hole to a filled hole, and indicates that for the same width-to-fastener-diameter ratio, similar results were obtained.

Subcomponent Tests—The subcomponent test plan and results are shown in Figure 24. The test results from this phase of the program were used to verify the design and durability of specific subcomponents prior to fabrication of the first elevator unit.

- **Cover Panel Padup at Ribs** (Test 8, fig. 25)—The test results (fig. 24) indicate that the ambient dry tension capability of this detail is 2.4 times the maximum required. Three ambient-temperature wet specimens also were tested in tension and the average failure strain for these was higher than the average for the dry specimens. Two fatigue specimens were tested dry and three specimens were tested wet at ambient conditions. All five specimens achieved 500,000 cycles with no detectable damage.
- **Spar Web Shear Test** (Test 9, fig. 26)—The shear web failed at a stiffener fastener hole for all three test panels at approximately 3-1/2 times the critical design shear flow for the front spar web.
- **Honeycomb Skin Compression Panel Stability Test** (Test 10, fig. 27)—All panels failed by local crippling in the edgeband region; therefore, panel buckling loads were higher than the test loads. The wet-tested panels produced the minimum values, which were 2.2 times the required value.
- **Honeycomb Skin Shear Panel Stability Test** (Test 10, fig. 28)—The wet-tested panels at 21°C(70°F), which provided the minimum values, indicated a capability 1.4 times the required value. Lightning and impacted panels, with visible damage, indicated a capability of 1.54 and 1.45 times the required values, respectively.

- **Panel Edge Shear and Bending (Test 12, fig. 29)**—The Type I specimens (fig. 29), which produced the minimum failure loads, developed an average shear load of 9.88 N/mm (56.4 lbf/in) along the supports, which is twice the requirement.
- **Actuator Support Rib Test (Test 14, fig. 30)**—The required capability of the splice was based on the same strength criterion as that of the current metal design. The strain in the chords at failure indicated that the test specimen failed at 1.33 times the design requirement.
- **Front Spar Actuator Fitting Splice Test (Test 11, fig. 31)**—The room-temperature/dry static specimen failed at 10.68 kN (2400 lbf) at a fastener hole, as shown in Figure 32. The elevated-temperature/wet static specimen was conditioned at 60°C (140°F) with 100% RH for approximately 70 days. When tested at 71°C (160°F), the failure load was 11.03 kN (2480 lbf) and the failure occurred at the same location as the dry static specimen. The similarity in failure load is consistent with open-hole coupon data that indicate that for quasi-isotropic laminates, room-temperature/dry and 71°C (160°F)/wet tension values are similar.

The fatigue specimen was subjected to two lifetimes of repeated-load testing. The applied loading was 1.045 kN (235 lbf) down and 0.516 kN (116 lbf) up. Blocks of 25,000 load cycles were applied alternately in an environment of 35°C (95°F) and 100% RH, and then at laboratory ambient temperature and relative humidity. After completion of two lifetimes, the specimen was deliberately damaged by impact, sawcut, and delaminations at several locations. The test specimen then was subjected to a design limit load, and two additional service lifetimes were applied. Inspections performed during the cyclic loading showed no damage propagation. The previously inflicted damage was extended to create significant and easily detectable damage. The test specimen was loaded to design limit load in an environment of 71°C (160°F) and 100% RH without failure. In an environment of ambient temperature and relative humidity, the specimen was loaded until it failed at 7.59 kN (1706 lbf).

Deflections were measured during both the limit load and destruction tests. A plot of the vertical deflection measured at the loaded end of the test specimen during the destruction test is shown in Figure 33. A load-versus-deflection plot for both the room-temperature/dry and elevated-temperature/wet static specimen also is presented in Figure 33. This comparison indicates that all three specimens had similar stiffness.

Significant conclusions from this test program are summarized as follows:

- The apparent static strength of an undamaged test article was unaffected by the effects of absorbed moisture in a high-temperature environment (see fig. 33).
- Modulus of elasticity values were not significantly changed by environmental conditioning and fatigue cycling (see fig. 33).
- Significant detectable damage did not propagate during two service lifetimes of fatigue cycling.

- **Elevator Outboard Section (Test 17)**—A photograph of the specimen and the test setup is shown in Figure 34. An ATLAS finite-element model of the elevator outboard section was extracted from the initial complete model of the elevator and stabilizer. A comparison in torsional windup between the test article and the finite-element model was made and the result is shown in Figure 35.

The test results are summarized as follows:

- The test box was loaded to 135% of design ultimate load with no failures. Thus, the basic design strength was verified.
- The torsion windup of the box agreed closely with the ATLAS finite-element predictions. Thus, stiffness predictions were verified.
- **Elevator Box Sonic Fatigue (Test 15, fig. 36)**—Two boxes were sonically tested to evaluate the effect of sonic environment on the elevator structure and were tested for an equivalent of two lifetimes of in-service damage. The honeycomb panel and edgebands then were impacted with visible damage. The boxes then were tested for an additional in-service lifetime, and post-test inspections revealed no apparent propagation of the damage areas.

Production Hardware Verification Tests—Tests of laminate and honeycomb coupons cut from an elevator production verification section were performed. The specimen configurations and the areas on the verification hardware from which the specimens were taken are shown in Figure 37. The test results, when compared with the ancillary test program coupon data, indicated that the production process produced an acceptable quality laminate.

Lightning Protection Panel Tests—Lightning protection system (see sec. 3.1.1) validation tests were performed on the elevator outboard upper surface. Figure 38 shows the elevator lightning protection system test article. The test article incorporated the production configuration of the graphite-epoxy elevator skin panel and its attachment to the aluminum elevator nose skin panel. The test article was struck with an energy pulse of 3.95×10^6 amp²-sec. There was no visible damage, and subsequent nondestructive inspection (NDI) of the test article indicated no damage.

Repair Tests—The objective of this test was to evaluate the strength of a typical honeycomb skin panel repair. Typical skin panels were damaged on one side, the damaged skin and core was removed, and the area was repaired.

The specimens were tested using a four-point beam bending specimen as shown in Figure 39. Undamaged specimens were tested to establish a baseline value. The wet specimens were moisture conditioned prior to being repaired to simulate parts being repaired after some flight-service time.

The repaired specimens were tested with the repair patch in compression, thus allowing the stability of the repaired area to be a contributing factor to the failure mode. Several specimens were impacted, tested, and compared to the baseline specimens. Results of these tests are summarized in Figure 39 and show that the repaired specimens were comparable to the baseline specimens at ambient test conditions. Both dry and wet impacted specimens showed lower strength capabilities than the baseline and repaired specimens.

Real-Time Exposure Environmental Tests—A test program to determine the effects of various real-time environmental exposures on several specimen configurations is defined in Figure 40. As noted in the test plan, specimens will be selected and tested after 12, 24, and 36 months of exposure.

At present, test data have been obtained for the ± 45 -deg tension coupons and the honeycomb compression coupons after 12 months of exposure. These results indicate a slight increase in strength for both specimen configurations. This program is scheduled to continue as planned, and complete program results will be published in a separate document.

3.2.2 Full-Scale Ground Test

The test elevator was supported in a vertical position (trailing edge up) by steel pedestals at each hinge fitting, as shown in Figure 41. The pedestals were calibrated with strain gages so that fore-and-aft loads in the stabilizer chord plane and loads normal to the stabilizer chord plane could be determined at each hinge.

Pedestal bases at the inboard end hinge and the four outboard hinges were moved in a plane normal to the stabilizer chord plane. Hydraulic jacks were used to duplicate the bending induced by the stabilizer. The pedestal bases of the two hinges on the actuator support fitting and the support for the actuator rod reaction link were held immobile and were used as a datum reference for deflection of the other five hinge points. These fixed and movable hinge points are defined in Figure 42.

Elevator airloads were applied to the lower and upper surfaces through pads bonded to the skin panels, as shown in Figure 41.

The pad locations and load distributions were optimized to match (a) vertical shear along the elevator, (b) hinge moment along the elevator, (c) skin panel out-of-plane moment along the front spar, and (d) maximum normal skin panel deflections. Thirteen hydraulic jacks were used to apply the loads, and a load cell was installed in series with each hydraulic jack to measure its applied load. One hundred and fifteen rosette strain gages and 16 axial strain gages were installed to measure strains at critical areas and verify internal load distributions.

The composite elevator was subjected to two static load conditions defined as follows:

- LC 128—positive maneuver at 852 km/hr (460 kn) at sea level
- LC 125—instantaneous elevator at 463 km/hr (250 kn) at sea level

The elevator was successfully tested to 67% of design ultimate LC 128 with no damage to the specimen. Strain, deflection, and load readings were recorded. Examination of measured strains, deflections, and hinge and actuator loads showed agreement with the finite-element ATLAS model values. After the limit load test, the elevator was subjected to 280,000 load cycles, which is equivalent to two service lifetimes.

Strain and deflection surveys were conducted for both up and down airloading before cycling began and again after 100 cycles had been applied. Similar surveys were conducted before resuming cycling for a second lifetime of testing. The respective measured strain and deflection values were in close agreement at each survey.

Visual inspections were conducted of all accessible structures at scheduled intervals during the testing. Ultrasonic inspections were made of critical areas at less frequent intervals, and X-ray inspections were performed before and after the second lifetime. No structural damage was found during any inspection.

The elevator was loaded to 100% of LC 128 (positive maneuver at dive speed ultimate condition). The strain-gage data showed good agreement with the linear extrapolated limit load data. Figures 43 and 44 show strain comparisons between the test elevator and the predicted finite-element model values for LC 128. Figure 45 shows the elevator torsional rotation comparison between test and predicted values for LC 128.

The elevator was set up for a Boeing-required fail-safe test by removing the station 209.96 hinge pin (fig. 42). The test objective was to achieve the fail-safe load level (67% design ultimate load, DUL) with the hinge failed. The LC 128 loading configuration was used for the test. At 60% of LC 128 design ultimate load, the elevator upper surface skin, (tension surface) spar chord, and web failed at station 172. The load at failure was equivalent to 96% of the fail-safe load condition. A failure analysis, which included a review of the finite-element model predicted strains, strain gage data, and coupon test data, was performed.

The loads that existed at the analysis location were the spar chord tension bypass load due to overall elevator bending and a fastener load due to the hinge loads.

Test data from the ancillary test program were reviewed and room-temperature/dry test values of bearing stress and bypass strain that would apply at this analysis location were obtained. These values are plotted on an interaction curve of fastener bearing stress versus bypass strain in Figure 46. The values of bearing stress and bypass strain that existed on the elevator at failure are plotted in Figure 46 as a ratio of the ancillary test program data. The test point, displayed in Figure 46, defines a circular arc interaction curve for combining fastener bearing stress normal to a tension bypass strain. The 100% level of the fail-safe load condition is plotted in Figure 46 as a reference. The test failure and subsequent analysis provided a good correlation between coupon and full-scale test results.

The full-scale elevator test program achieved all certification goals and the required data were submitted to the FAA.

3.2.3 Ground Vibration Test

Ground vibration testing was performed on a 727 flight test aircraft with the composite elevator installed. The primary purpose of these tests was to compare the measured natural frequencies of the composite elevators with the values used in the flutter analysis.

The test airplane was positioned on a level surface in an operating-empty weight configuration. The airplane was supported on the main and nose gears with reduced tire pressure. Portable vibration shakers were used to excite the elevator with the horizontal stabilizer in the neutral position. Tests were conducted with hydraulic power on and off, and with the right- and left-hand elevator excitation in and out of phase.

Accelerometers, located on both right- and left-hand stabilizers, elevators, tabs, and control columns, were used to measure control system natural frequencies, mode shapes, and damping characteristics. The measured natural frequencies of the advanced

composite elevators were in close agreement with those used in the flutter analysis, as shown in Table 4.

3.3 MANUFACTURING DEVELOPMENT

The manufacturing development organization provided a team of people from Manufacturing Engineering, Industrial Engineering, Manufacturing Research and Development, Quality Control Research and Development, and Manufacturing to work in close collaboration with engineering on the 727 Advanced Composite Elevator Program. They established and evaluated producibility and cost of various design concepts and determined the tooling and process development required to produce the advanced composite elevator.

3.3.1 Detail Tooling

Test parts and production tools were fabricated from aluminum or steel using photo-contact-master drawings and master-dimensioning-index drawings developed through computer-aided design. Figures 47 through 52 illustrate the various major part and tool dimensions and geometry.

3.3.2 Kitting, Layup, and Bagging

To minimize errors in ply orientation and drawing interpretation, a prepreg kit consisting of plies cut using tool templates was prepared for each detail part. The plies, with honeycomb in a sandwich structure (when required) are laid up on the tool (as shown in fig. 53) according to the following procedures:

- The tool surface is cleaned with methyl ethyl ketone.
- Mold release, Frekote 33, is applied to the tool and baked on at 121°C (250°F) for 30 minutes.
- Every two to three plies laid up are compacted (debulked) using a temporary vacuum bag and a minimum vacuum of 560 mm (22 in) of mercury.
- Peel ply is used on all surfaces that are to be secondarily bonded or painted.
- Bondable Tedlar is applied to laminate surfaces where isolation from aluminum elements is required and to all honeycomb details as a moisture barrier.
- With the nylon bag sealed to the tool surface, a minimum vacuum of 560 mm (22 in) of mercury is drawn and the bag is checked for conformity to the part and for leaks. Unacceptable leakage is defined as a loss of 127 mm (5 in) or more of mercury in 5 minutes.

3.3.3 Cure Cycle

The bagged part was placed in an autoclave and the vacuum connection was coupled to an outside vent line. When the autoclave was closed, pressure and heat were applied (see fig. 54); at 138 kPa (20 psi) the vacuum was vented to the outside atmosphere and pressure was increased to 586 to 689 kPa (85 to 100 psi) for solid laminates, or 276 to 345 kPa (40 to 50 psi) for honeycomb parts. The heatup rate was held to 0.5 to 2.8°C (1 to 5°F) per minute to a maximum temperature between 174 and 185°C (345 and 365°F), where it was

held for 120 to 180 minutes. The part then was cooled at a maximum rate of 2.8°C (5°F) per minute to 60°C (140°F), where the pressure was released and the part debagged and inspected (fig. 54).

3.3.4 Nondestructive Inspection

Reference standards for nondestructive inspection (NDI), representing anticipated production designs, were built with defects, 0.05-mm (2-mil) Teflon¹, incorporated during the layup. The production NDI standards, duplicating exactly the various sections of production parts, were also laid up with built-in defects. Both were used to evaluate the following NDI techniques and to determine the most suitable technique to be used for each part.

- Through-transmission ultrasonic (TTU) with automated scanning and computerized C-scan recording and/or a visual display
- Portable and semiportable TTU, manual scanning with light meter and audible defect indication
- Sondicator, Models -1 or S-2B, manual ultrasonic inspection
- Fokker bond tester
- Radiographic inspection, low kilovoltage, (15 to 40 kV)

All defects in the standards were detectable by one or more of these NDI techniques. The TTU inspection with computerized C-scan capability was the most sensitive technique, with detection limits going down to 0.64 by 0.64 cm (0.25 by 0.25 in). Portable TTU, the Sondicator, and the Fokker bond tester were effective for defects not smaller than 1.27 by 1.27 cm (0.5 by 0.5 in) in rib and spar flange areas where manual scanning was required.

Radiographic inspection was the only technique suitable to detect voids in the sealed area of the trailing edges for voids as small as 0.03 by 0.03 cm (0.01 by 0.01 in).

Quality control criteria required rejection for any inclusions. For voids or delaminations less than 3.0 by 5.1 cm (1.5 by 2.0 in) and occurring less than once in each square foot of solid laminate or edgeband area, repair by resin injection was acceptable. In facing plies over honeycomb core, delaminations of less than 2.54 by 2.54 cm (1.0 by 1.0 in) and occurring less than once in each square foot of surface were deemed repairable by resin injection.

In-service maintenance inspection using any of the portable techniques is expected to have realistic defect detection capability to 2.54 by 2.54 cm (1.0 by 1.0 in), which will show the need for, or suitability of, field repair. The NDI standards and evaluation details are described and illustrated in Volume 2 (ref. 1) of this report.

¹Teflon: Registered trademark of E. I. duPont de Nemours & Co., Inc.

3.3.5 Problems and Solutions

Fiber breakout that occurred when drilling through panels that were laid up with uni-directional tape required the evaluation of material form and surface finish fabricability and cost-effectiveness. Woven fabric layup was compared with various tape layups and was found to require less labor and had fewer rejections for fiber breakout. Surface finish time was greater for the fabric; however, the woven fabric layup remained the most cost-effective form. Table 5 lists the relative costs of the systems studied.

Fabrication studies of a full-scale, but only 203-cm (80-in) long, elevator section to test detail tools and to ensure that major assembly problems would not be encountered during production resulted in the following:

- Spars for the subject test section did not reproduce the warpage that occurred in the longer, 442-cm(174-in) production spars. From this it is concluded that verification hardware should be full scale in all dimensions.
- Assembly fitup discrepancies occurred between rib spars and skins in the concept verification hardware. The discrepancies, which were caused by dimensional inaccuracies in scaling the photo contact master to make the male rib tool, were corrected in the rib tool design for the actual verification and production hardware by using master dimensioning index data.
- The verification hardware was fabricated by research mechanics. Although these mechanics were later involved in training the production assembly personnel, it would have been more effective if the production people themselves had built the verification hardware.

3.4 FABRICATION AND ASSEMBLY

3.4.1 Part Fabrication

Production facilities at Boeing's Fabrication Division in Auburn, Washington, were selected to produce advanced composite components and certain new metal components. The facilities were modified as necessary to accommodate the unique processing requirements of the composite materials. To support the composite program, systems and procedures in use for ongoing commercial airplane manufacturing were used to release engineering drawings, production plans, and part fabrication orders and to ensure schedule compliance. Personnel were assigned from production tooling workers already engaged in normal fiberglass and metal manufacturing operations because of their familiarity with similar materials.

The system used for fabricating the composite components is a no-bleed resin system with a 176.7°C (350°F) cure cycle. Figure 55 illustrates the typical operational flow for both laminate and honeycomb structure kitting, layup, cure, inspection, and net trim. Layup of the graphite fabric and tape materials is a manual process using templates to assist in proper location, orientation, and final sizing of the plies and to locate honeycomb cores.

The production phase was successful and verified the program approaches established early in the proposal phases. At the same time, it demonstrated that fabricating parts from composite materials was more complex than originally anticipated. This experience refined the production system procedures and data, and will be the basis for future production commitment decisions.

3.4.2 Problems and Solutions

- The rear spar exhibited a spanwise warp relative to the spar centerline. Revisions were introduced that changed the layup to all fabric with revised ply orientation, and warpage was reduced to acceptable levels. The assembly tooling provided final straightening.

The outboard portion of the front spar exhibited a cross-section warp. Because assembly clamping and installation of spar stiffeners and nose rib attach angles straightened the spars, changes to the layup were not necessary.

The skin panels warped away from the tool surface after cure. The panels were acceptable when their condition was compared to specification warp allowances.

- It was determined that a growth factor must be incorporated into the layup of core details, since graphite-epoxy cured on the large aluminum tools grows to the point of resin gel as a function of aluminum expansion. Development results showed an overall length increase of 1.02 cm (0.4 in) or 0.0019 cm/cm (0.0019 in/in) for the core and graphite-epoxy. Based on these data, core-location templates were reworked to incorporate the growth factor.
- Female layup mandrels caused materials in the outside radius of the flanges to bridge, creating resin ridges and voids. Some of the problem was corrected by changing the staged compaction and the radius size, where allowable. In other cases, the ridges were sanded and the voids were filled with adhesive.

3.4.3 Joining Methods

Titanium Hi-lok bolts with corrosion-resistant steel collars and washers were the predominant fasteners used to mechanically join the assembly components. However, in the rear spar and lower skin panel areas, the following installation problems prompted changes to an alternate fastener:

- Accessibility of standard tools to the collar and Allen pin recess
- High torque range for collar breakoff
- Size of Allen pin recess

The Hi-lok bolts were replaced by Hi-torque bolts that had slotted heads, and Hi-lok collars were replaced with self-locking nuts. This was to solve the problem by driving the bolts from the outside and eliminating the Allen pin problem. However, the Hi-torque bolt head was difficult to grip and presented problems in obtaining proper clamp-up torque. To resolve this condition, a new bolt (the Torque-set) was qualified and used in place of the Hi-torque bolt. This bolt has an offset Phillips-head configuration that provides a positive grip without a high degree of pressure being applied to keep the drive tool seated.

The initial system used to install the upper skin panels on the closeout side of the assembly was nutplates with Hi-torque bolts. In addition, blind rivets, along with the nutplate/bolt fastener, were used in the nose rib area, and hollow-ended rivets were used in the trailing edge. Because the nutplate installation was time consuming and the Hi-torque bolts were a problem, the Visu-lok blind fasteners were qualified and substituted at the majority of these fastener locations. The Visu-lok blind fastener was used in conjunction with a stainless-steel washer bonded to the inner surface of the composite

stackup. Use of the "Bigfoot" blind fastener, which qualified after completion of the fifth shipset of elevators, will eliminate the washer requirement in future applications.

There were no significant problems with installation of the NAS blind fasteners in the nose rib area, but the hollow-ended rivets used along the trailing edge required development of special rivet dies.

3.4.4 Assembly Tools

New tools were designed and fabricated for elevator assembly operations. These tools are similar to existing metal elevator tools, but are fewer in number because the major assembly work of the composite units is accomplished in one stage versus three stages for the metal elevator. The reduced number of internal structural members and one-piece cover panels for composite units allows this one-stage operation. These features and other engineering design variances disallowed the use of existing tool designs and construction of dual-purpose tools for elevator production. Tooling consisted of left- and right-hand units for rear spar, front spar/leading edge, and major assembly operations. Existing master tooling was used as a control medium to ensure interchangeability at the stabilizer/elevator hinge centerline. A new master gage was constructed for control of the tab/elevator hinge line.

Existing control tab and balance panel tools were revised so that either metal- or composite-configured assemblies could be produced.

Conventional tooling methods were used to design and construct all tools, but unique features were included to accommodate the special equipment developed for drilling and trimming composite parts. This equipment included such items as high-speed (18,000 rpm) tapered drills, diamond-coated router bits, and dust-collection systems. For the latter, vacuum nozzles adapted to drill motors and router units were used in conjunction with portable vacuum cleaners.

Index holes sized to the drill motor vacuum nozzle diameter were used in assembly tool drill plates to provide positive dust management during drilling operations, as well as proper hole location and drill alignment. Restricted access prevented use of this system in some areas of the spars and major assemblies. In these areas, a hand-held vacuum hose was used.

Tools tried out on initial units did require some modification but, for the most part, the conventional tool approach, as developed, worked quite effectively.

3.4.5 Assembly Techniques

Part Fitup—Fitup of components was not the problem originally anticipated, and only in isolated areas was shimming required. The warpage of the spars and skin panels during cure cycles was a problem causing concern during detail fabrication relative to fitup on assembly; however, assembly operations were not appreciably affected. Examples of warp and shimming are as follows:

- The front-spar parts exhibited a cross-section warp that was removed by the clamping action of the assembly tool and the installation of nose rib attach angles. In only two instances were shims required to allow proper fastener installation.

- The rear-spar channel exhibited a lengthwise warp relative to the spar centerline, and the clamping action of assembly tools held the channel in position without excessive preload. Also, the channel legs of the spar had a tendency to close in toward the trailing edge when curing. The channel could be opened sufficiently by hand or by tool pressure to allow installation of rear-spar headers and tab hinge fittings. The amount of closedown varied from shipset to shipset.
- Warpage across the width of the skin panels was prevalent in all panels. Pullup of the skin to the inspar structure could be accomplished without causing excessive pressure or preloading. The trouble area with the skin fitup was along the leading edge where the stiffness and warp of the skin panels, coupled with tolerance variation in the metal nose ribs, created shimming requirements to meet process requirements for installation of fasteners (meets minimums for exposure of fastener shank within material stackup).

Hole Preparation—Drilling and countersinking techniques developed during fabrication of verification hardware were applied in the production program through training sessions. The training and experience gained from assembling additional units had a direct effect on workmanship quality.

Composite Stackup—Drilling through composite materials was accomplished with 18,000-rpm air motors and special high-speed, tapered drills made with carbide materials. Hole preparation by this method was relatively trouble free. The exception was the drill exit through the outer surface of the skin panels. The outer layers of the panels were a tape material that caused the graphite fibers to break out as the drill exited. This breakout was generally cleaned up during countersink operations except in an area along the trailing edge. Here, a strip of fiberglass fabric was added to the exterior ply of the panels to eliminate the problem.

If misguided, the taper drills would rapidly cut through the material in a sidewise direction like a router, thus making the hole too large. This was alleviated by establishing positive guidance in the assembly tool. However, in the front-spar area, certain holes were located by pilot holes rather than by tool. In these cases, the mechanics had to be careful to avoid oversizing the finished hole.

Composite/Aluminum Stackup—The original plan for hole preparation was a one-step operation with the carbide-tipped twist drills operating at 2,000 rpm. In stackups where the metal was entered first, no problems were experienced. However, in the leading edges where the stackup was such that the graphite skin panel was entered first, metal chips backing up the drill flutes caused a problem with fiber breakout. To correct this problem, a two-step operation was used. First, the hole was drilled undersize with a carbide-tipped twist drill and then brought to full size with the special taper drill.

Countersinking—Tool life, depth control, surface quality, and fiber breakout were the startup problems that required the most attention. Ultimately, it was determined that three fluted cutters with carbide inserts provided the desired quality and tool life. When a nylon pad was added to the nose of the microstop countersink tool, it effectively controlled the depth and size of the countersink and provided enough pressure close around the cutting area to eliminate breakout. In addition, operator training and techniques contributed to proper countersinks.

3.5 REPAIR TECHNIQUES

Repair techniques using precured graphite-epoxy patches for composite sandwich structure were developed. Patches were bonded to the panel using an elevated temperature and pressure cure. Refer to Volume 2 of this report for details of these techniques (ref. 1). Three types of inspection were used to ensure high-quality repair:

- In-process inspection, including surface preparation, cleanliness, material verification, and Quality Control organization acceptance of cure cycle for pressure, time, and heat rate during actual repair.
- Visual inspection for obvious defects; e.g., bubbles, blisters, or other areas exhibiting nonbonds.
- Nondestructive testing, including through-transmission ultrasonic, Sondicator, and/or Fokker bond tester for bonding, and X-ray for voids and porosity.

3.6 WEIGHT

The five advanced composite elevator systems showed weight reductions of 26.4 to 27.3% from that of the comparable metal elevator system. Table 6 provides a component weight comparison between the metal baseline and the advanced composite elevators.

Figure 56 shows the actual weight and center of gravity location for five shipsets of elevator systems, together with the predicted values. The plot shows a decreasing weight trend throughout the program. The reduction in shipsets Nos. 4 and 5 is attributed partly to the deletion of the surfacer from the skin panel outer surfaces.

3.7 FLIGHT TESTS

Boeing-funded flight tests were conducted to demonstrate flutter clearance and stability and control performance.

Flight flutter tests were conducted at the speeds and altitudes shown in Figure 57. Measured displacement and rotation of the fin, rudder, stabilizer, and elevator, due to sharp control inputs from the elevator and rudder, were used to evaluate the natural frequency and damping characteristics of the empennage with graphite-epoxy elevators.

Stability and control flight tests consisted of two phases. Phase I flight tests were conducted on a production aluminum elevator to establish baseline data. For Phase II, the aluminum elevator was replaced by the composite elevator and Phase I flight tests were repeated. The effect of the composite elevator on the stability and control characteristics and autopilot operation of the Model 727 was evaluated by comparing the two sets of test data. These test results indicated no detectable difference in aircraft response between the composite and production aluminum elevators. The flight-test airplane was flown by a Federal Aviation Administration (FAA) pilot as part of the stability and control and autopilot certification flight testing.

3.8 FAA CERTIFICATION

The flight flutter and stability and control test results were submitted to the FAA. Both sets of test results indicated that all FAA requirements had been achieved.

A formal strength analysis of the graphite-epoxy elevator was submitted to and accepted by the FAA. Certification of the graphite-epoxy elevator was granted on December 7, 1979.

4.0 COST ANALYSIS

It is projected that advanced composite material waste will be reduced with the implementation of advanced manufacturing technology and more uniform quality material. It also is projected that cost per pound of advanced composite material will decrease 20% as industry usage of the material increases. Based on these projections, the production experience gained during this program, and assumptions of other cost-reducing factors as detailed in Section 4.3, the cost of advanced composite elevators will become comparable to the cost of similar metal components.

When the increasing value of weight reduction is considered together with the adoption of innovative manufacturing methods and engineering designs, the economic justification for advanced composite aircraft structure is assured.

This section presents the production cost data for the five-and-one-half-shipset production run.

4.1 PRODUCTION COSTS

4.1.1 Production Environment

The total production program costs shown in Figure 59 reflect the fabrication and manufacturing processes used in a semiproduction environment for the five-and-one-half-shipset program. Tooling and component manufacturing percentages shown in Figure 58 are relative to overall costs in dollars; engineering costs are not included.

Work was performed in production shops by people whose experience and skill level were a representative cross section of the shop work force. Component fabrication was performed with hand cutting and layup of broadgoods, ply-by-ply inspection, and hand trimming. Tooling was designed for extended production, but the tool rework and improvement effort was restricted to the five-and-one-half-shipset contract.

These activities were representative of the production processes that would, when practical, be used to produce a large number of elevators. It is likely, however, that by adopting improved manufacturing processes, the per-unit cost of elevators produced in a regular production environment would be significantly lower. Projections of production cost trends are discussed in Section 4.3.

4.1.2 Total Costs

Of the total production expenditures for the five-and-one-half shipsets, labor was 82.4% and nonlabor was 17.6%. The major cost elements of the total production costs are shown as percentages in Figure 59. The component production labor hours shown in Figure 59 are broken down further in Figure 60: fabrication (61.8%), assembly (28.0%), and manufacturing research and development (10.2%). Total production labor hours are presented in Figure 61 showing the breakout between recurring (31.5%) and nonrecurring (68.5%) costs. Many nongraphite parts used in the composite elevator are common to both the metal and the composite elevator. Some of these had to be modified from the configuration provided by the part vendor or metal elevator subcontractor to make them usable in the composite elevator assembly. The cost for the rework of these parts has been segregated and is identified in Figure 60. Recurring fabrication and assembly efforts are broken out by task and presented in Figure 61. A percentage breakout of recurring fabrication effort by major graphite component is provided in Figure 62.

4.2 COMPOSITE MATERIAL USAGE FACTORS

Usage factors experienced for graphite-epoxy materials were 1.8 lb of tape and 2.8 lb of fabric for each unit of weight of graphite-epoxy flyaway weight in the finished elevator. This included indirect usage for receiving tests, kitting trim loss, process test panels, process and miscellaneous rejections, and layup trim loss. It is estimated that these factors could be reduced to 1.5 and 2.0, respectively, over a 200-shipset program, with more uniform quality materials, revised handling methods, and improved manufacturing processes. With the advent of automated material cutting/ part nesting and new layup and processing technology, these factors would be further reduced.

4.3 COST COMPARISONS

Based on costs incurred in producing the five-and-one-half shipsets of composite elevators, the average cost of 200 shipsets is estimated to be 40% higher than the average cost of the first 200 shipsets of the current all-metal configuration. However, the cost penalty would be substantially reduced and possibly eliminated through the adoption of improved manufacturing processes; this includes using the aforementioned automated tape layup and cutting machines, using material more efficiently, and reducing material prices in real terms by increasing production volume.

The effect of improved composite technology on the trend of competitive cost relationships initial 200-shipset quantities of Model 727 metal and composite elevators at current and future time periods is illustrated in Figure 63. The figure shows that the present 40% cost penalty could be reduced to 13% by 1985. By 1990, this cost penalty may be either eliminated or turned into an advantage based on the current elevator design and the assumptions listed in Table 7. Further optimization of the design would be expected to produce additional cost benefits.

The cost projection comparison of 200 shipsets of metal versus composite elevators shown in Figures 64 and 65 is based on the following ground rules:

- Estimated production costs are scoping level.
- No additional engineering or developmental sustaining effort is required.
- Nonrecurring costs such as production release and duplicate tooling are excluded.
- Recurring costs include only material, outside production, and operations labor to be expended directly on the deliverable end item.
- Production delivery rate for a 200-airplane program is 12 shipsets per month.
- Material supplier-quoted unit cost per pound of composite material will decrease by 20% as industry usage doubles.

Other ground rules, which are the average of high and low cost projection factors, are listed below. For the high cost projection, it is assumed that:

- 707/727/737 Division assembly hours will follow a 77.5% learning curve.
- Fabrication Division process assembly hours will follow an 80% learning curve.

- Composite material dollars include a 1.75 usage factor.
- Fabrication Division sheet metal and machine hours will follow a 90% learning curve.
- Production material will follow a 95% improvement curve.

5.0 CONCLUDING REMARKS

Key program results are highlighted below:

- Weight saving of 27% over current metal assembly was achieved.
- Components were produced on schedule.
- Parts and assemblies were readily produced on production-type tooling.
- Quality assurance methods were demonstrated.
- Repair methods were demonstrated in factory production and airline service.
- Strength and stiffness analytical methods were substantiated.
- Cost data base information was accumulated in a semiproduction environment.
- Federal Aviation Administration certification was achieved.
- Five shipsets were committed to routine airline revenue service.

The program was successful and timely and provided the necessary confidence to commit usage of graphite composite structure in similar applications on a new generation of commercial aircraft.

6.0 REFERENCES

1. Chovil, D. V., W. D. Grant, E. S. Jamison, H. Syder, O. E. Desper, S. T. Harvey, and J. E. McCarty: Advanced Composite Elevator for Boeing 727 Aircraft. Volume 2--Final Report. NASA CR-159258, 1980.
2. Oghi, George Y.: "Advanced Composite 727 Elevator and 737 Stabilizer Programs," a paper presented at the 1978 SAMPE Conference, Anaheim, California. 2-4 May 1978.
3. Syder, H.: "Using Graphite Composites in Aircraft Structures," a paper presented at the 1980 Design Engineering Conference, Chicago, Illinois. 24-27 March 1980.

7.0 ABBREVIATIONS AND SYMBOLS

A	ampere
ACEE	Aircraft Energy Efficiency program
ATLAS	computer program
cg	center of gravity
\bar{C}	centerline
D	diameter
deg	degree
DUL	design ultimate load
FAA	Federal Aviation Administration
f_{BRG}	applied bearing stress
\bar{H}	hingeline
Hz	hertz
$K_{B_{\infty}}$	B-basis statistical factor
kg	kilogram
km	kilometre
kn	knot
kN	kilonewton
kPa	kilopascal
kV	kilovolt
lbf	pound force
LC	load case
M_D	Mach number at dive speed
mm	millimetre
mm/mm	millimetre per millimetre
M_{MO}	Mach number at maximum operating speed
MPa	megapascal
N	newton
NDI	nondestructive inspection
N/mm	newton per millimetre
psi	pounds per square inch
R	stress ratio
R_{BRG}	bearing stress ratio
$R_{\epsilon_{gross}}$	gross area strain ratio
RH	relative humidity
rpm	revolutions per minute
RT	room temperature
s, sec	second
Sta	station
t	thickness
T	temperature
TTU	through-transmission ultrasonic
V_D	design dive speed
V_{MF}	variation magnification factor
V_{MO}	maximum operating speed
W	width
ΔT	temperature increment
ν_{ϵ}	ultimate shear strain
ν	ultimate axial strain
ν	Poisson's ratio
ν_{MAX}	maximum test value ratio
ν_{xy}	inplane Poisson's ratio

ϕ	tortional rotation
$^{\circ}\text{C}$	degree Celsius
$^{\circ}\text{F}$	degree Fahrenheit

All measurement values are expressed in the International System of Units (SI) with the U.S. Customary Units appearing after in parentheses; the U.S. Customary Units were used for principal measurements and calculations.

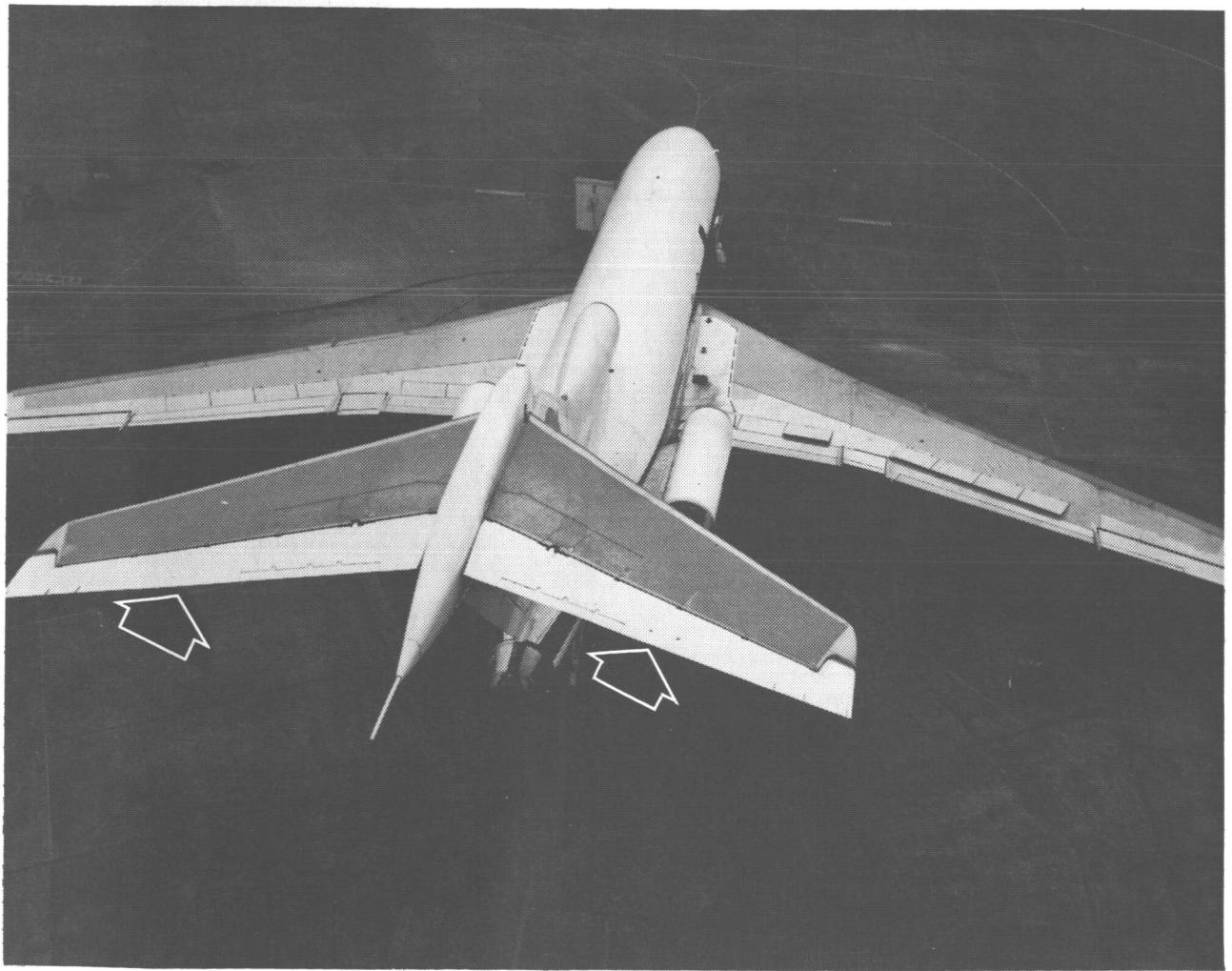


Figure 1. First Advanced Composite Elevator Installed on a Commercial Aircraft

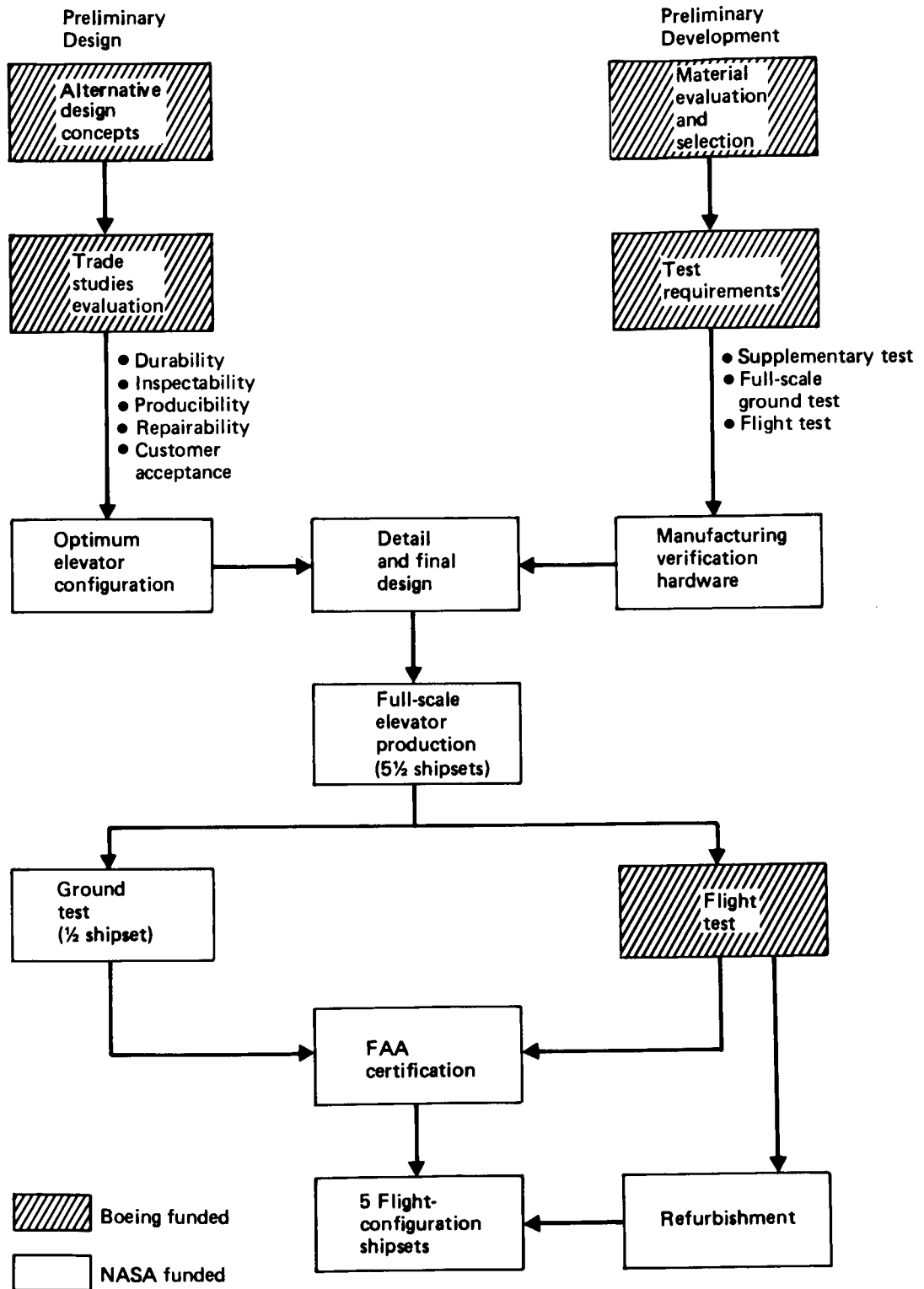


Figure 2. Program Technical Approach

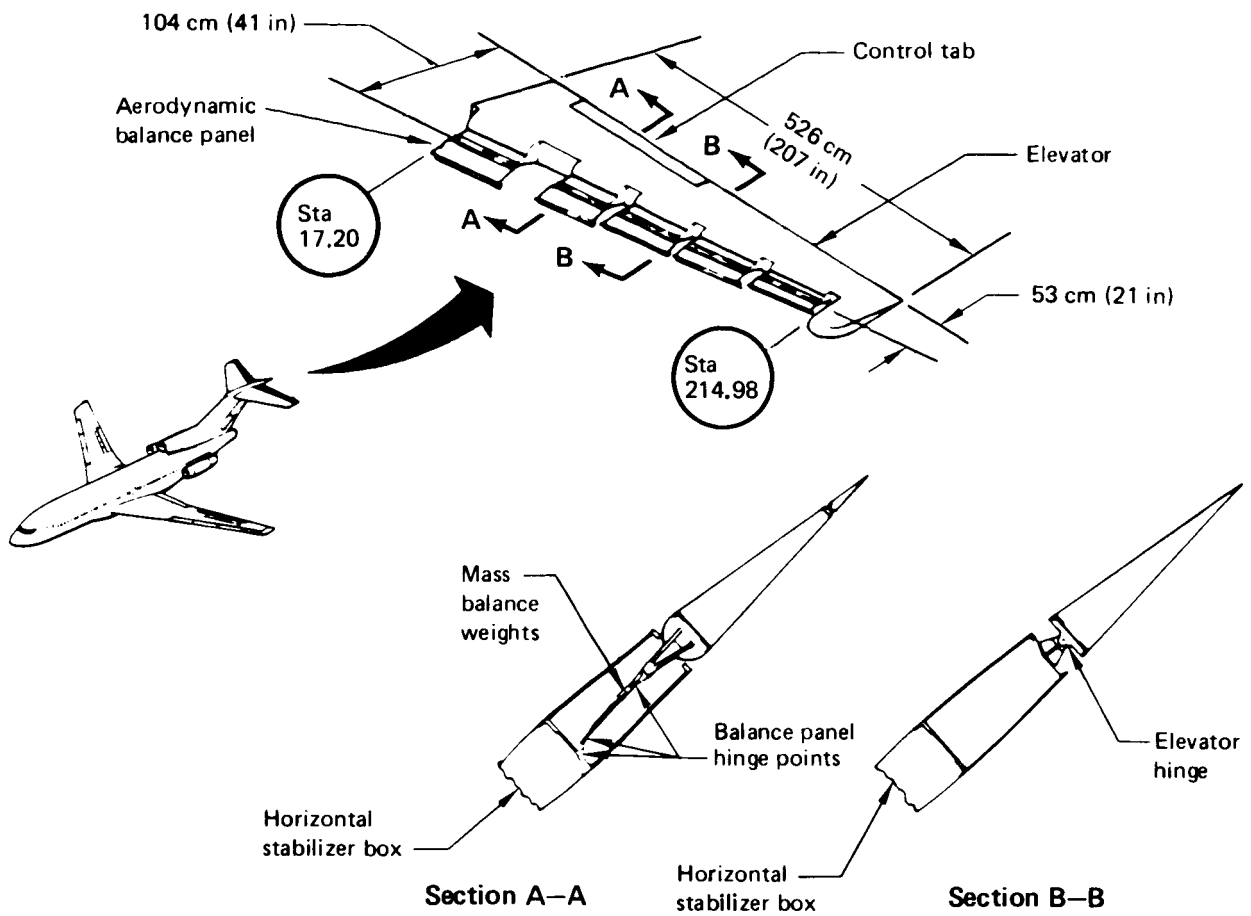


Figure 3. 727 Elevator General Arrangement

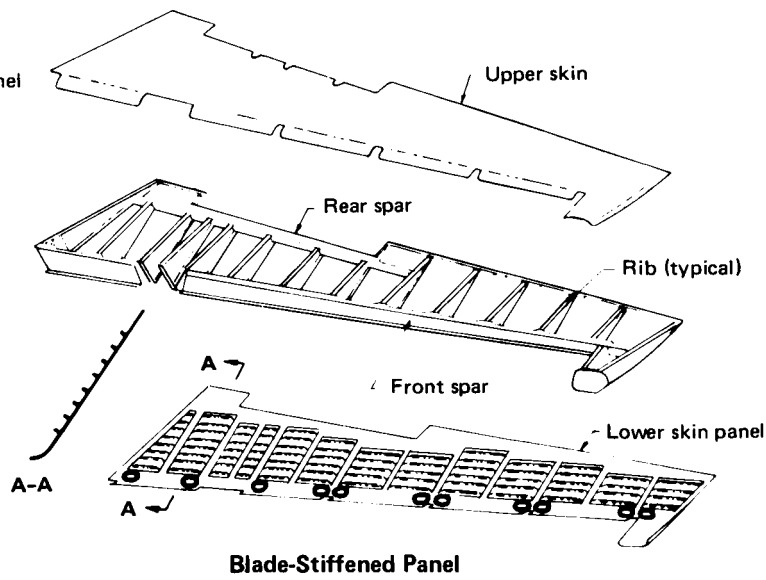
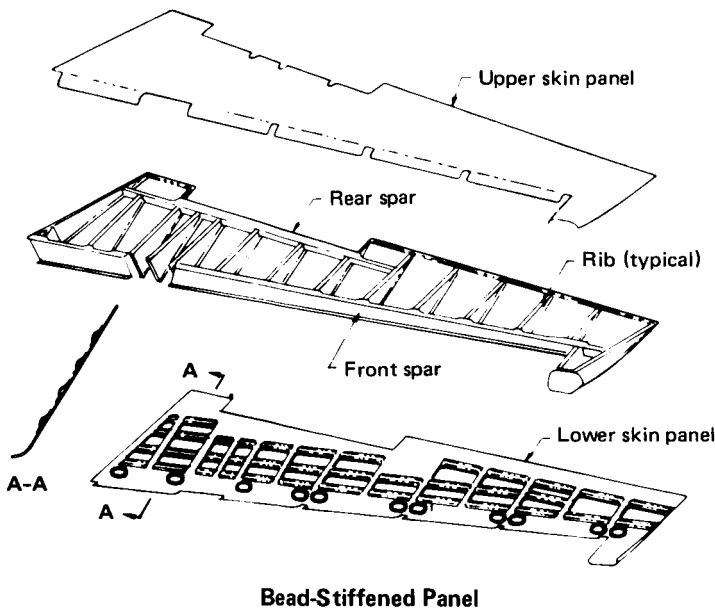
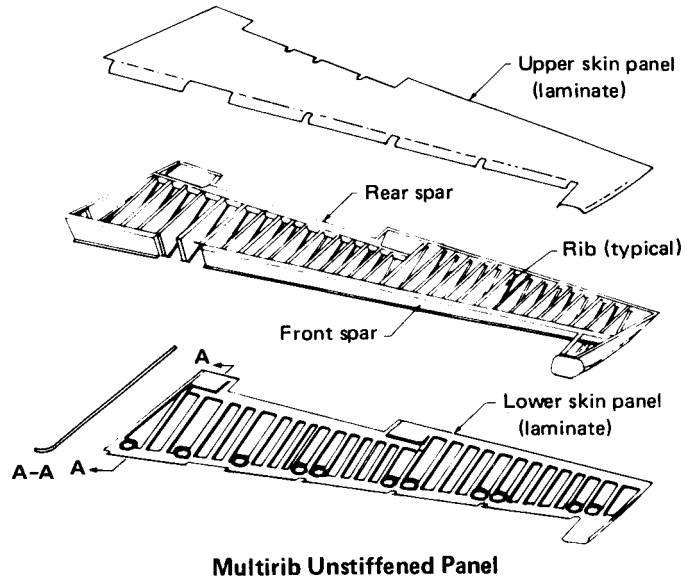
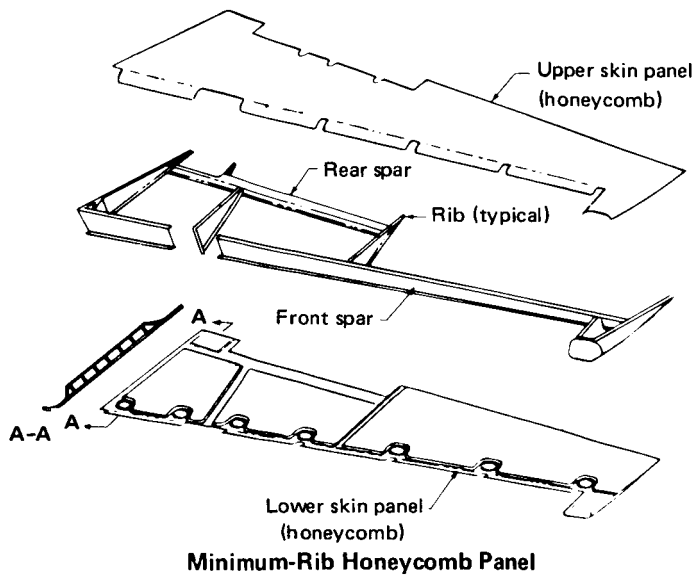


Figure 4. Preliminary Composite Elevator Configurations

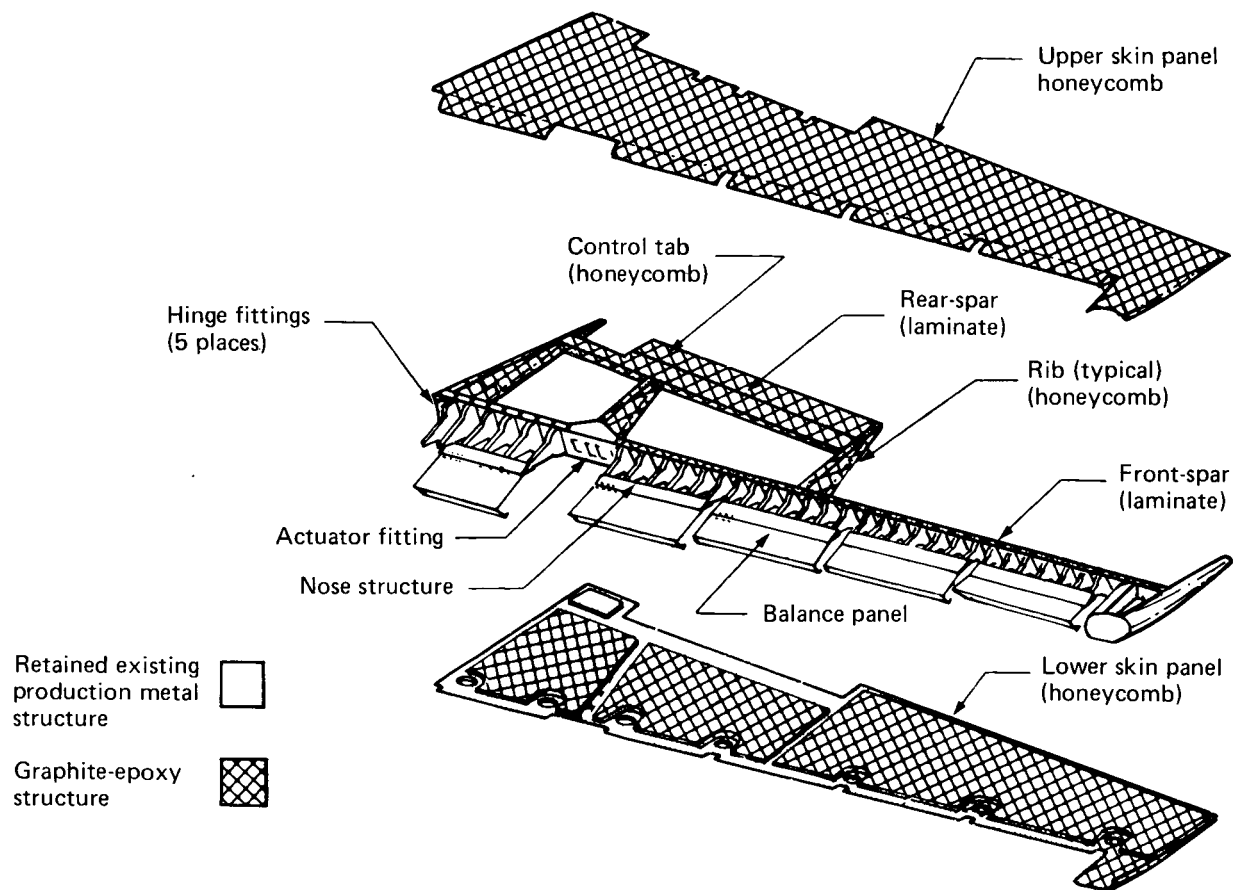


Figure 5. 727 Composite Elevator Structural Arrangement

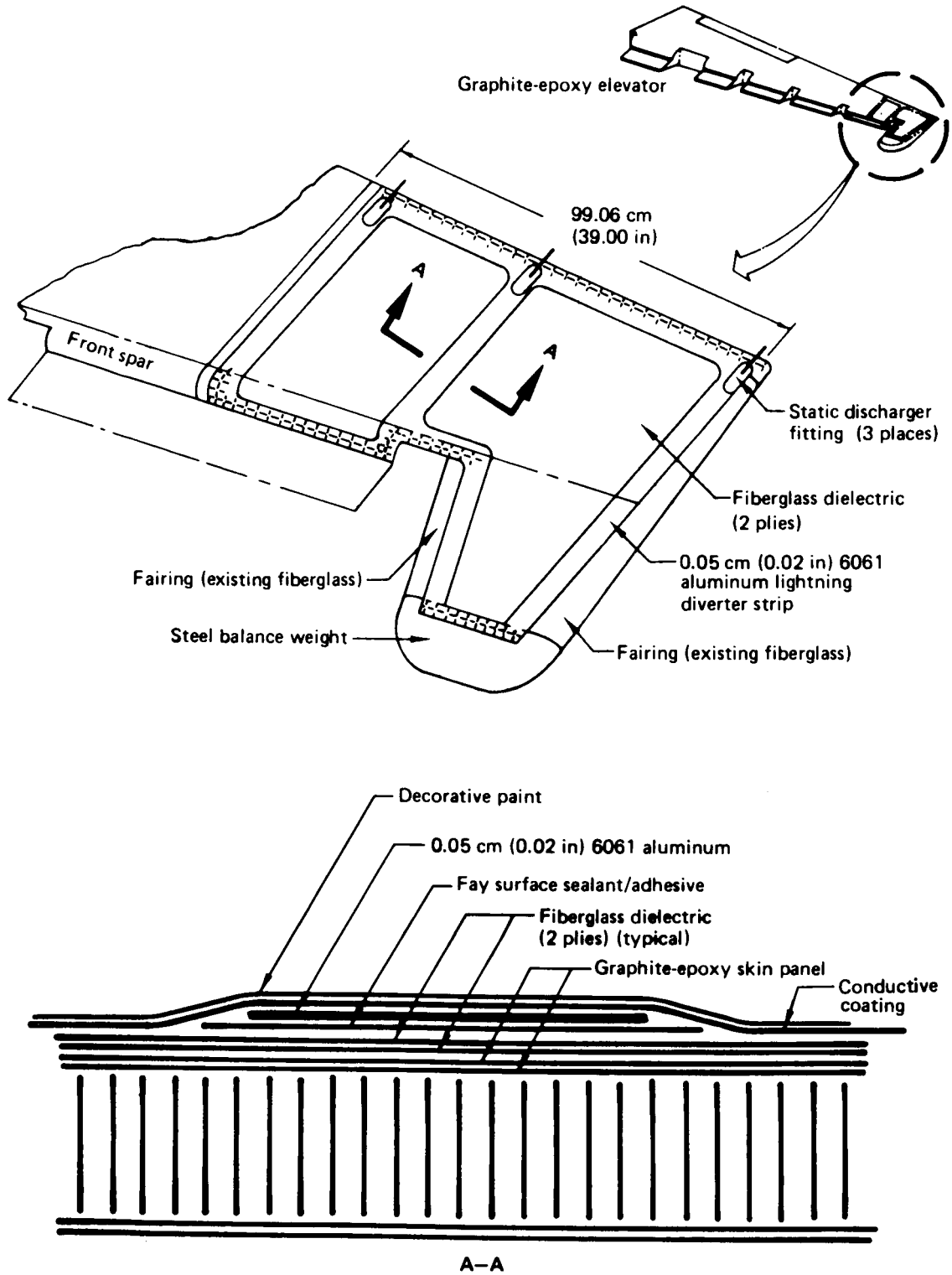


Figure 6. Lightning Protection System

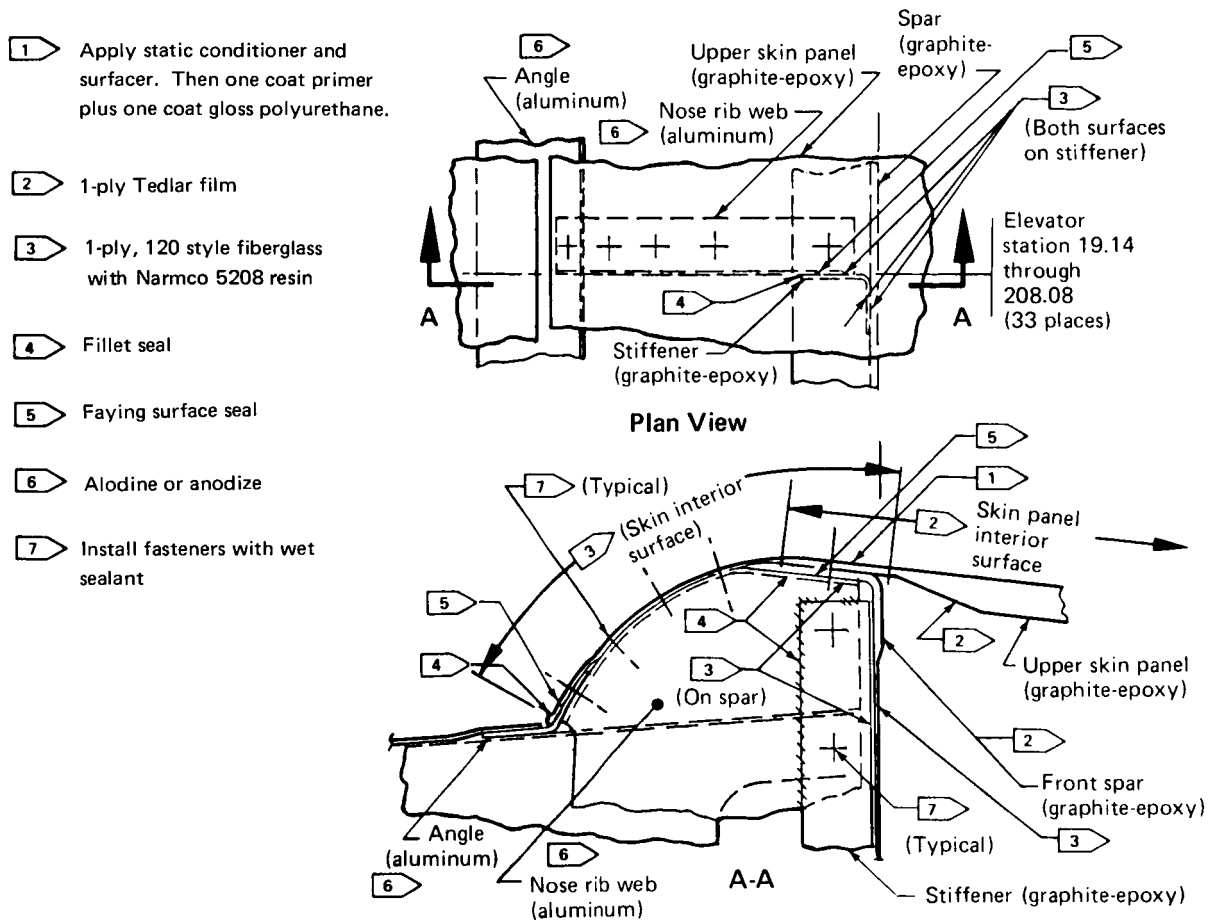


Figure 7. Corrosion Protection—Typical Graphite-Epoxy/Aluminum Interface

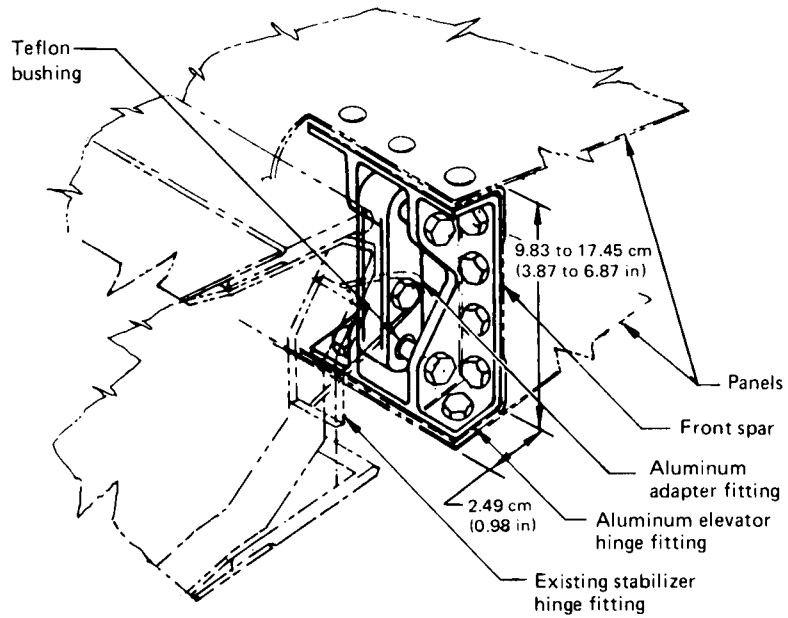


Figure 8. Elevator and Stabilizer Hinge Concept

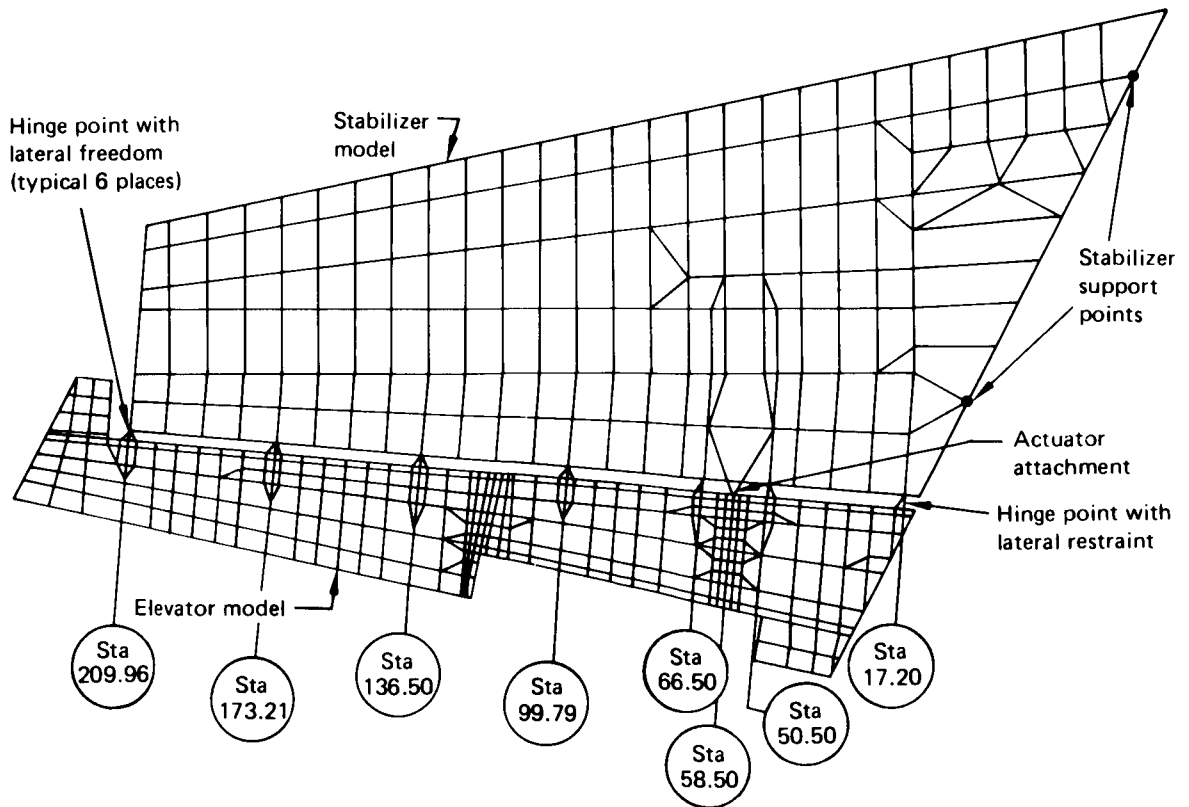


Figure 9. Elevator/Stabilizer Finite Element Model

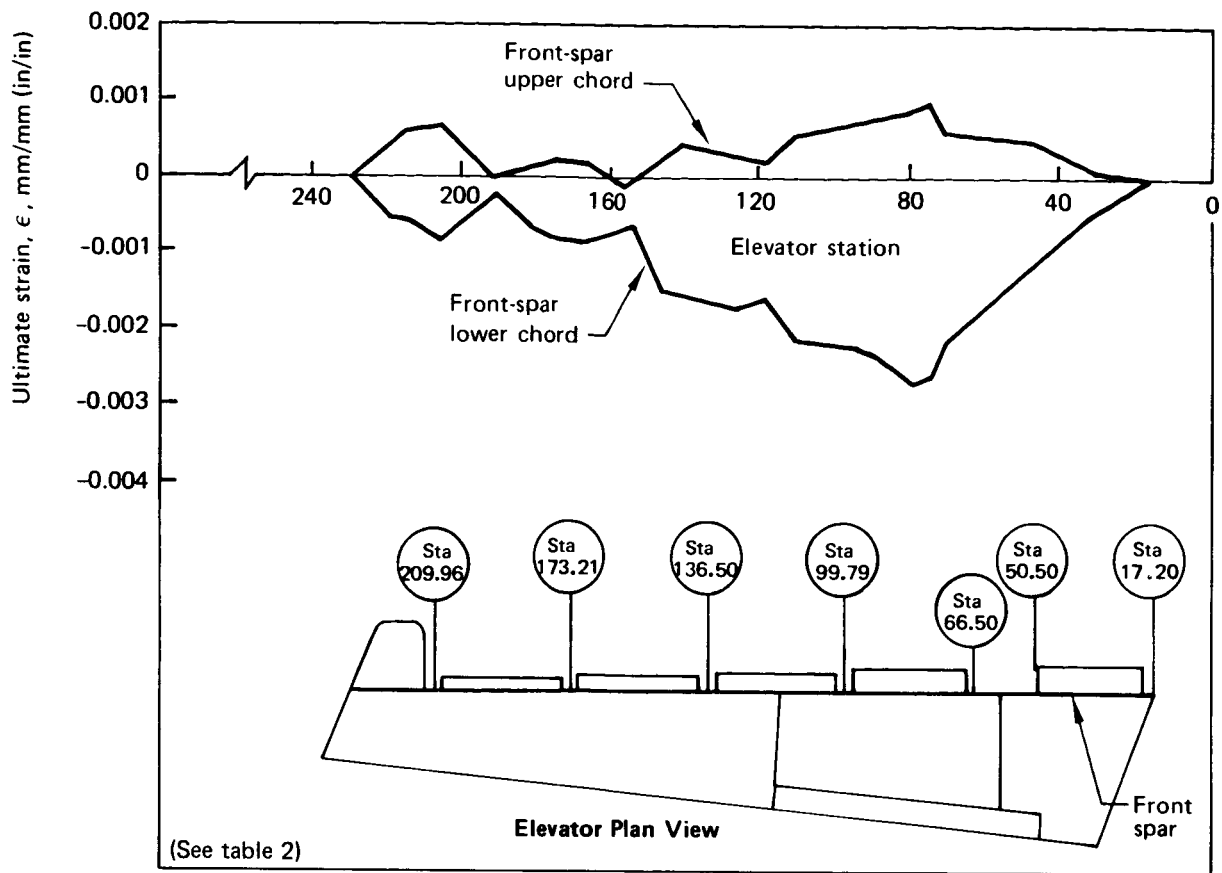


Figure 10. Ultimate Front-Spar Chord Strains for Load Case 125

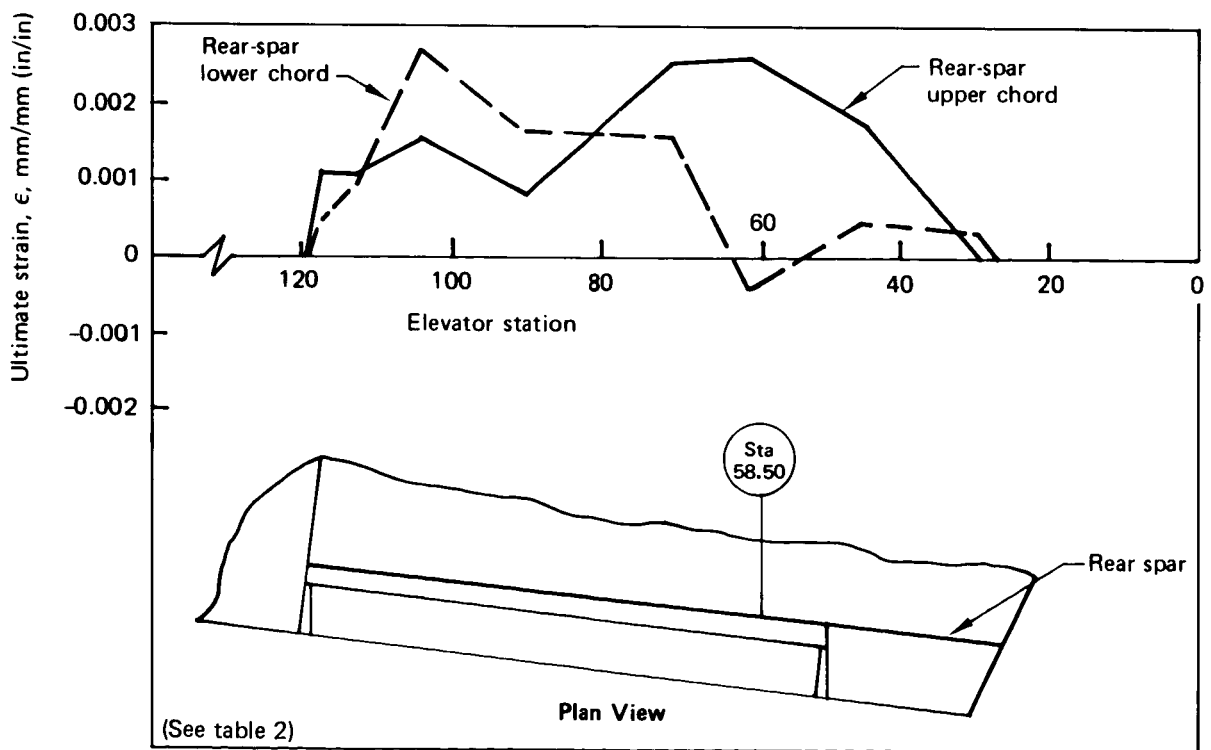
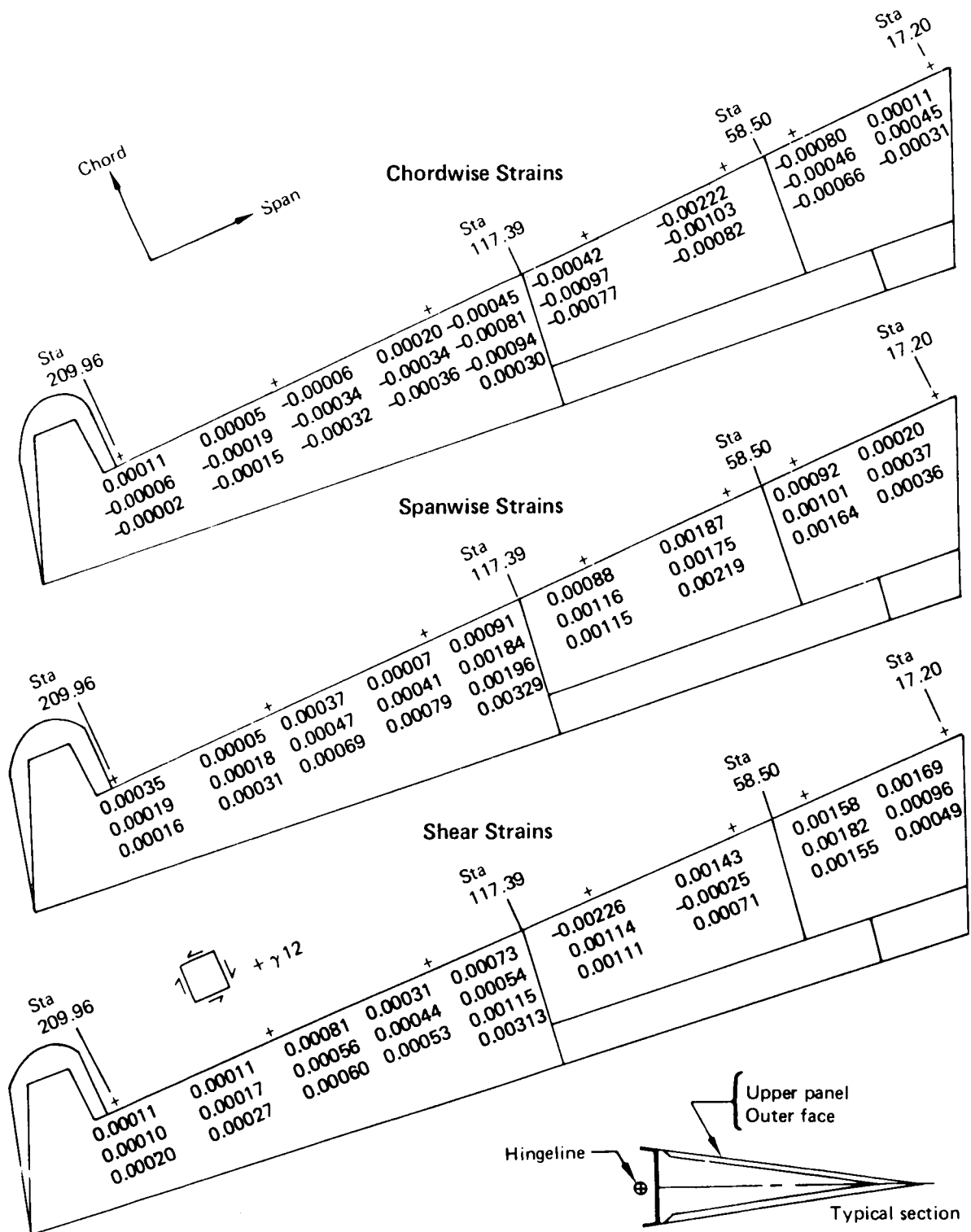


Figure 11. Ultimate Rear-Spar Chord Strains for Load Case 125



(See table 2)

Figure 12. Ultimate Skin Panel Strains, Load Case 125

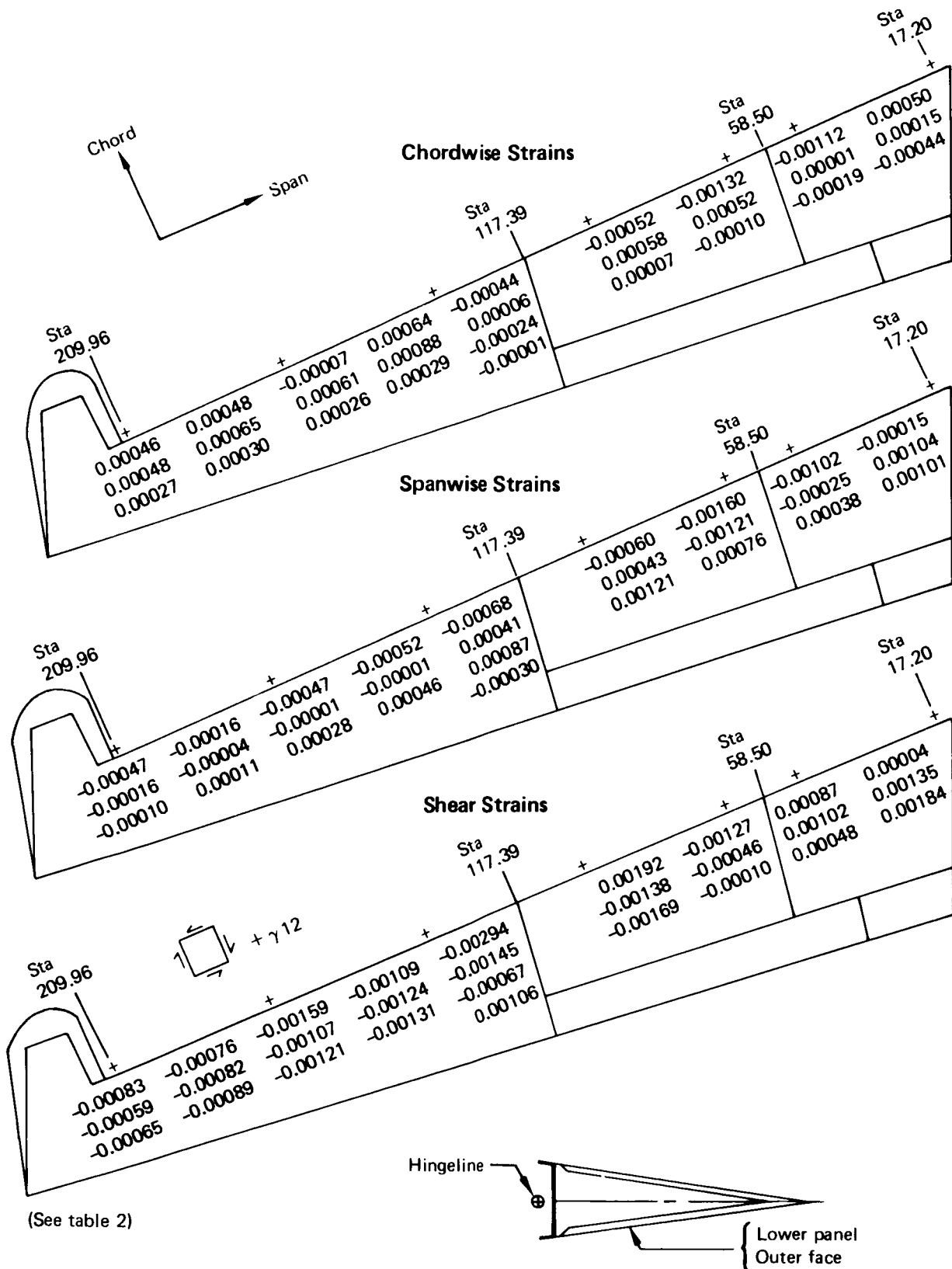


Figure 13. Ultimate Skin Panel Strains, Load Case 125

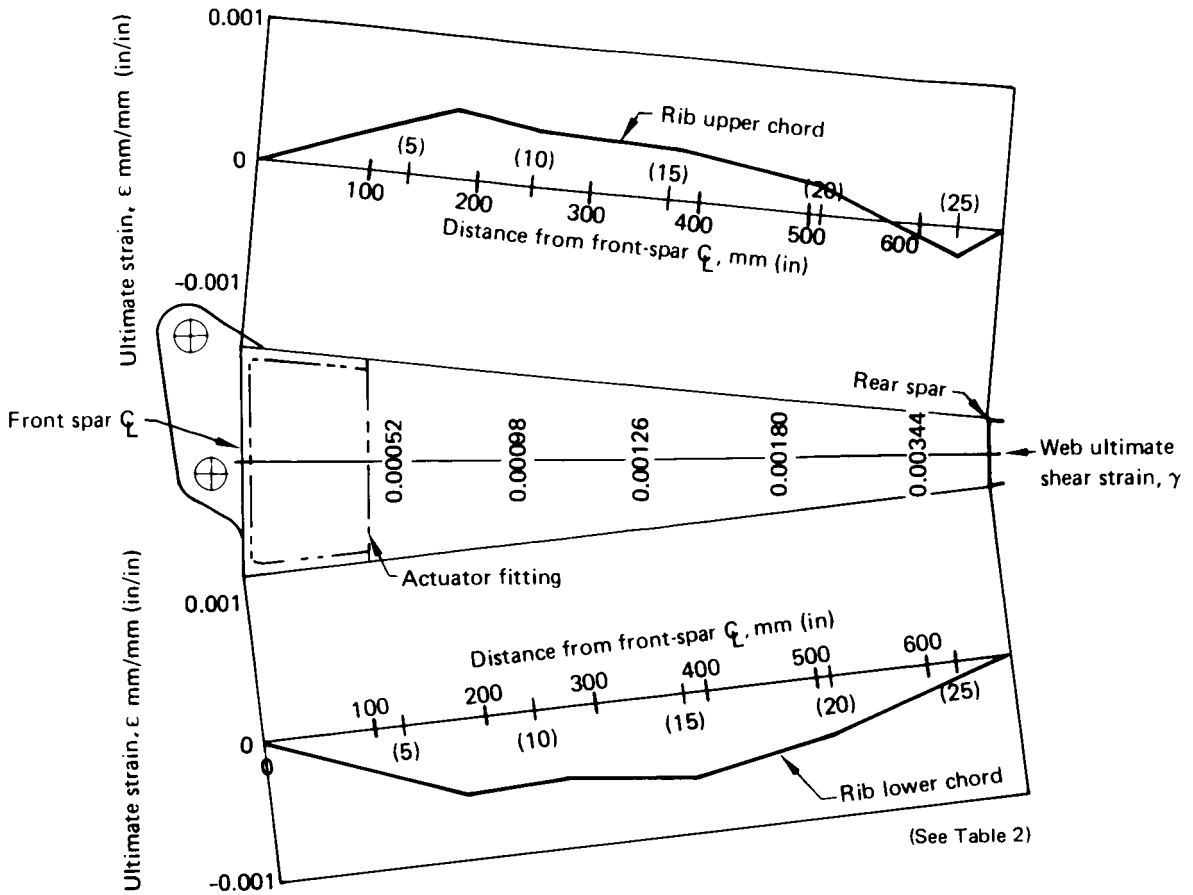


Figure 14. Ultimate Actuator Rib Strains for Load Case 125

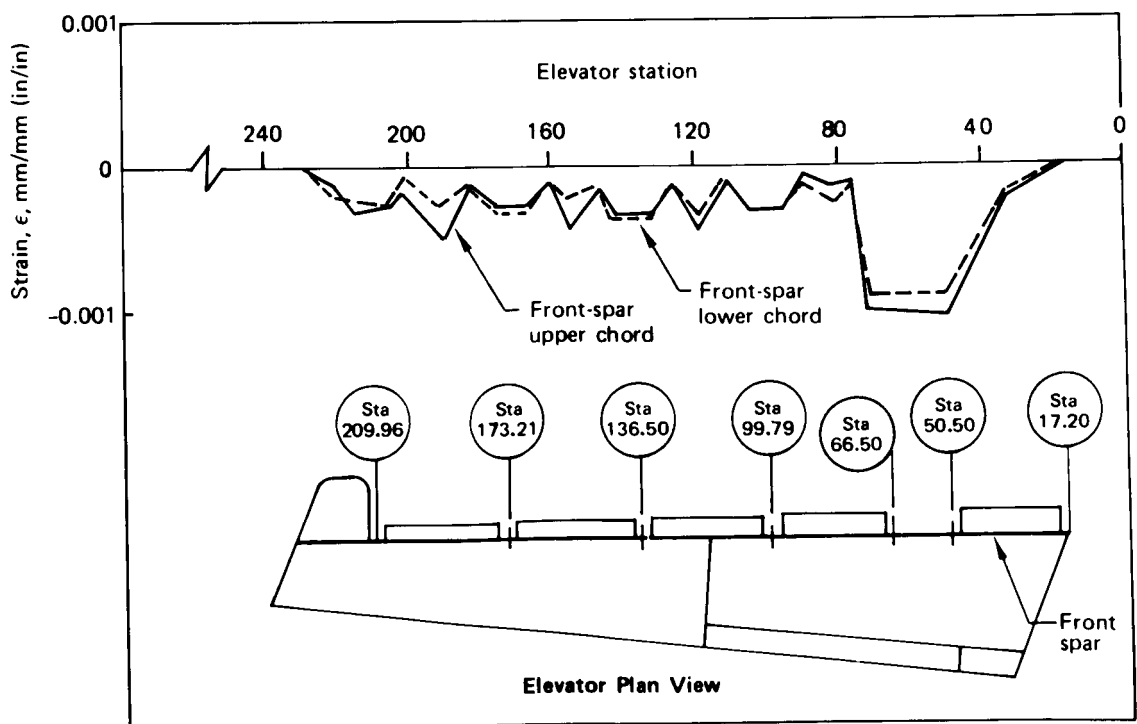


Figure 15. Front-Spar Chord Strains, Thermal Load Case $\Delta T = 81^{\circ}\text{C}$ (145°F), at $T = -59^{\circ}\text{C}$ (-75°F)

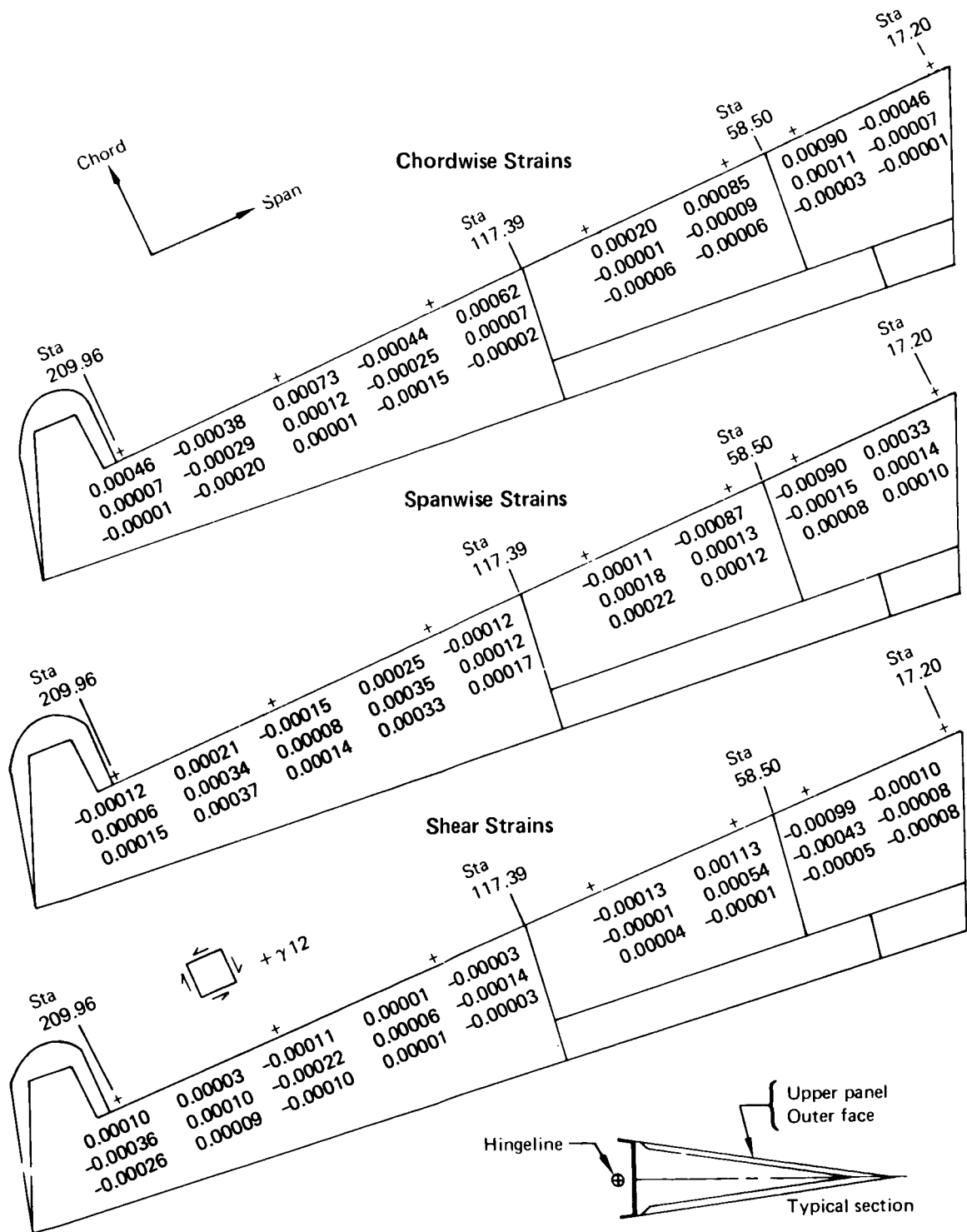


Figure 16. Skin Panel Strains, Thermal Load Case $\Delta T = 81^{\circ}\text{C}$ (145°F), at $T = -59^{\circ}\text{C}$ (-75°F)

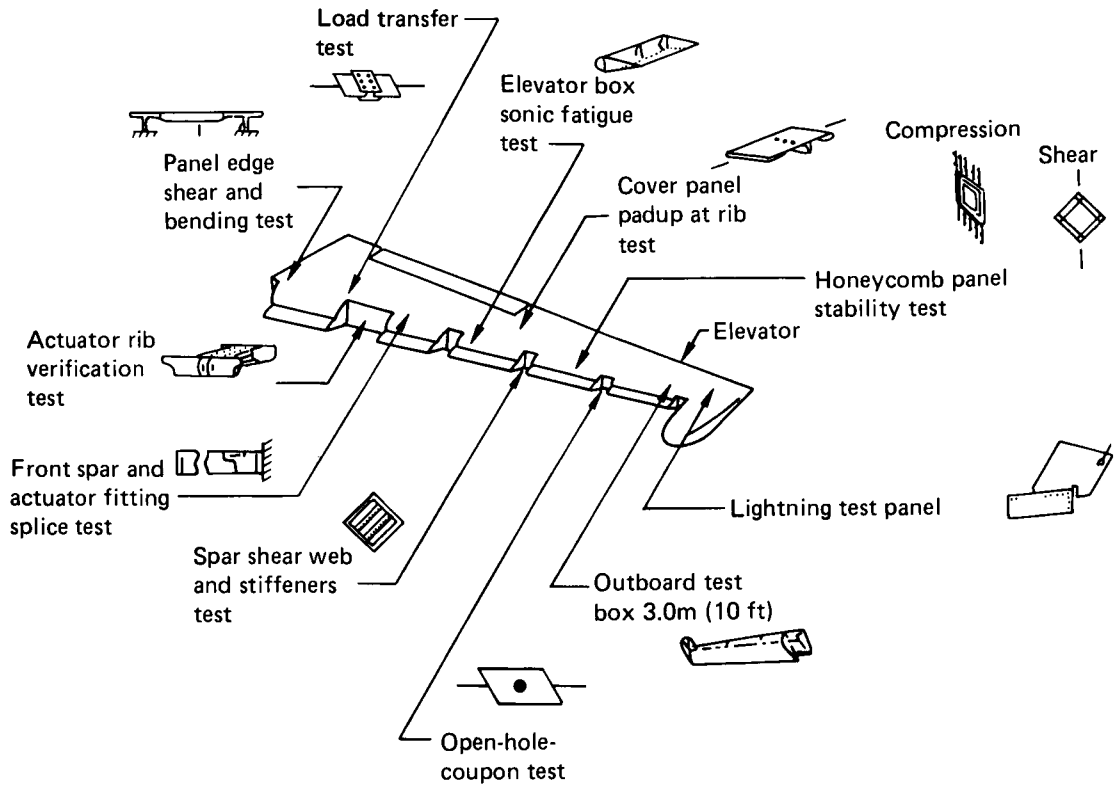


Figure 17. Ancillary Test Program

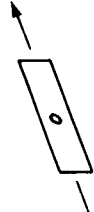
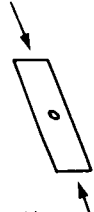
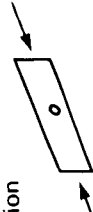

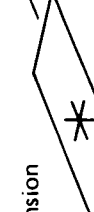

Specimen (drawing number)	Fabric layout	Size, mm (in)	Test condition	Number of specimens			Data	Purpose	Remarks
				RT (-65°F)	-53.9°C (-65°F)	+71°C (160°F)			
 Tension test (65C17702)	±45	381.0 (15.0) x 38.1 (1.5)	Wet Dry	3 9	3 3	3 3	Load/strain	Effect of stress con- centration	Parameters: edge margin hole size layout
		381.0 (15.0) x 38.1 (1.5)	Wet Dry	3 9	3 3	3 3			
 Compression test (65C17702)	±45	381.0 (15.0) x 38.1 (1.5)	Wet Dry	3 9	3 3	3 3	Load/strain	Residual strength	
		381.0 (15.0) x 38.1 (1.5)	Wet Dry	3 9	3 3	3 3			
 Defect compression test (65C17702)	0/90/±45	381.0 (15.0) x 38.1 (1.5)	Wet Dry	3 9	3 3	3 3	Load/strain	Effect of stress con- centration	Parameters: defect size layout
		381.0 (15.0) x 38.1 (1.5)	Wet Dry	3 9	3 3	3 3			
 Inplane shear test (65C17702)	±45	152.4 (6.0) x 76.2 (3.0)	Wet Dry	3 9	3 3	3 3	Load/strain	Residual strength	
		152.4 (6.0) x 76.2 (3.0)	Wet Dry	3 9	3 3	3 3			
 Impact defect-tension test (65C17702)	0/90/±45	381.0 (15.0) x 38.1 (1.5)	Wet Dry	3 12	3 12	3 12	Load/strain	Effect of stress con- centration	Parameters: defect size layout
		381.0 (15.0) x 38.1 (1.5)	Wet Dry	3 12	3 12	3 12			
 Impact defect- compression test (65C17702)	±45	381.0 (15.0) x 38.1 (1.5)	Wet Dry	3 12	3 12	3 12	Load/strain	Residual strength	Parameters: defect size layout
		381.0 (15.0) x 38.1 (1.5)	Wet Dry	3 12	3 12	3 12			

Figure 18. Material Coupon Test Plan (Test 1)


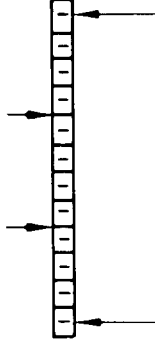
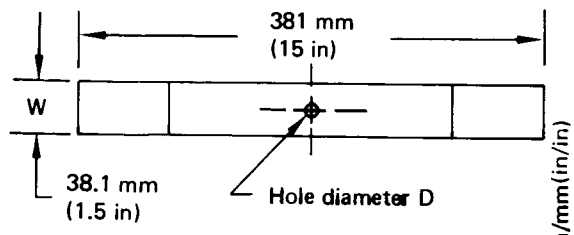
Test program	Specimen (drawing number)	Layup	Size, mm (in)	Test condition	Number of specimens				Data	Purpose
					RT	-59°C (-75°F)	86°C (180°F)	93°C (200°F)		
7313 -16	Tension test (65C19913-3) 	Fabric ±45	381.0 (15.0) x 38.1 (1.5)	Dry	5	5	4	5	Load/strain	Basic material properties
		Fabric 0/90/±45	381.0 (15.0) x 38.1 (1.5)	Dry	5	5	5	5		
	Fabric ±45	381.0 (15.0) x 38.1 (1.5)	Dry	5	5	5	5			
	Fabric 0/90/±45	381.0 (15.0) x 38.1 (1.5)	Dry	5	5	5	4			
7313 -36	Honeycomb sandwich beam (65C17727) 	Tape 0 Fabric ±45	406 (16.0) x 76 (3.0)	Dry	12	-	-	-	Wet	
					-	8	7	-		

Figure 19. Basic Laminate Properties Test Plan (Boeing Funded)



- 12 plies of fabric
- $\pm 45/0/90$ -deg orientation
- Extensional modulus, $E = 4.62 \times 10^4$ MPa
(6.7×10^6 lbf/in²)
- Hole diameter
 - $D_1 = 7.95$ mm (0.313 in), $W/D = 4.8$
 - $D_2 = 2.46$ mm (0.097 in), $W/D = 15.5$
 - $D_3 = 12.7$ mm (0.500 in), $W/D = 3.0$
- Data from NASA test 1, appendix C (ref 1)

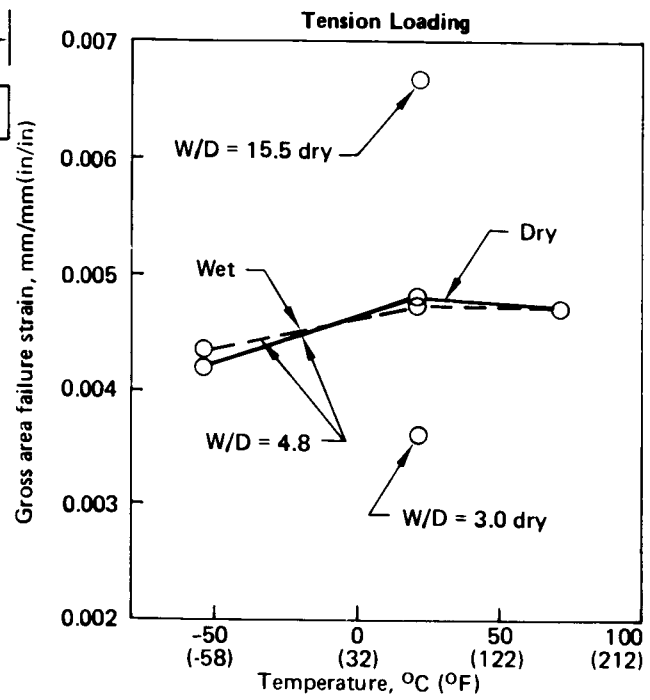


Figure 20. Effect of Moisture, Temperature, and W/D on Tension Strains of $\pm 45/0/90$ -deg Fabric Laminate Coupons

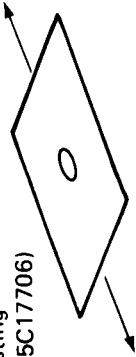
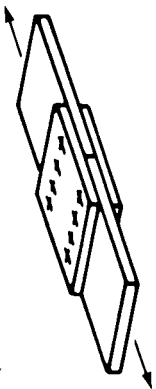
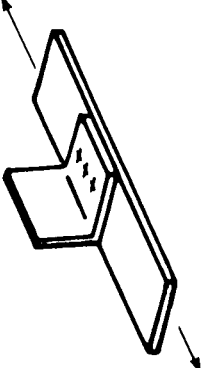
Speciman (drawing number)	Fabric layup	Size mm (in)	Condition	Number of specimens						Data	Purpose	Remarks
				Static		Fatigue R = -1.0						
				RT -53.9°C (-65°F)	+71°C (160°F)	RT	-53.9°C (-65°F)	+71°C (160°F)	RT			
Mechanical joint testing (65C17706) 	0/90/±45	381.0 (15.0) x 38.1 (1.5)	Dry	9	-	9	3	3	3	No load transfer strength and fatigue life	Parameters: Edge margin Hole size	
			Wet	3	-	3	3	3	3			
Mechanical joint testing (65C17702) 	0/90/±45	Varies	Dry	33	3	33	3	3	3	Life and failure load and mode	Parameters: Edge margin Fastener diameter Thickness Defects	
			Wet	15	3	15	3	3	3			
			Dry	6	-	6	-	-	-			-
			Wet	6	-	6	-	-	-			-
Mechanical joint testing (65C17706) 	0/90/±45	381.0 (15.0) x 25.4 (1.0)	Dry CSK	6	-	6	-	-	-	Effect of locally induced load transfer	Parameters: Thickness Defects	
			Dry non-CSK	3	-	3	-	-	-			
			Dry CSK	3	-	3	-	-	-			-
			Dry non-CSK	3	-	3	-	-	-			-

Figure 21. Structural Elements Test Plan (Test 4)

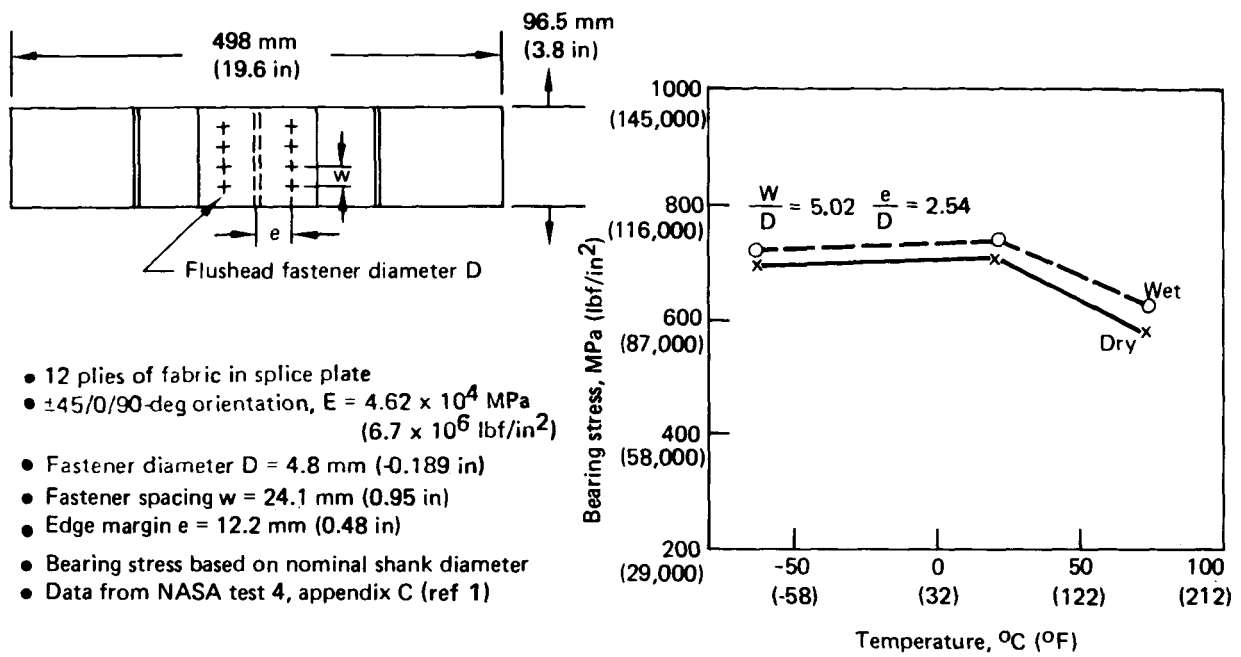


Figure 22. Effect of Moisture and Temperature on Fastener Bearing Stress

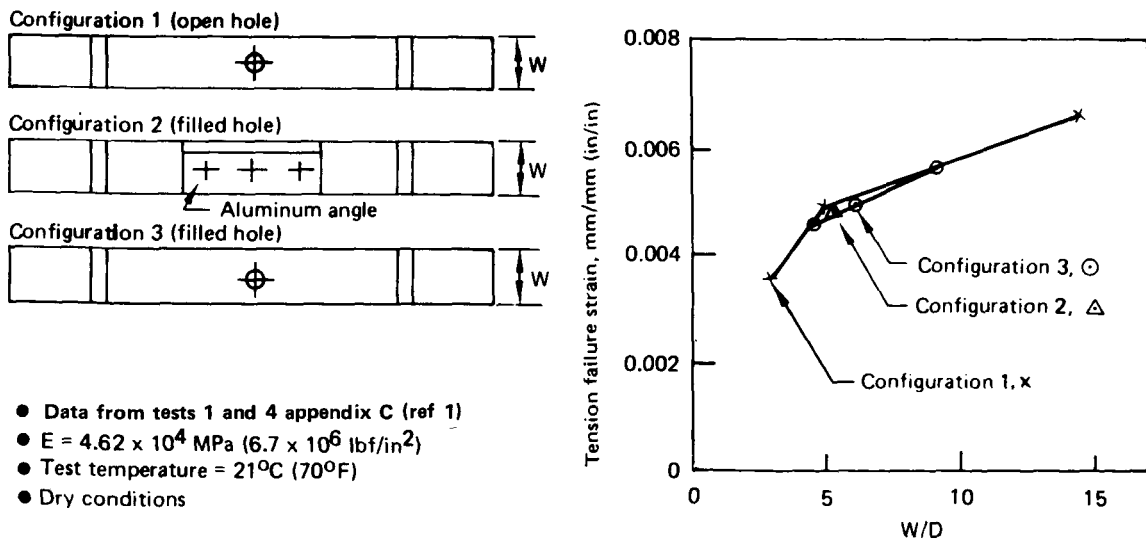


Figure 23. Effect of W/D on Tension Failure Strain Values for Open and Filled Holes

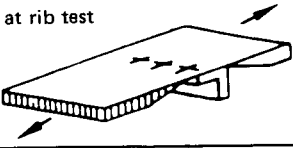
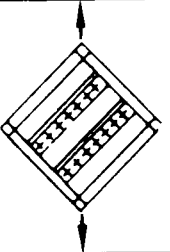
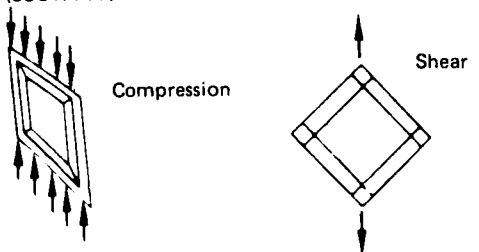

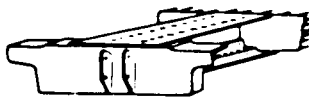
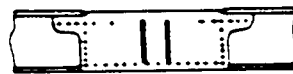
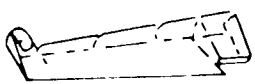
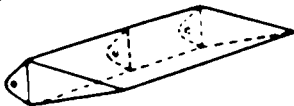





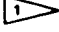
Test No.	Specimen (drawing number)	Layup	Size, mm (in)	Condition	Number of specimens	
					Static	Fatigue
8	Cover panel padup at rib test (65C17708) 	90/±45 2-ply faces honeycomb	63.5 (2.5) x 658.0 (25.9)	RT, dry RT, wet	5 3	5
9	Spar shear web and stiffeners test (65C17711) 	+45	521.0 (20.5) x 521.0 (20.5)	RT, dry	4	—
10	Honeycomb panel stability test (65C17709) 	90/±45 2-ply faces honeycomb	Com- pression 597.0 (23.5) x 610.0 (24.0)	RT, dry RT, wet RT, dry damaged	3 2 2	— — —
			Shear 610.0 (24.0) x 610.0 (24.0)	RT, dry RT, wet RT, dry damaged	3 2 2	— — —
12	Panel edge shear and bending test (65C17710) 	90/+45 2-ply faces honeycomb	254.0 (10.0) x 50.8 (2.0)	RT, dry +load -load	3 3	3 3
14	Actuator rib verification test (65C17712) 	Per drawing	589.3 (23.2) x 203.2 (8.0)	RT, dry	1	
11	Front spar/actuator fitting splice test (65C17704) 	Per drawing	914.4 (36.0) x 203.2 (8.0)	RT, dry 71°C wet (160°F)	1 1	1
17	Elevator outboard sections (65C17707) 	Per drawing	2 997.2 (118.0) x 762.0 (30.0)	RT, dry	1	—
15	Elevator box sonic fatigue test (65C17705) 	Per drawing	1676.4 (66.0) x 711.2 (28.0)	RT, dry	—	2

Figure 24. Elevator Subcomponent Test Plan

Test No.	Results	Requirements
8	Average static tension, RT dry, 0.00687 mm/mm (in/in) Fatigue specimens, 500 000 cycles at $\pm 1112\text{N}$ (± 250 lbf), no damage	Ultimate tension strain, 0.00283 mm/mm (in/in) 
9	Average shear flow, 164 N/mm (937 lbf/in)	Ultimate shear flow, 46.9 N/mm (267.7 lbf/in) 
10	Average minimum at RT wet condition, 51.8 N/mm (296 lbf/in)	Ultimate end load, 23.5 N/mm (134 lbf/in) 
	Average minimum principal shear strain at RT wet condition, 0.008084 mm/mm (in/in)	Ultimate principal shear strain, 0.005774 mm/mm (in/in) 
12	Average minimum, 9.88 N/mm (56.4 lbf/in) Fatigue specimens, 500 000 cycles at $\pm 44.5\text{N}$ (± 10 lbf), no damage	Air pressure shear load, 4.5 N/mm (25.7 lbf/in)
14	Ultimate rib chord strain, 0.00431 mm/mm (in/in)	Ultimate rib chord strain, 0.00316 mm/mm (in/in) 
11	Ultimate load: RT dry, 10.68 kN (2400 lbf) 71°C (160°F) wet 11.03 kN (2480 lbf) Residual strength, 759 kN (1706 lbf) after four lifetimes of repeated loads and with major cuts in the spar chord	Ultimate load, 7.65 kN (1720 lbf)  One lifetime, 225 000 cycles
17	Tested to 135% design ultimate load with no failure	Design ultimate load
15	Sonic tested to two equivalent lifetimes of service; tested to an additional equivalent lifetime with visible impact damage, no damage growth	One equivalent service lifetime

 Requirements from finite element analysis model

Figure 24. Elevator Subcomponent Test Plan (Concluded)

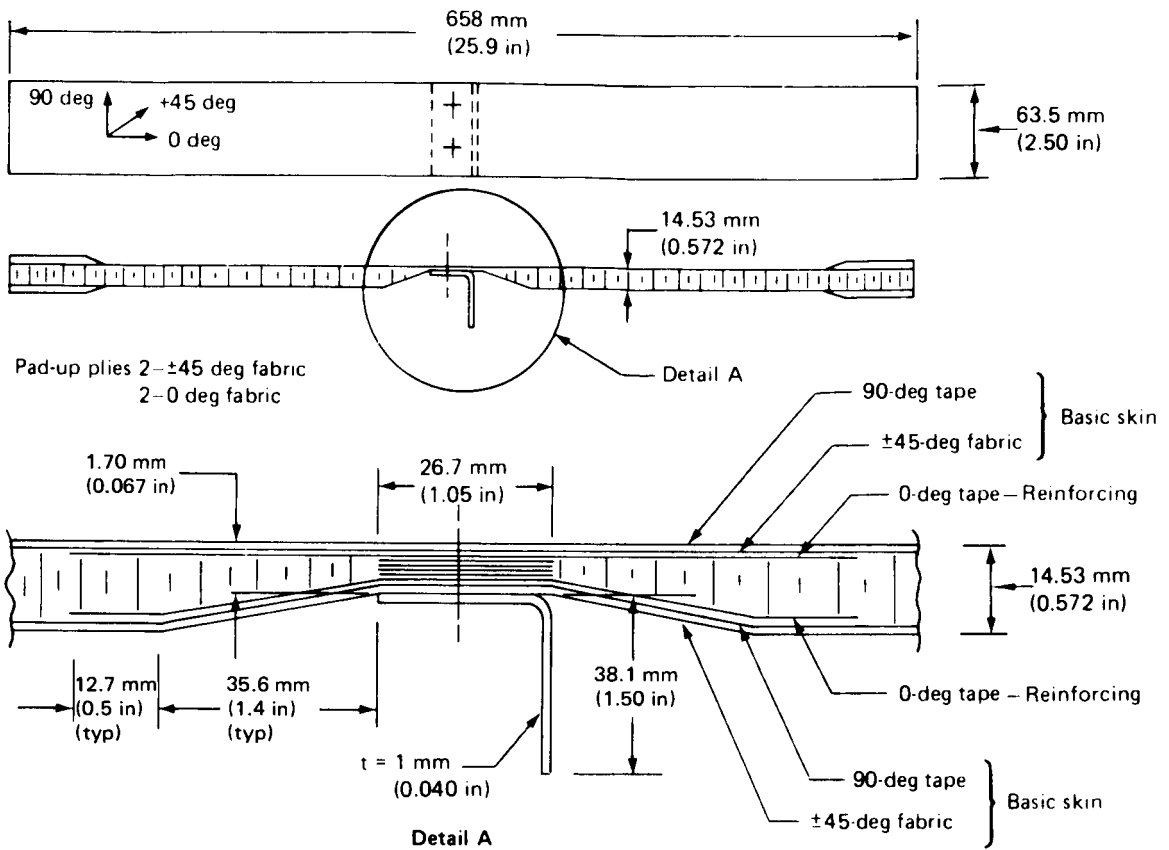


Figure 25. Cover Panel Padup Specimen Geometry (Test 8)

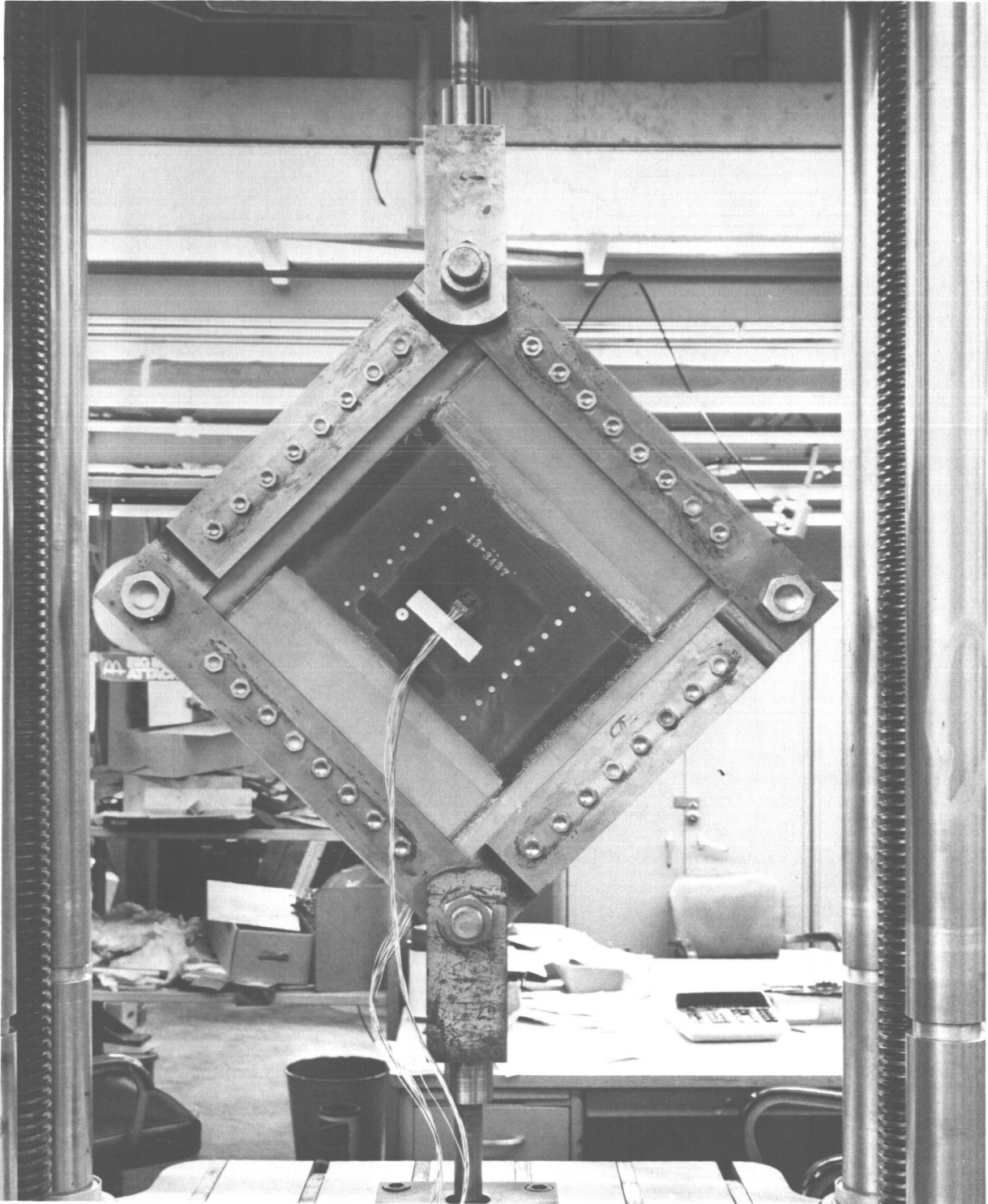


Figure 26. Spar Web Shear Test Setup (Test 9)

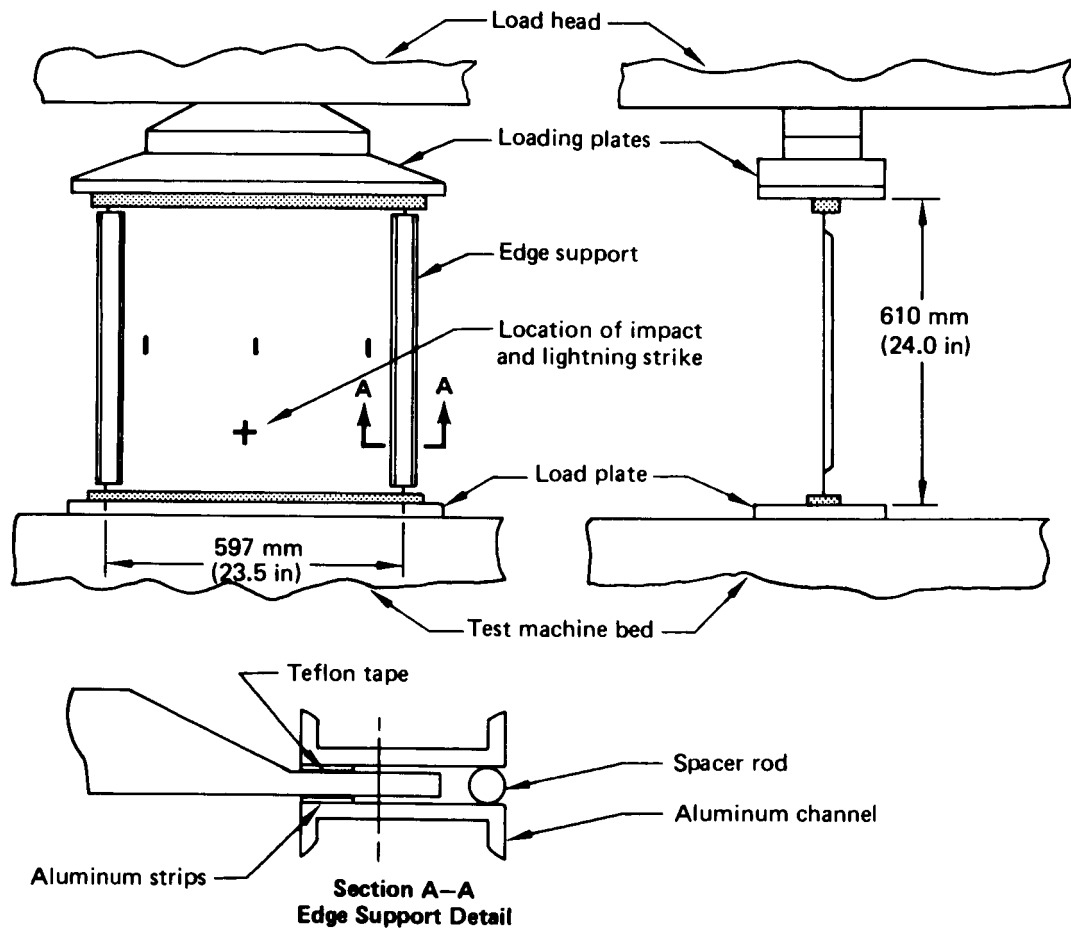


Figure 27. Honeycomb Skin Compression Panel Stability Test Setup (Test 10)

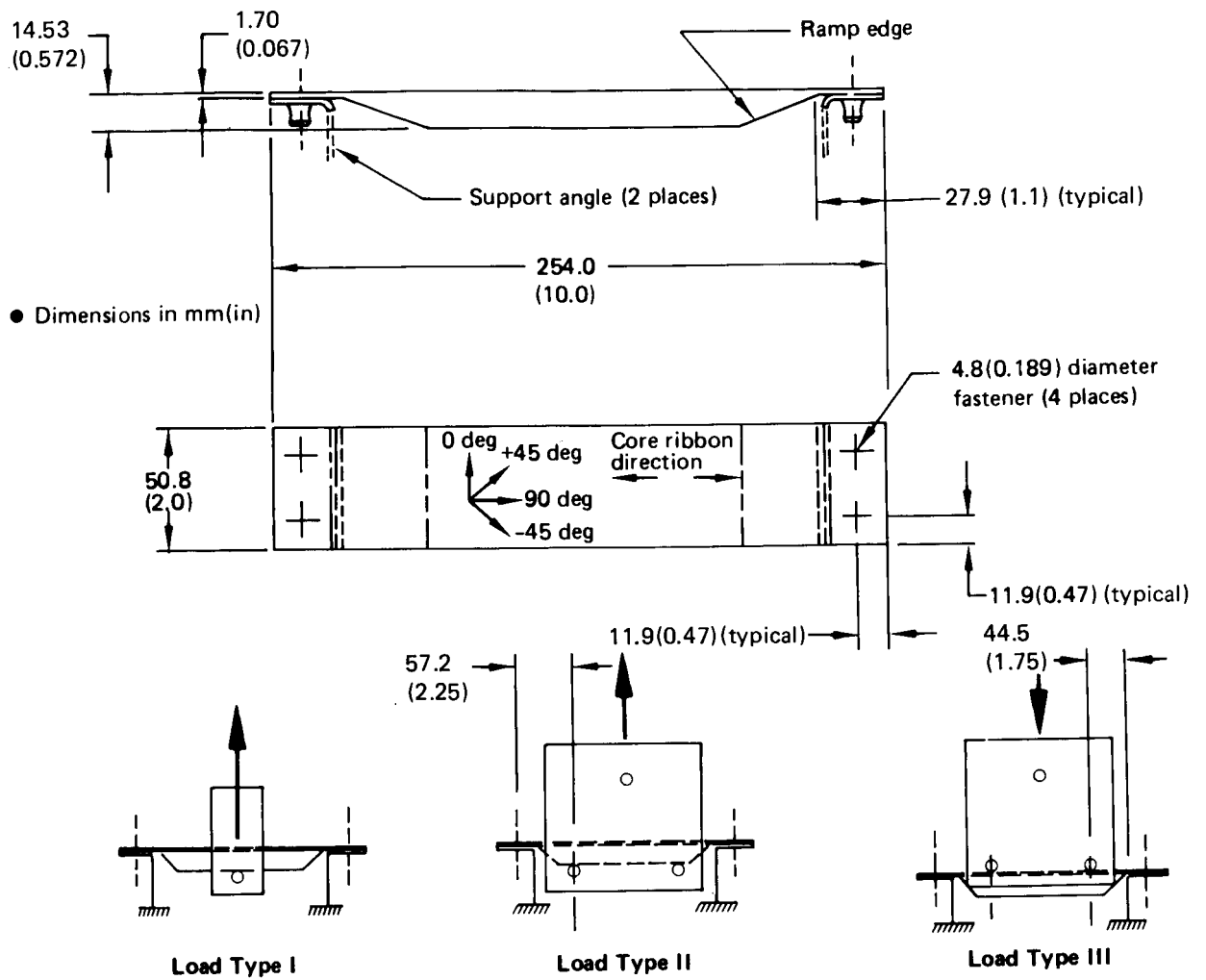


Figure 29. Panel Edge Shear and Bending Test Specimen Geometry (Test 12)

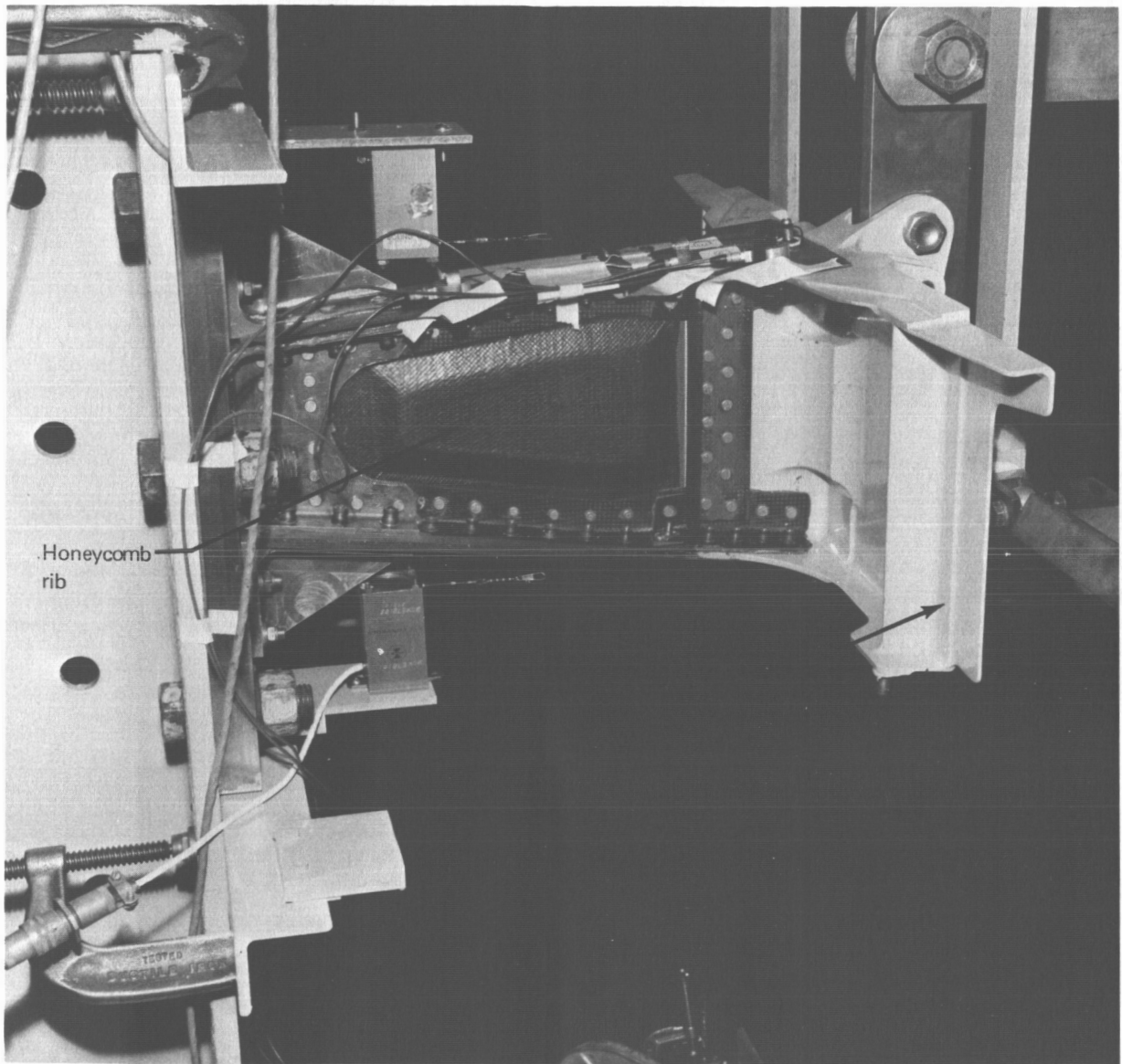


Figure 30. Actuator Support Rib Test (Test 14)

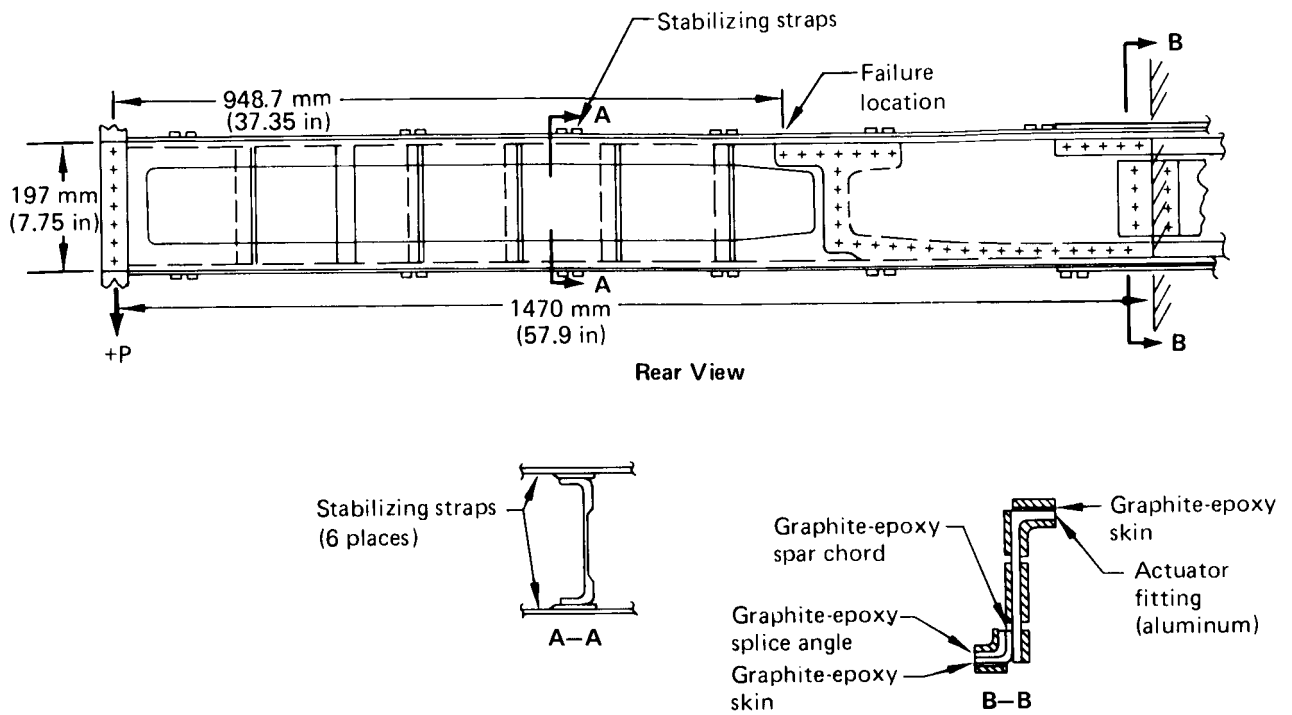


Figure 31. Front-Spar Actuator Fitting Splice Test Schematic (Test 11)

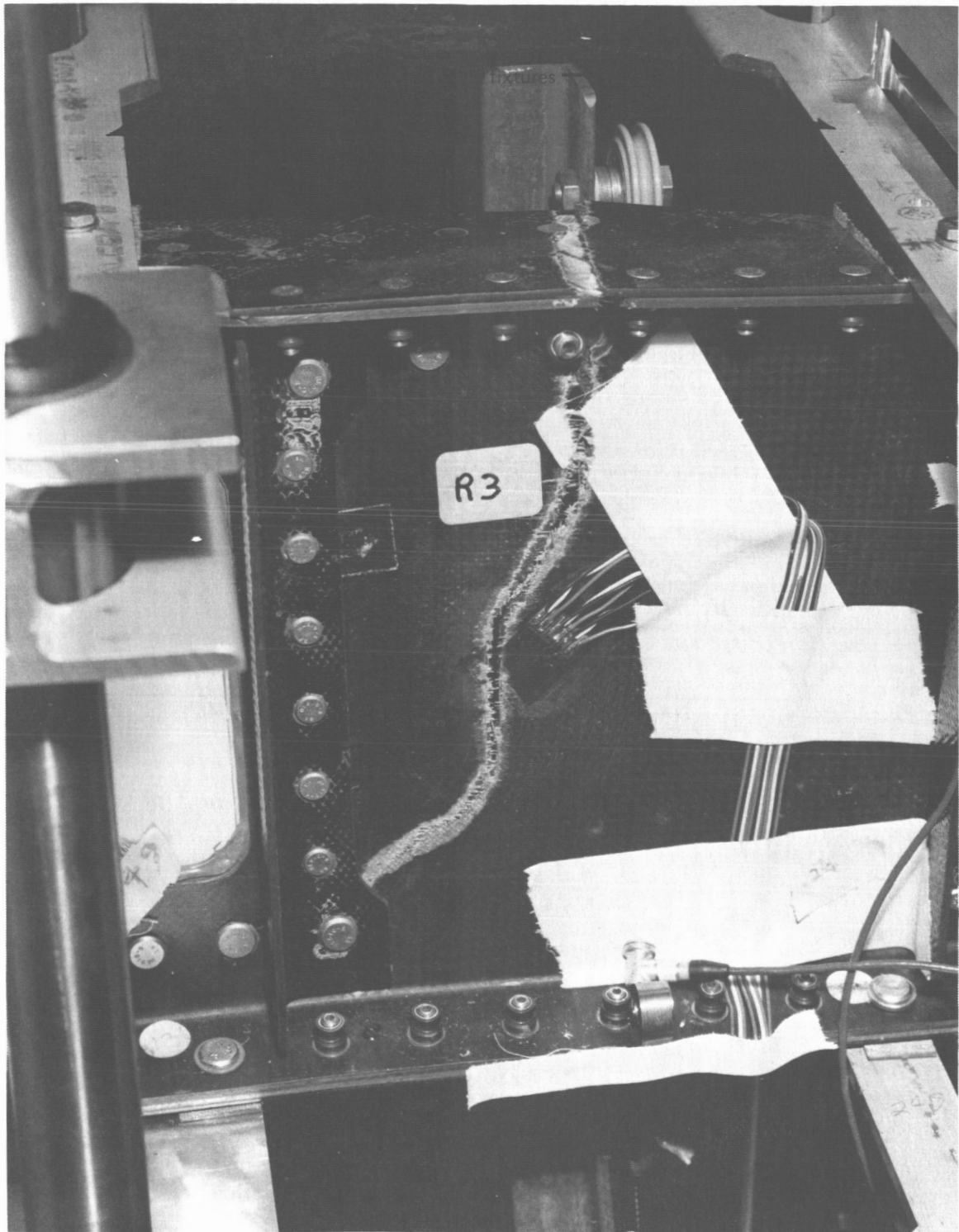


Figure 32. Front-Spar Actuator Fitting Splice Test Specimen Failure

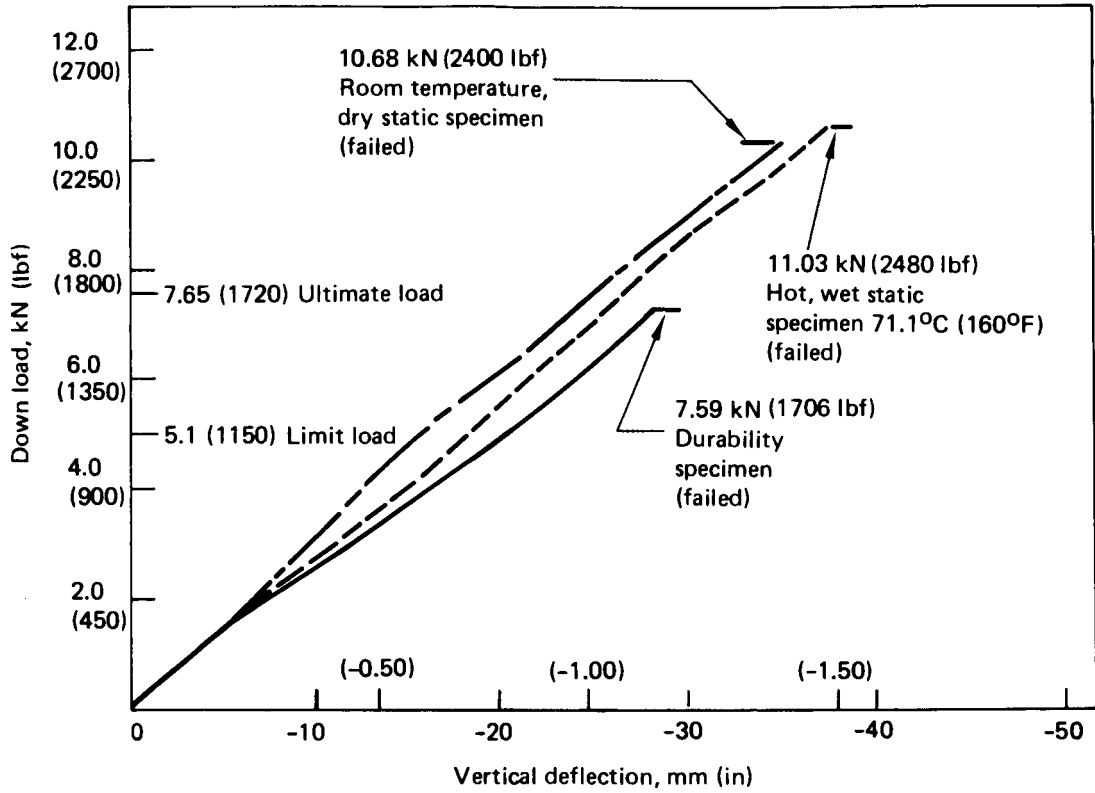


Figure 33. Front-Spar Actuator Fitting Specimen, Measured Vertical Deflections

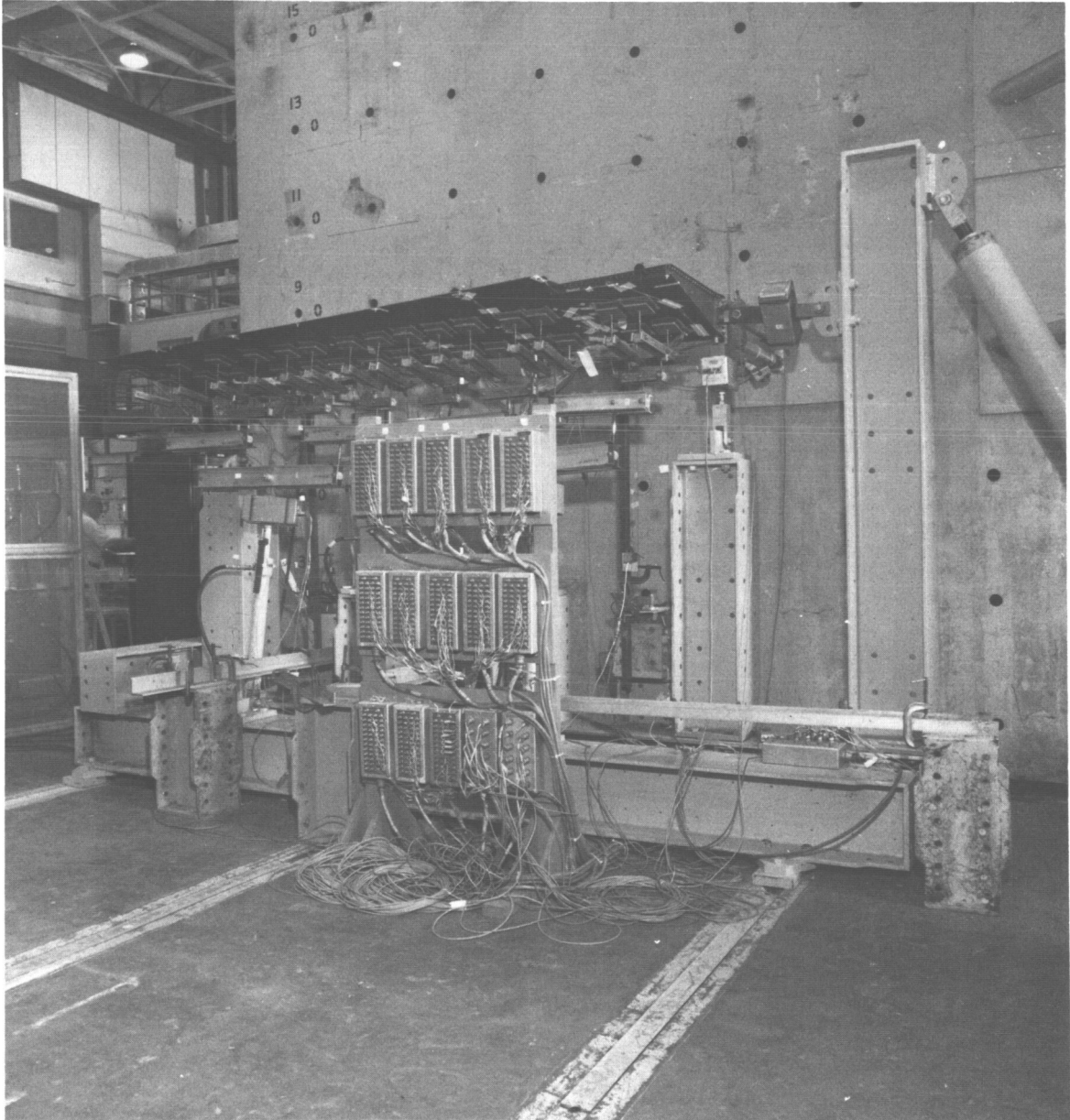


Figure 34. Elevator Outboard Box Test Setup (Test 17)

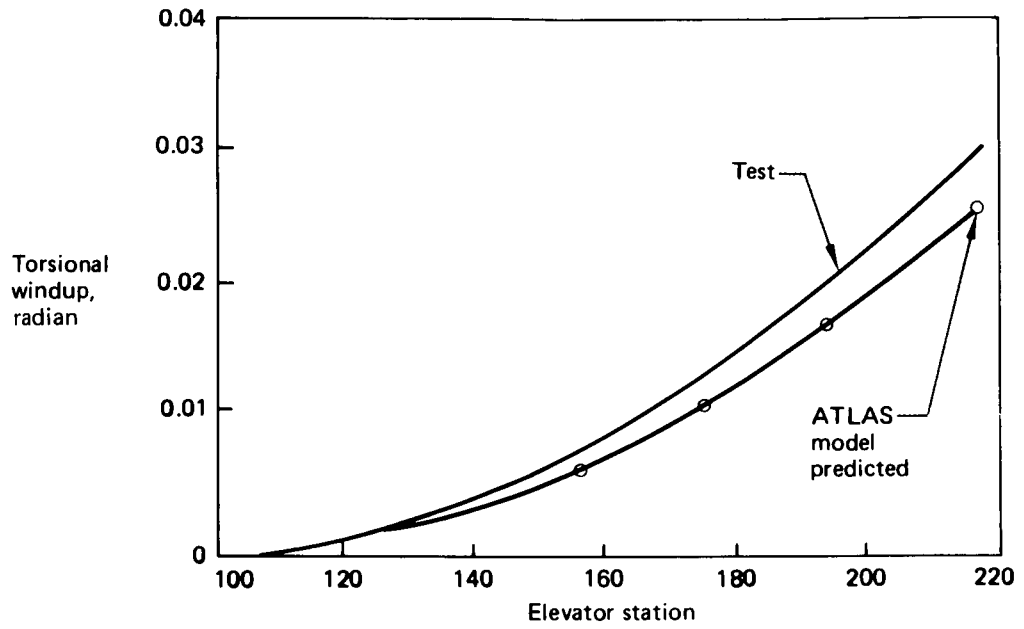


Figure 35. Elevator Outboard Box Section Test—Torsion Windup Test and Prediction Comparison

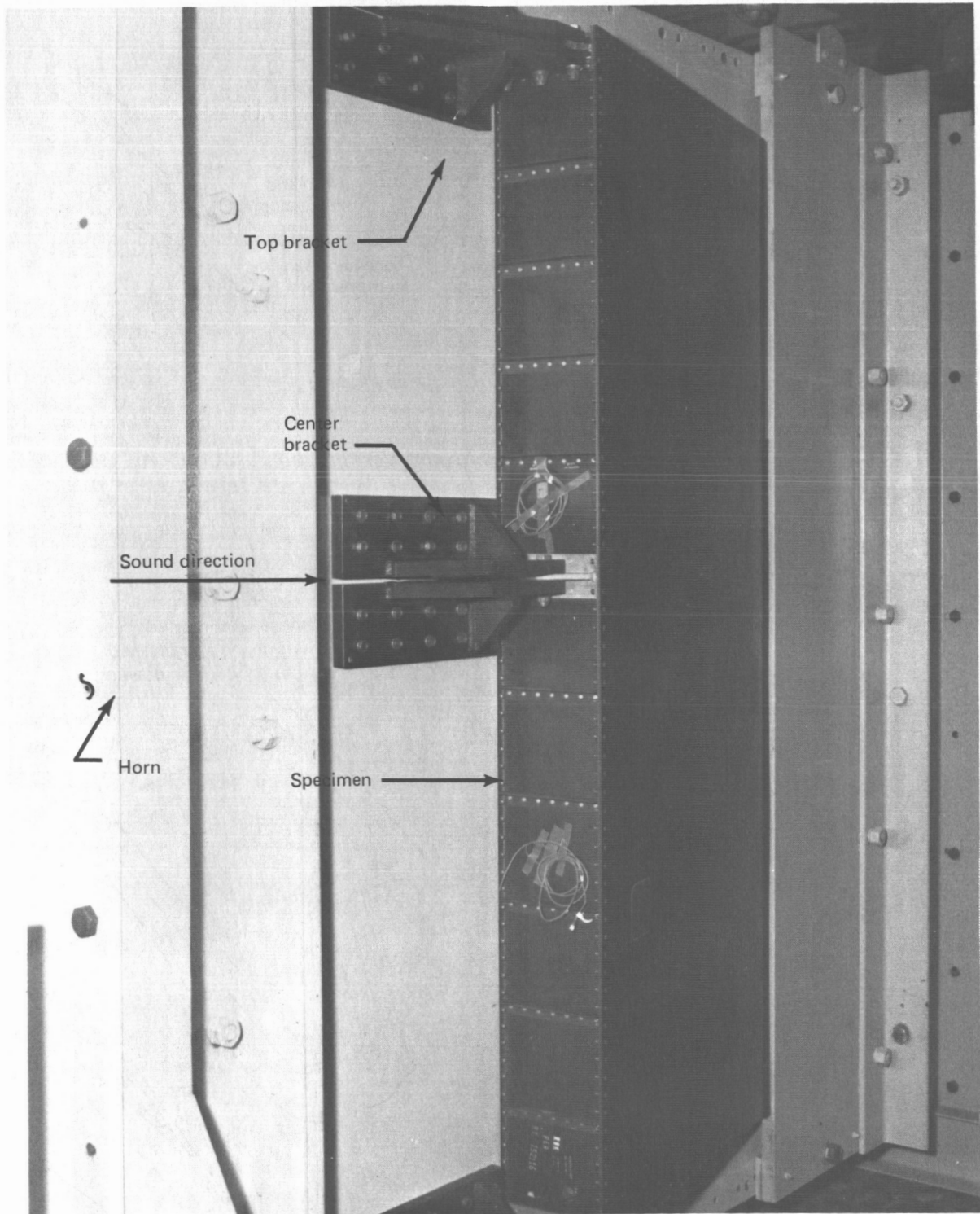
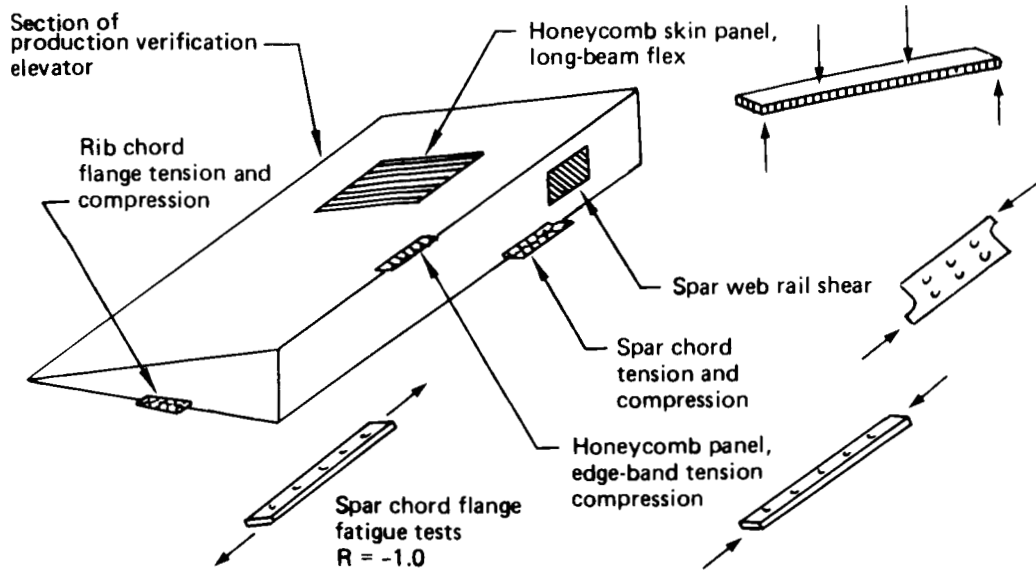


Figure 36. Elevator-Box Sonic Test Setup (Test 15)



- Specimens taken from parts fabricated on production tools
- All tests conducted at room temperature

Figure 37. Production Hardware Verification Test Coupons

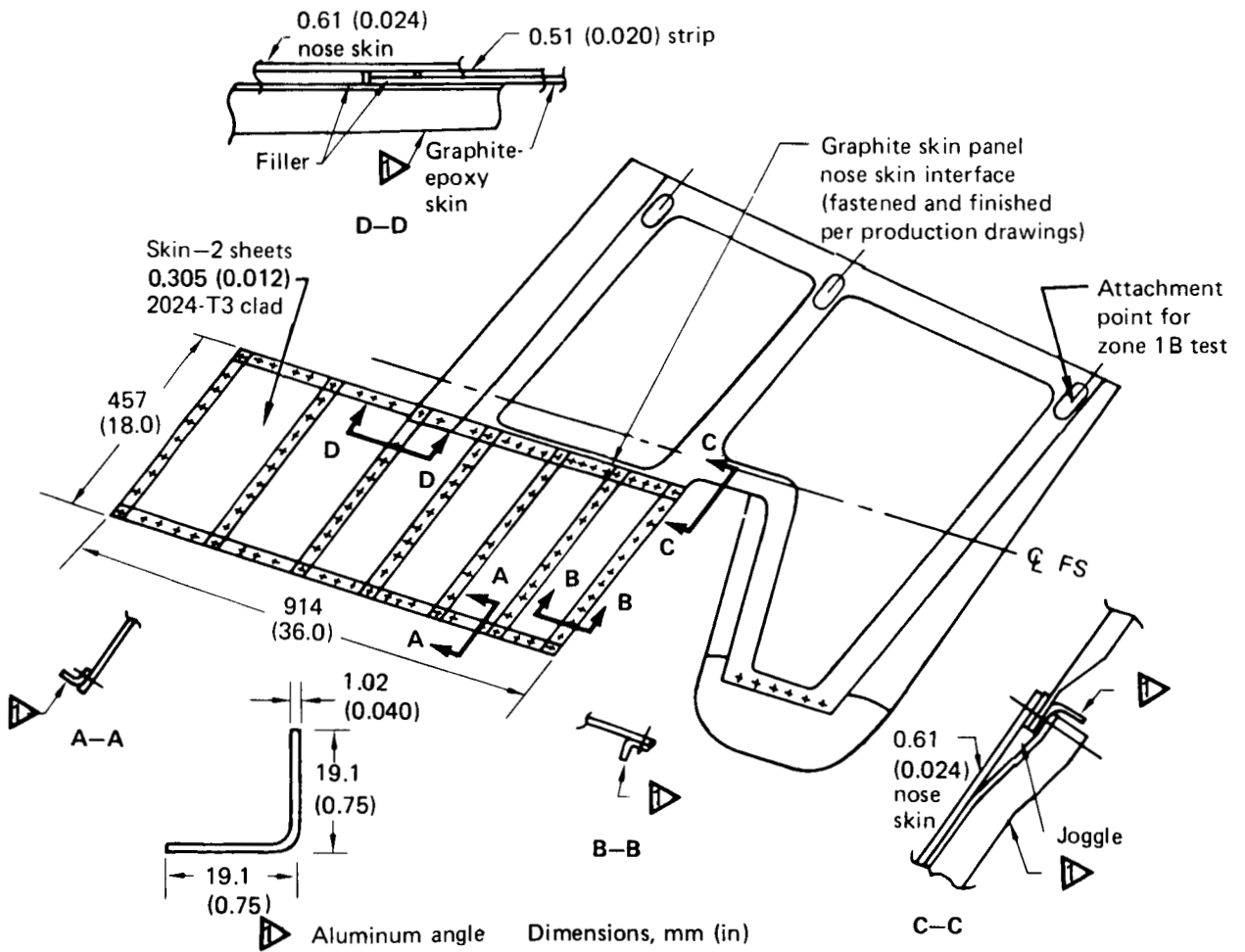
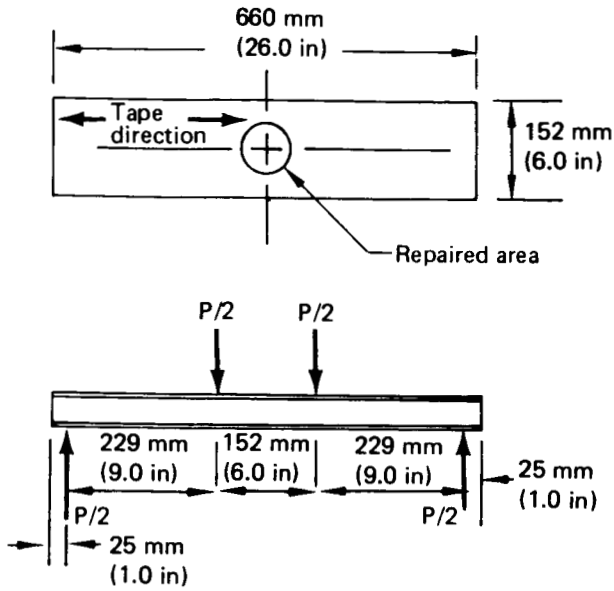


Figure 38. Graphite-Epoxy Elevator Lightning Test Article



- Face sheets: 1-ply fabric ± 45 -deg
1-ply tape 0-deg
- Nomex honeycomb core is 14mm (0.55 in) thick
- Data from (ref 1)

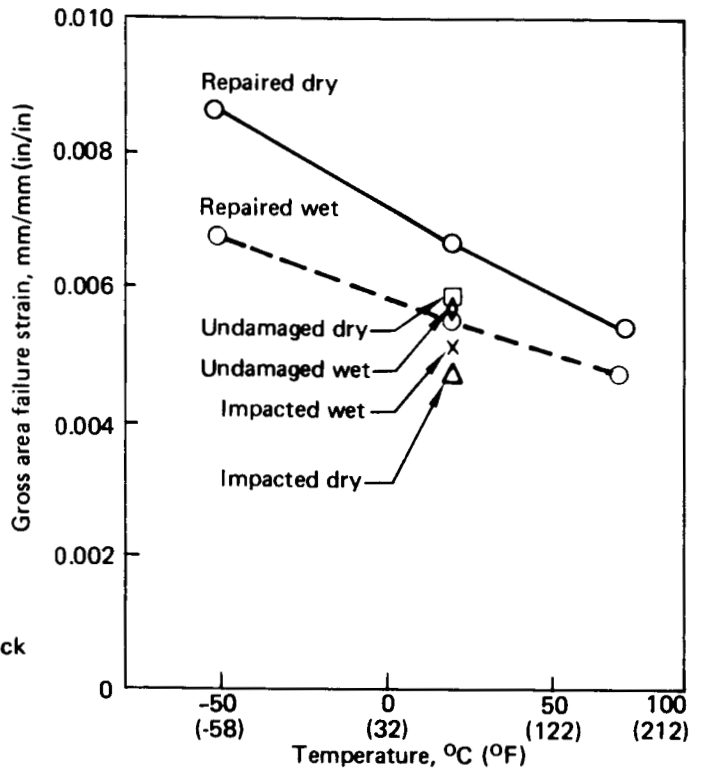
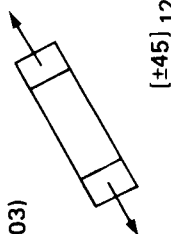

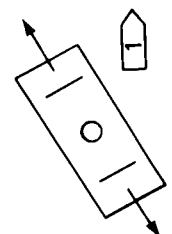

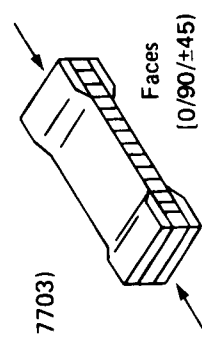

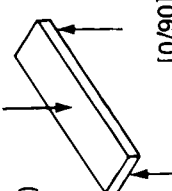





Figure 39. Honeycomb Repair Test Results

Specimen configuration 0.18-mm (7-mil) fabric (drawing number)	Size, mm (in)	Exposure conditions	Exposure time (months and hours)				Type of test after exposure (test at room temperature)	Exposure conditions	
			0	12	24	36			
			0	8760	17520	26280			
(65C17703)  [±45] 12	304.8 (12.00) x 25.4 (1.00)	I	6	6	6	6	Static tension	I Laboratory shelf exposure	
		II 	6	6	6	6		II Outdoor rack exposure strained during exposure	
		IV		5	5	6		IV Environmental chamber temperature, humidity, and pressure cycling, strained during exposure	
		V						V Humidity chamber exposure, strained during exposure	
(65C17703)  [0/90/±45] 3S	304.8 (12.00) x 50.8 (2.00)	I	6	6	6	6	Fatigue test to failure R = -1.0		
		II 		6	6	6		6	
		IV		6	6	6		6	
(65C17703)  [0/90/±45]	304.8 (12.00) x 25.4 (1.00)	I	5	5	5	5	Static compression		
		II 		5	5	5		5	
		IV		5	5	5		5	
		V		5	5	5		5	
(65C17703)  [0/90] 12	15.2 (0.60) x 6.35 (0.25)	I	6	6	6	6	Static interlaminar shear test		
		II 		6	6	6		6	
		IV		6	6	6		6	
		V		5	5	5		5	

 Three of each series of six specimens will be initially fatigue cycled to equivalent flight cycles corresponding to scheduled calendar time of exposure

 One side painted (all other honeycomb specimens unpainted)


 Both sides painted (no ultraviolet exposure of unpainted specimens)

Figure 40. Environmental Test Plan

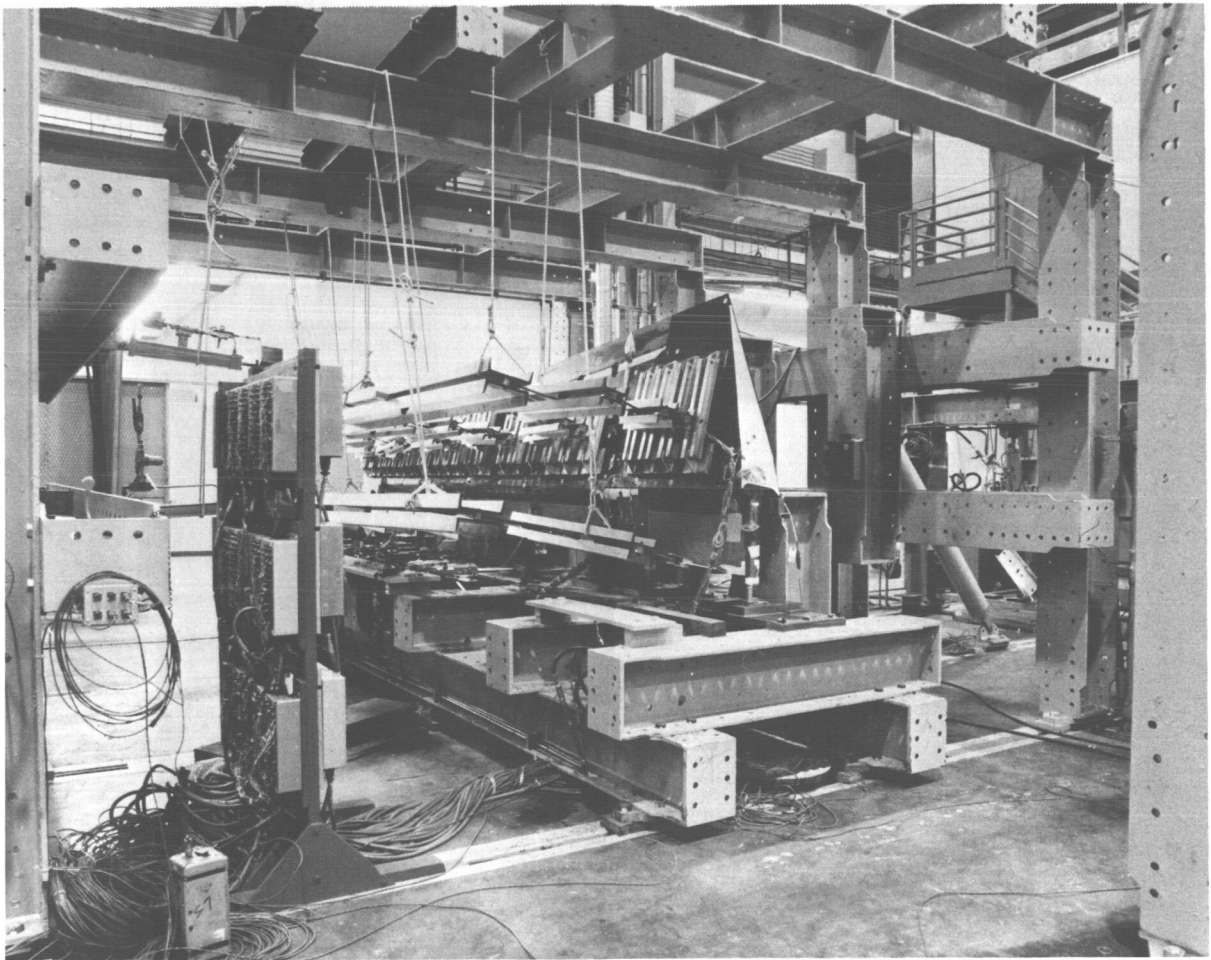


Figure 41. Elevator Ground Test Setup

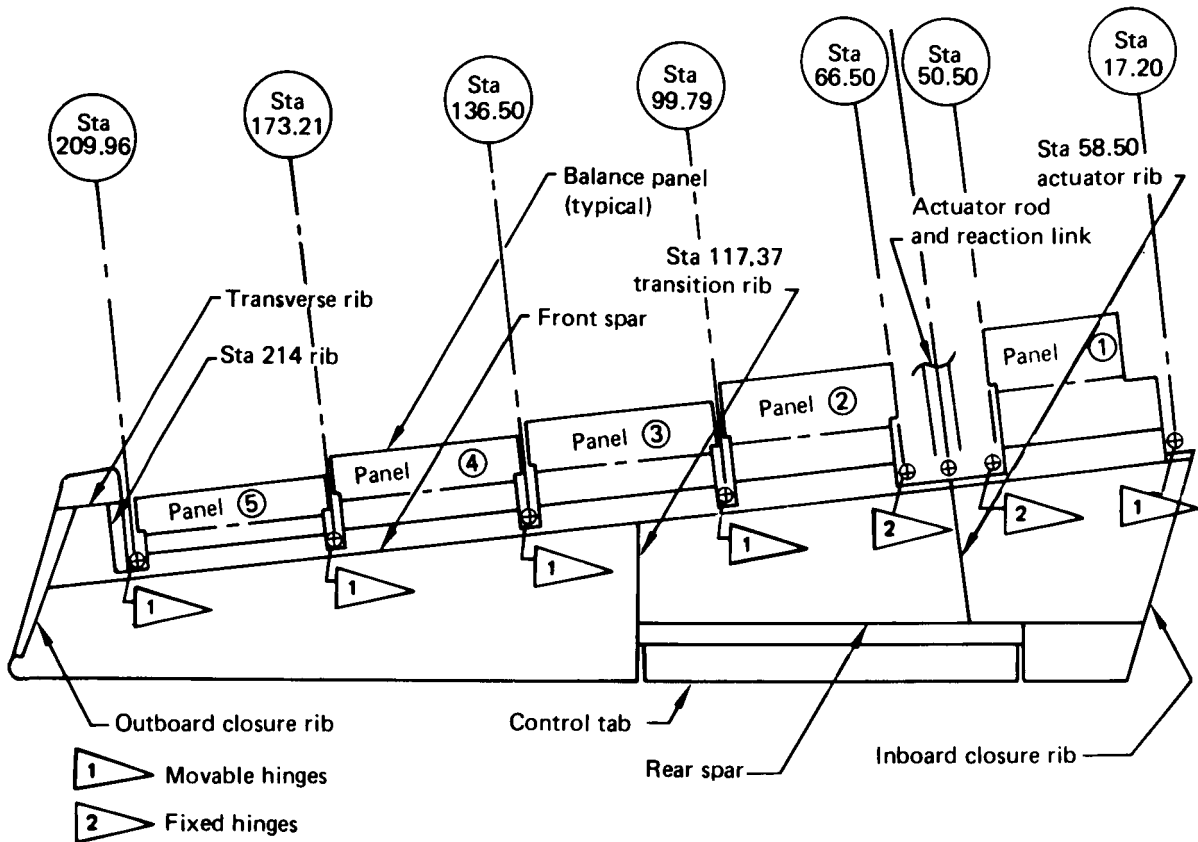


Figure 42. 727 Composite Test Elevator Hinge Locations

Load Case 128 Ultimate (see Table 2)

Legend:

- ↙ Rosette strain gage location
- ε Maximum principal axial strain
- γ Maximum principal shear strain
- Upper number is measured test value
- () Number is predicted value

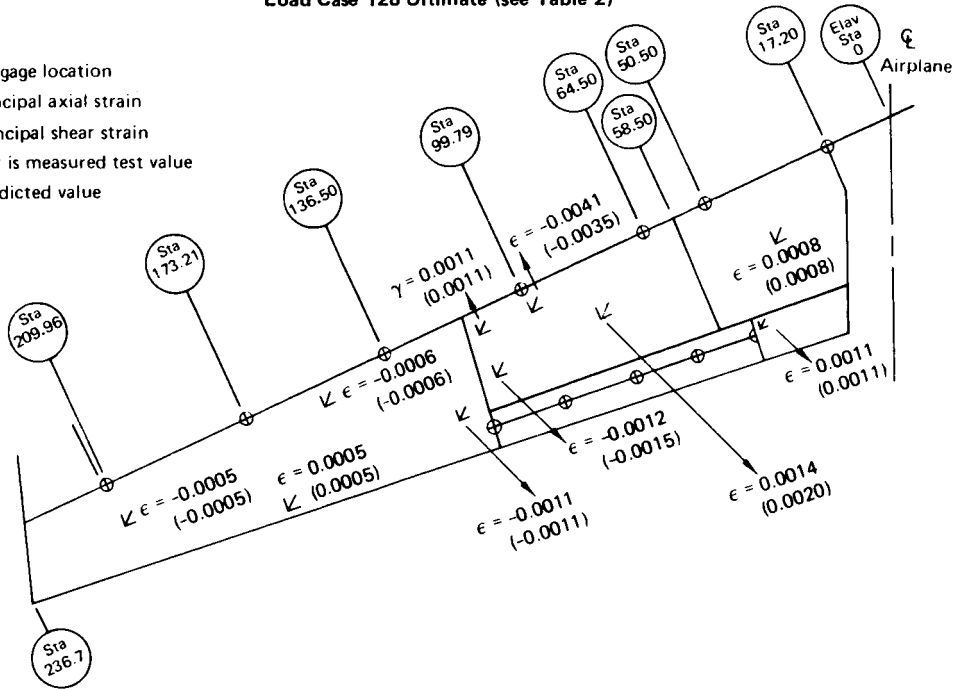


Figure 43. Lower Skin Panel Outer Face Strain Comparisons—Predicted Versus Test

Load Case 128 Ultimate (see Table 2)

Legend:

- ↙ Rosette strain gage location
- Axial strain gage location
- ε Maximum principal axial strain
- γ Maximum principal shear strain
- Upper number is measured test value
- () Number is predicted value

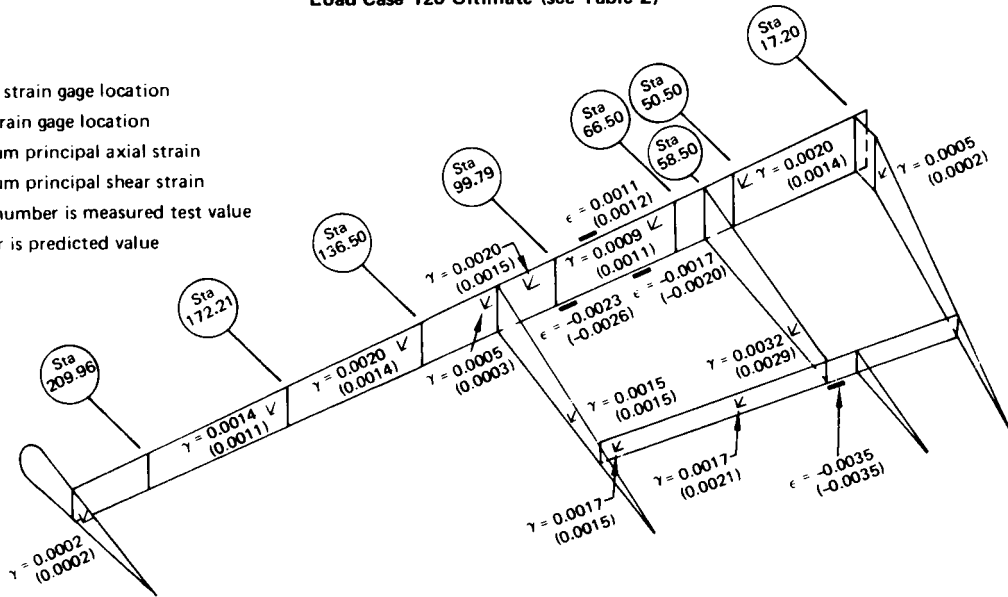


Figure 44. Spar and Rib Strain Comparisons—Predicted Versus Test

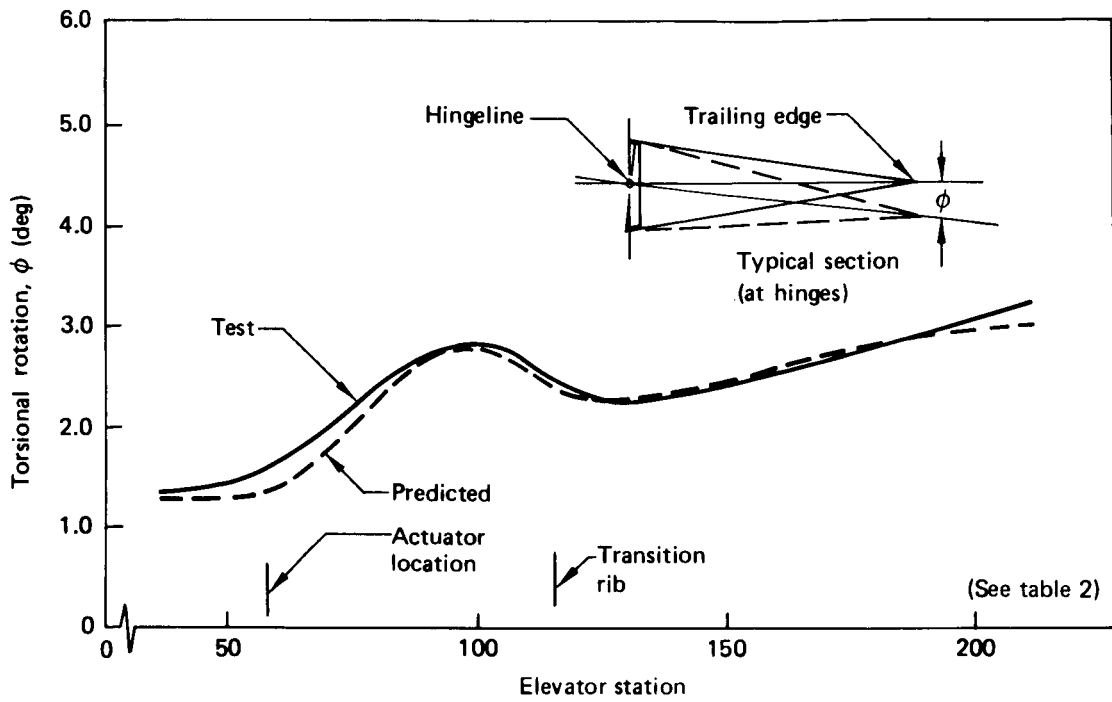
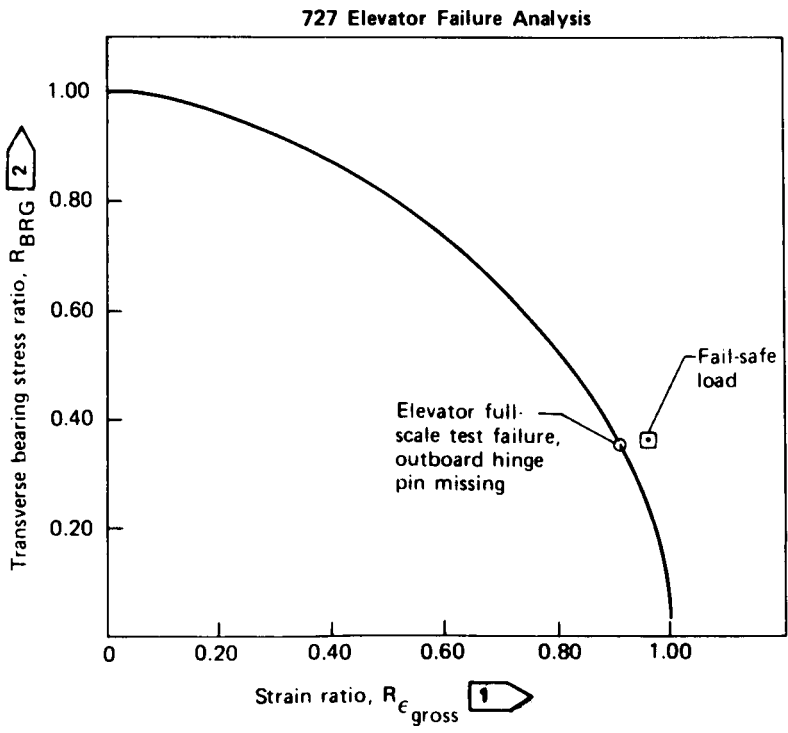


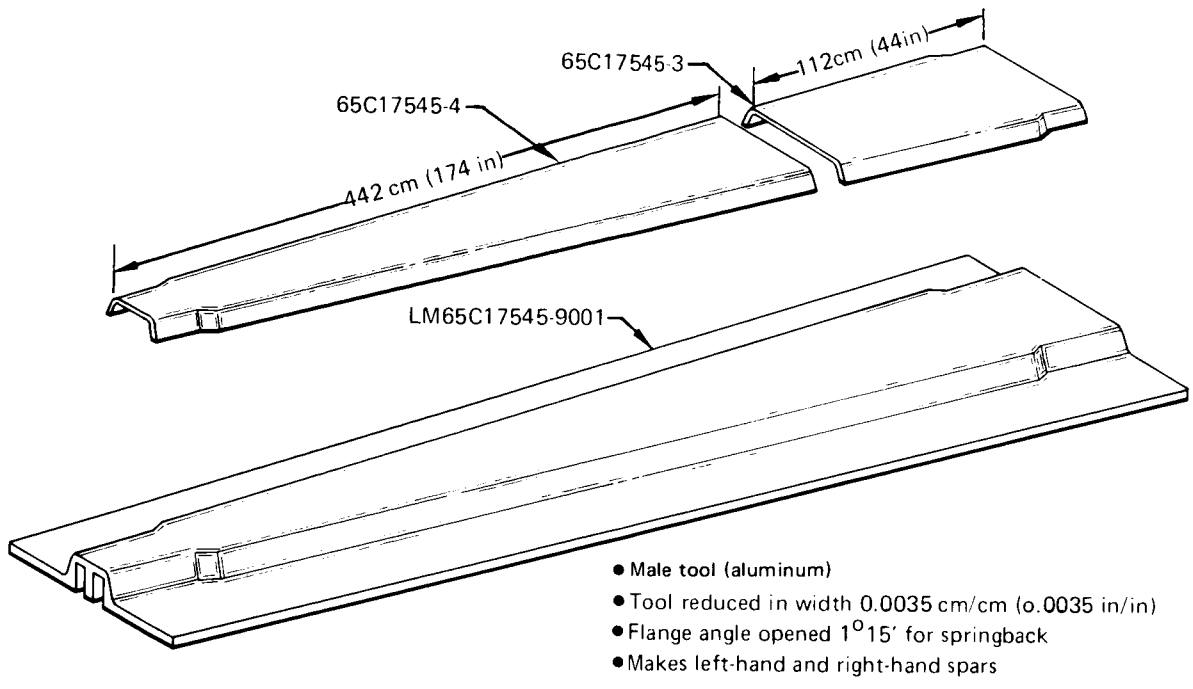
Figure 45. Elevator Rotation Comparison for Load Case 128



1 $R_{\epsilon_{gross}}$ of 1.00 based on $\epsilon_{gross} = 0.0046$ mm/mm, (in/in), from room temperature, dry test specimens (fig. 23)

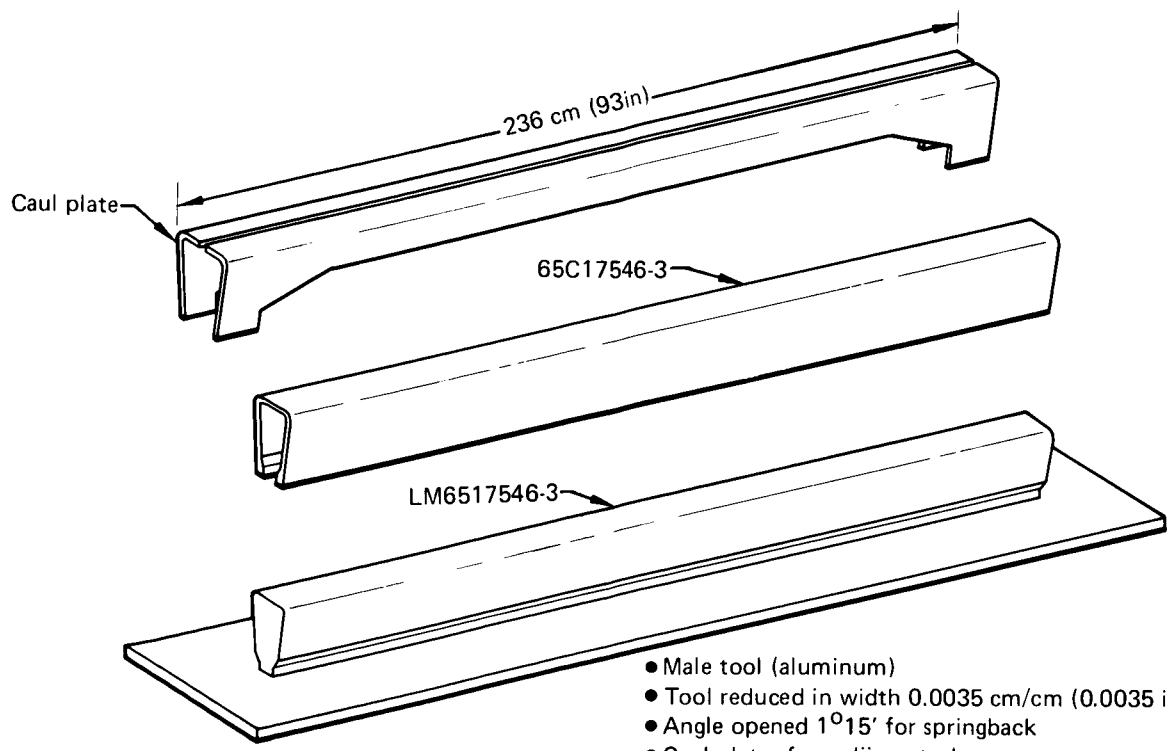
2 R_{BRG} of 1.00 based on $f_{BRG} = 709$ MPa (102 800 lbf/in²) from room temperature, dry test specimens (fig. 22)

Figure 46. Interaction Curve Bearing Stress Versus Tension Bypass Strain



- Male tool (aluminum)
- Tool reduced in width 0.0035 cm/cm (0.0035 in/in)
- Flange angle opened 1°15' for springback
- Makes left-hand and right-hand spars

Figure 47. Front Spar and Layup Mandrel



- Male tool (aluminum)
- Tool reduced in width 0.0035 cm/cm (0.0035 in/in)
- Angle opened 1°15' for springback
- Caul plates for radii control
- Makes left-hand and right-hand spars

Figure 48. Rear Spar and Layup Mandrel

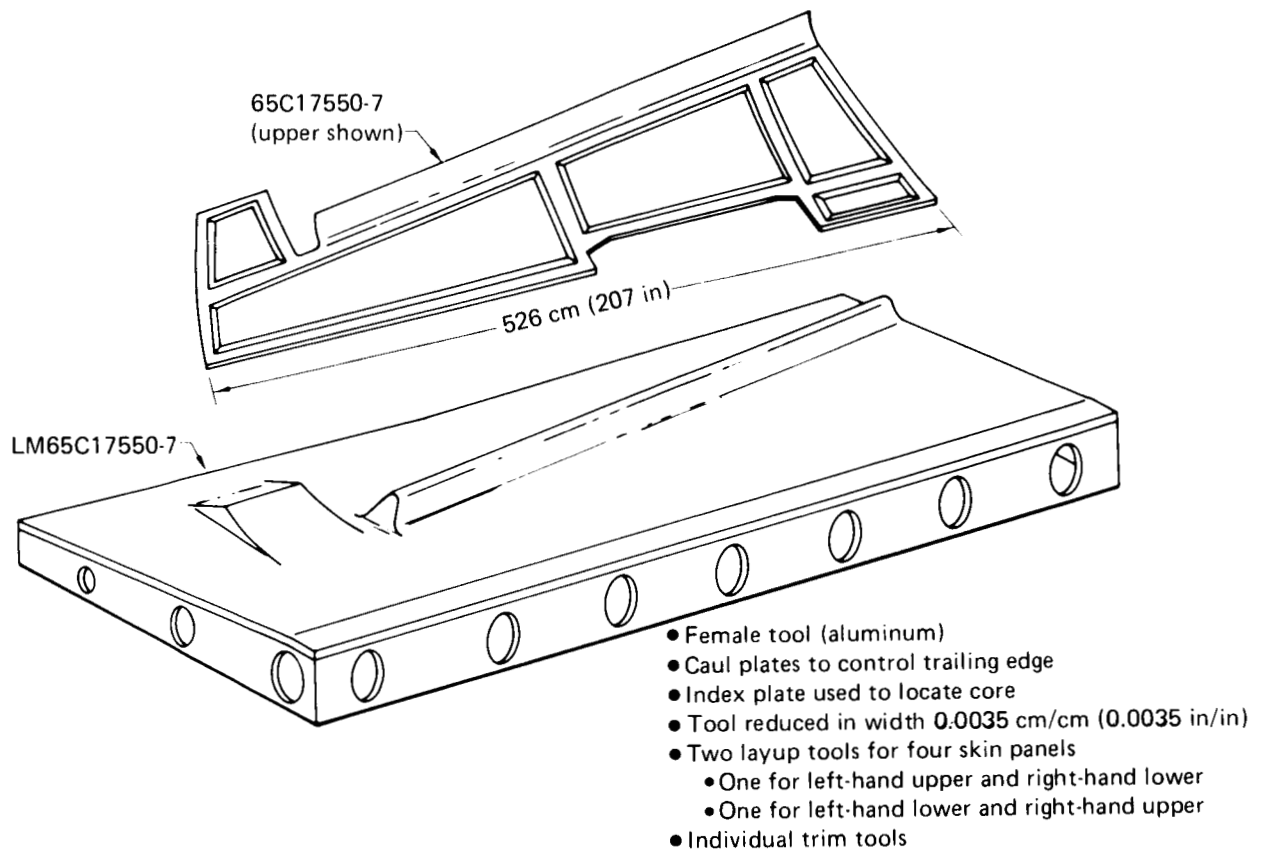


Figure 49. Skin Panel and Layup Mandrel

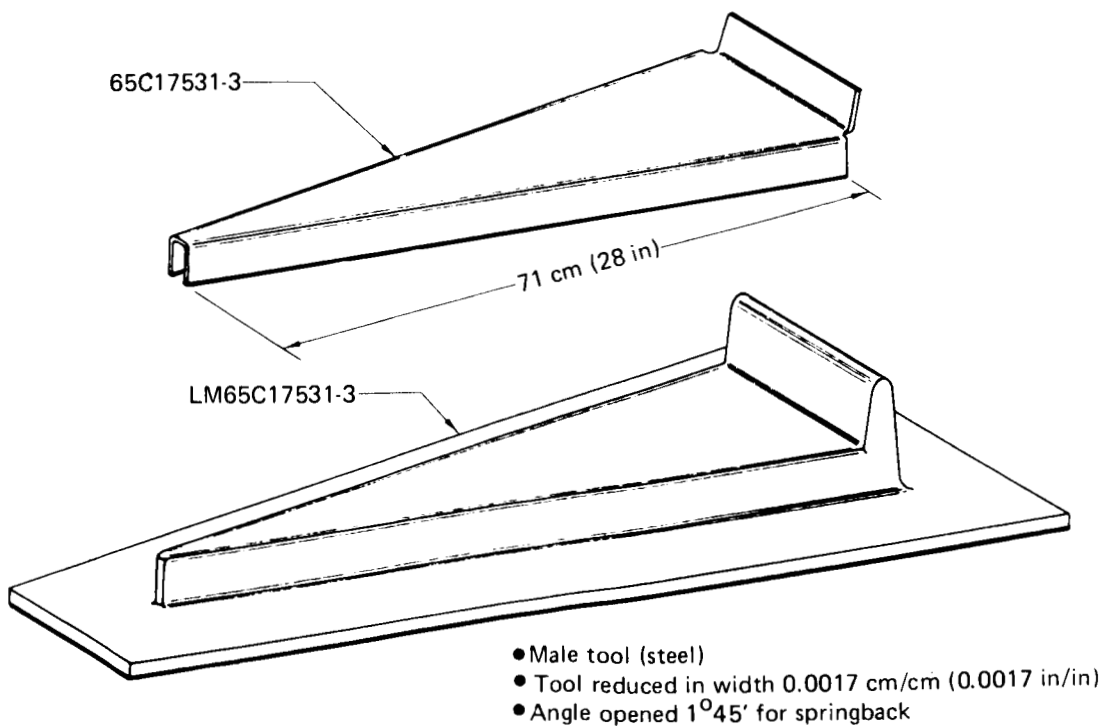


Figure 50. Rib-Station 117.37 and Layup Mandrel

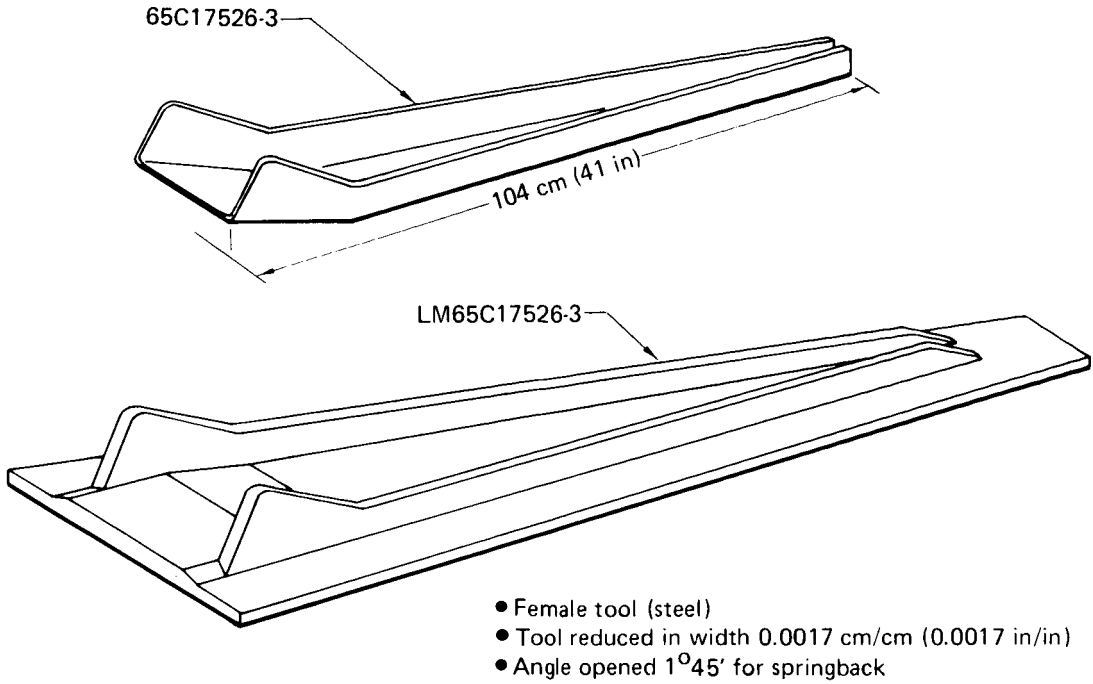


Figure 51. Inboard Closure Rib and Layup Mandrel

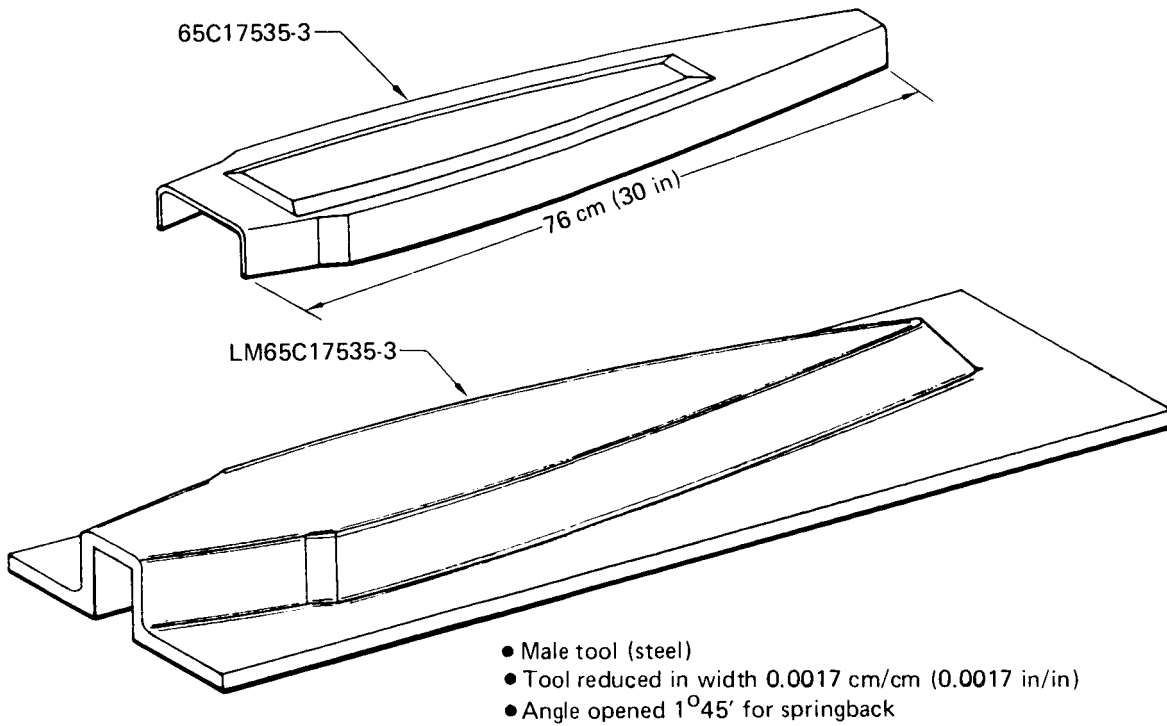


Figure 52. Outboard Closure Rib and Layup Mandrel

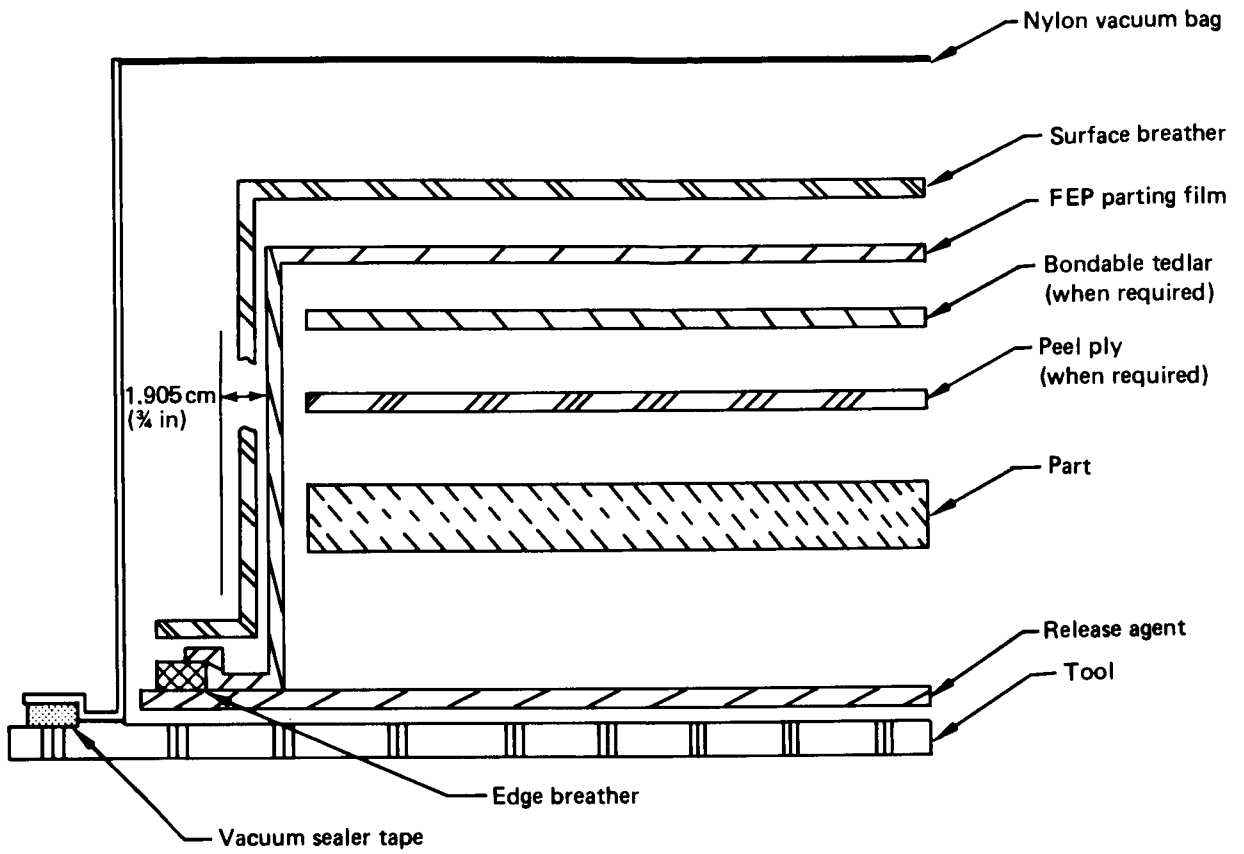
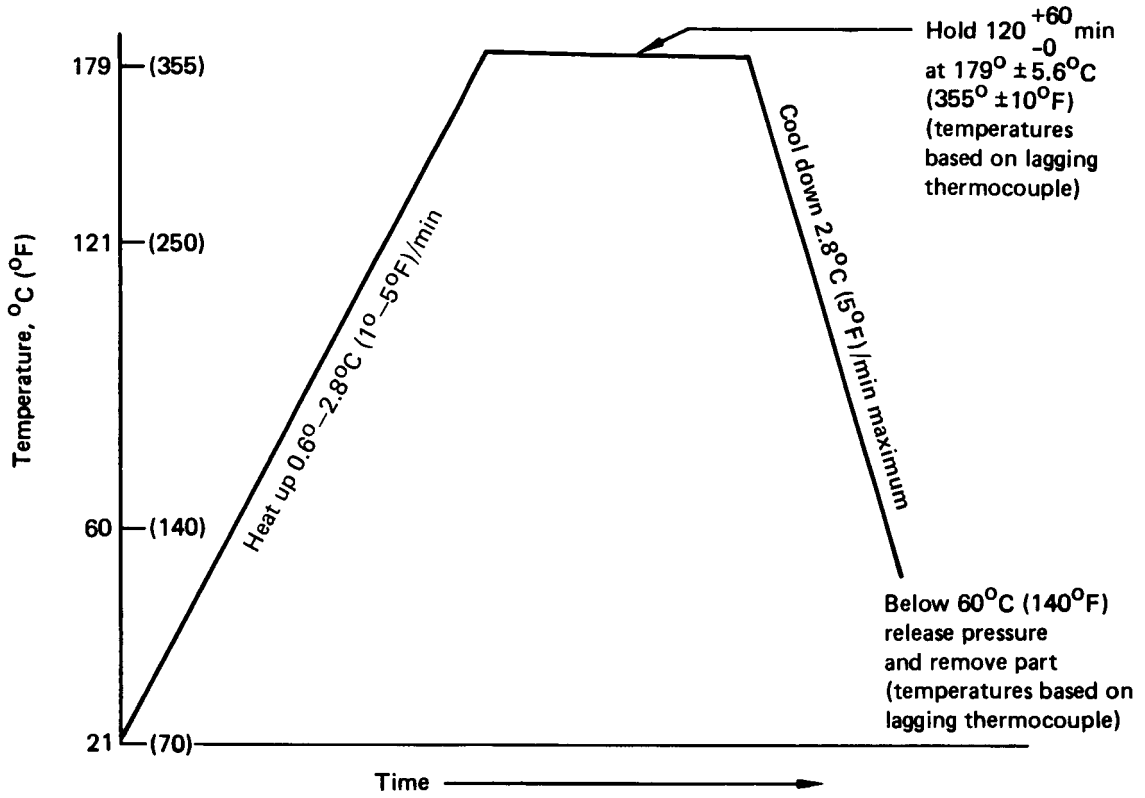


Figure 53. BAC 5562 Bagging Procedure (No-Bleed Material)



Apply 559 mm (22 in) of mercury-vacuum	} Vent vacuum bag to atmosphere when pressure reaches 138 kPa (20 lb/in ²)
Apply 586 + 10 kPa (85+15 lb/in ²) pressure for laminate	
Apply 310 + $\frac{34}{-41}$ kPa (45+5 lb/in ²) pressure for sandwich	

Figure 54. BAC 5562 Cure Cycle (No-Bleed Material)

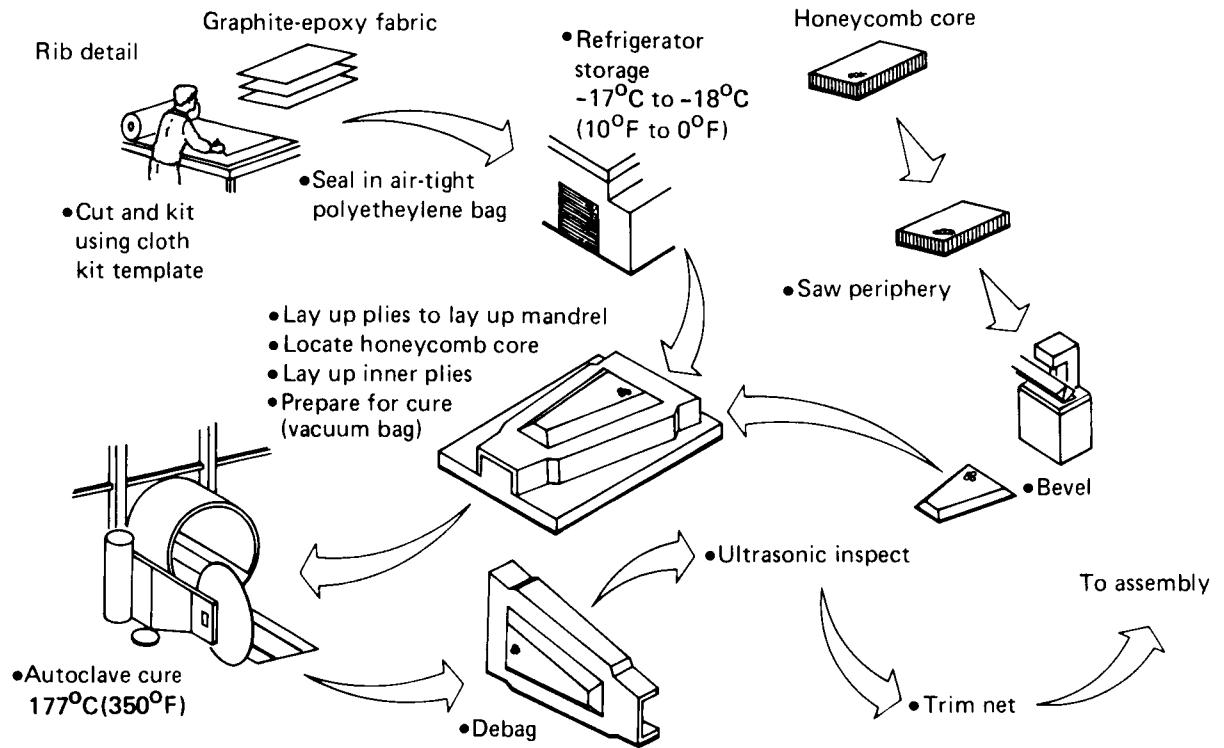


Figure 55. Typical Advanced Composite Fabrication Process

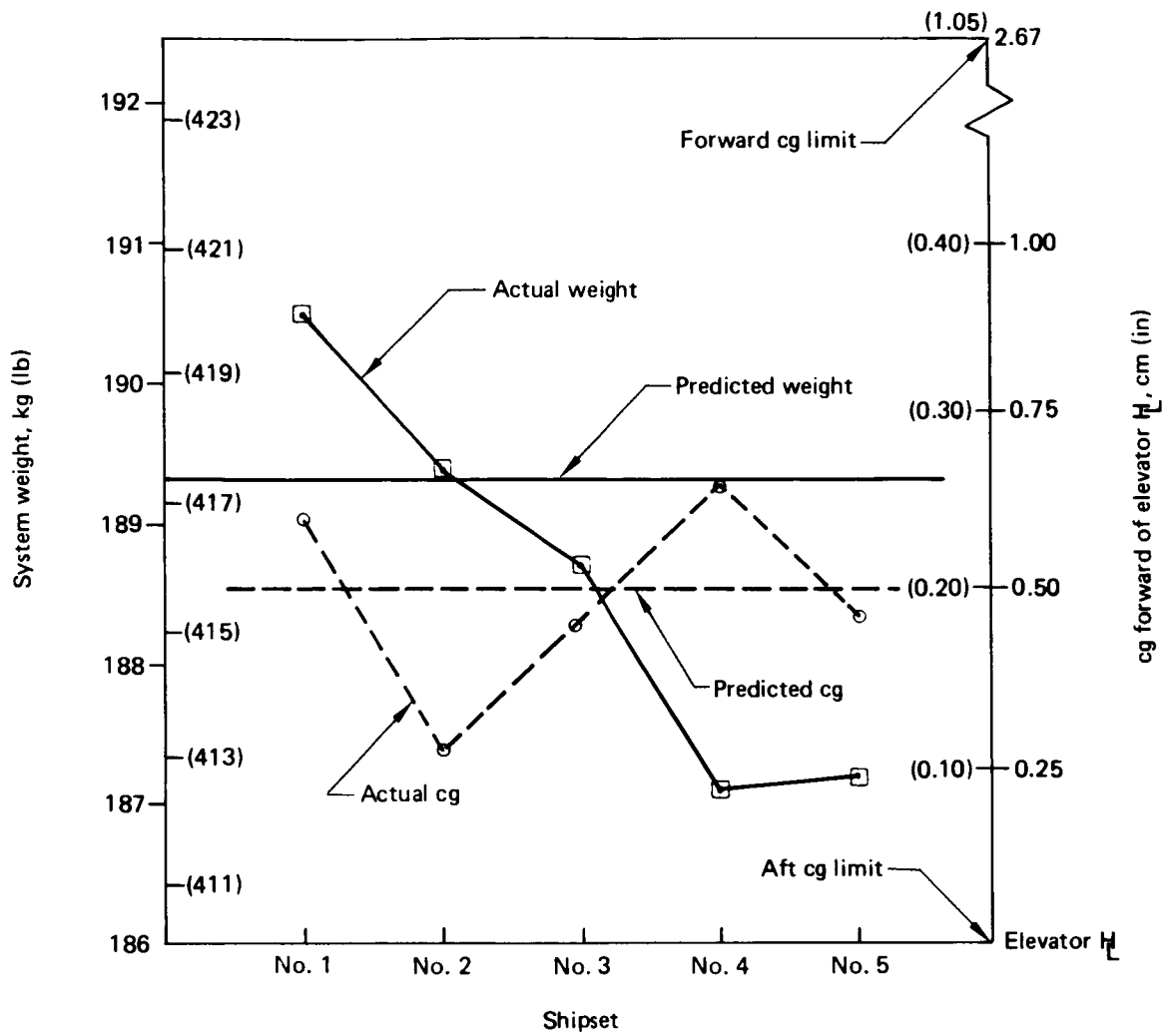


Figure 56. Elevator System Actual Weight and Balance Data (Elevator Surface, Control Tab, and Balance Panels)

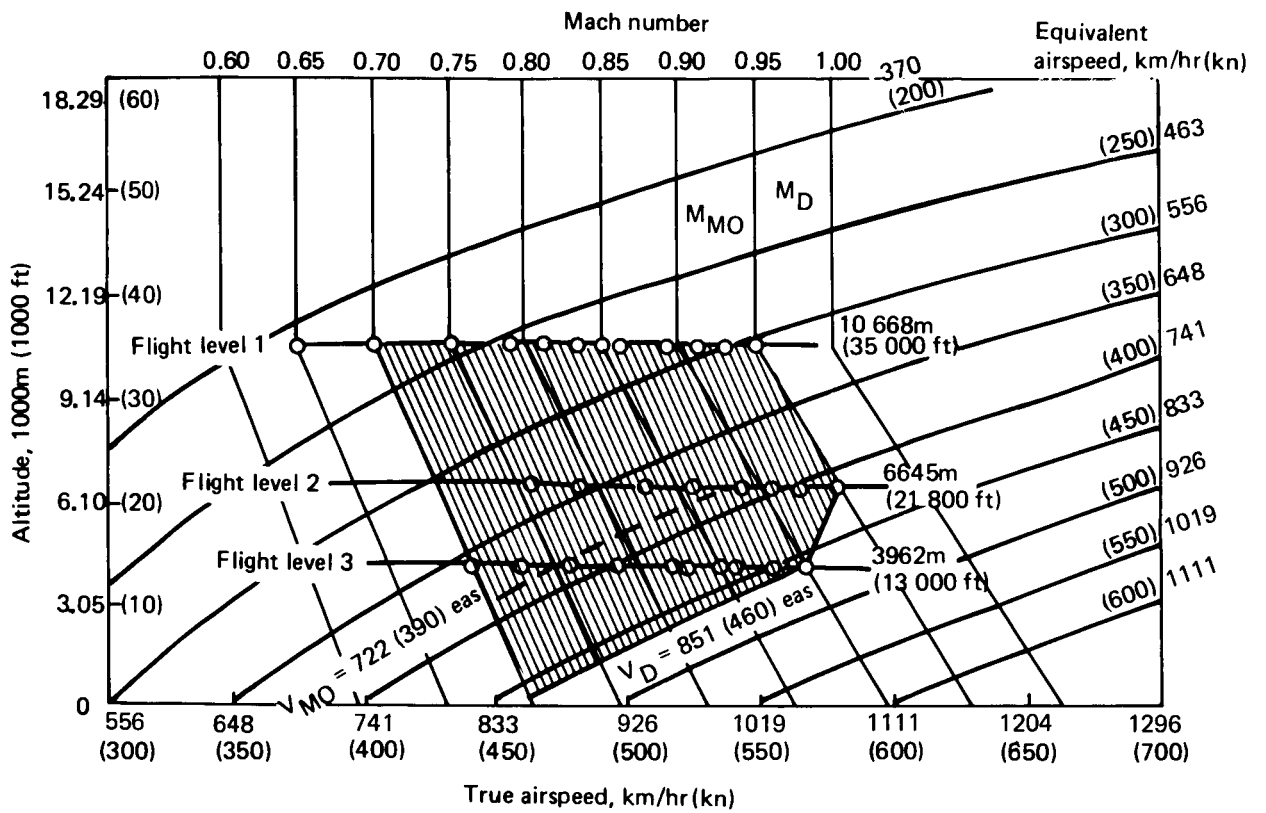


Figure 57. Flight Flutter Altitude and Speed Test Conditions

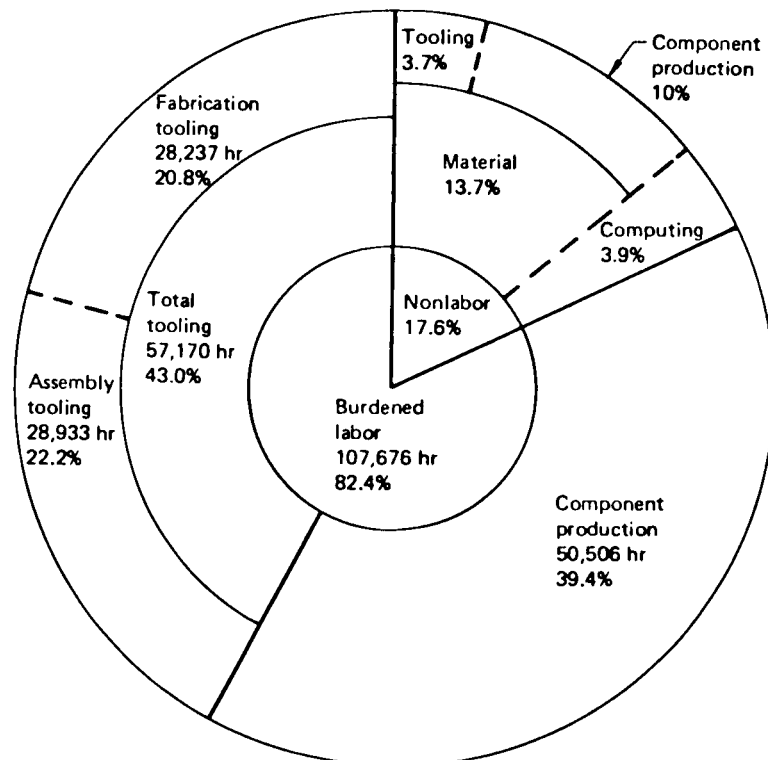


Figure 58. Total Recurring and Nonrecurring Production Costs by Major Element (5 1/2 Shipsets)

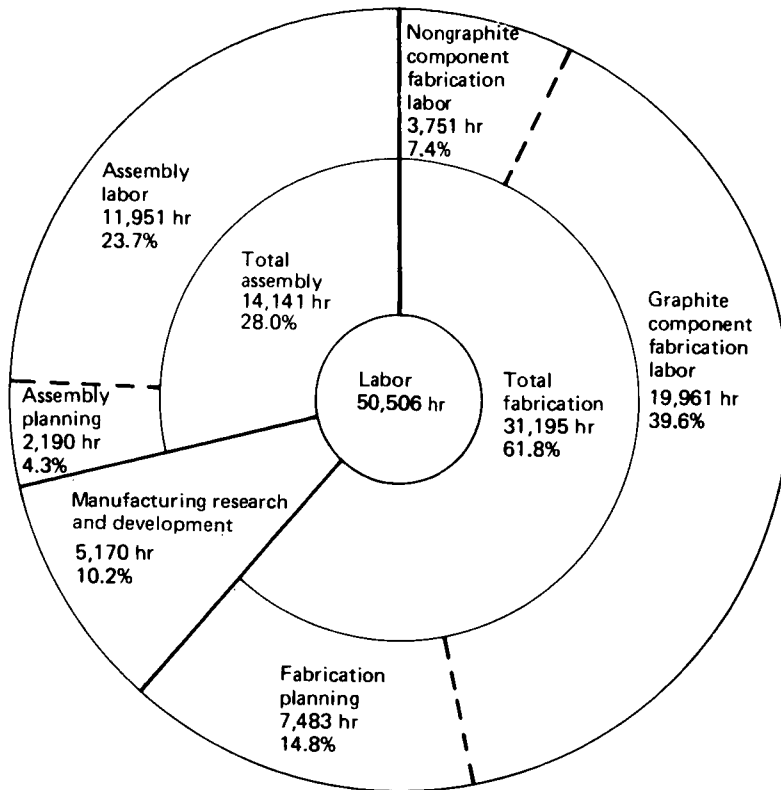


Figure 59. Total Recurring and Nonrecurring Component Production Labor Hours (5 1/2 Shipsets)

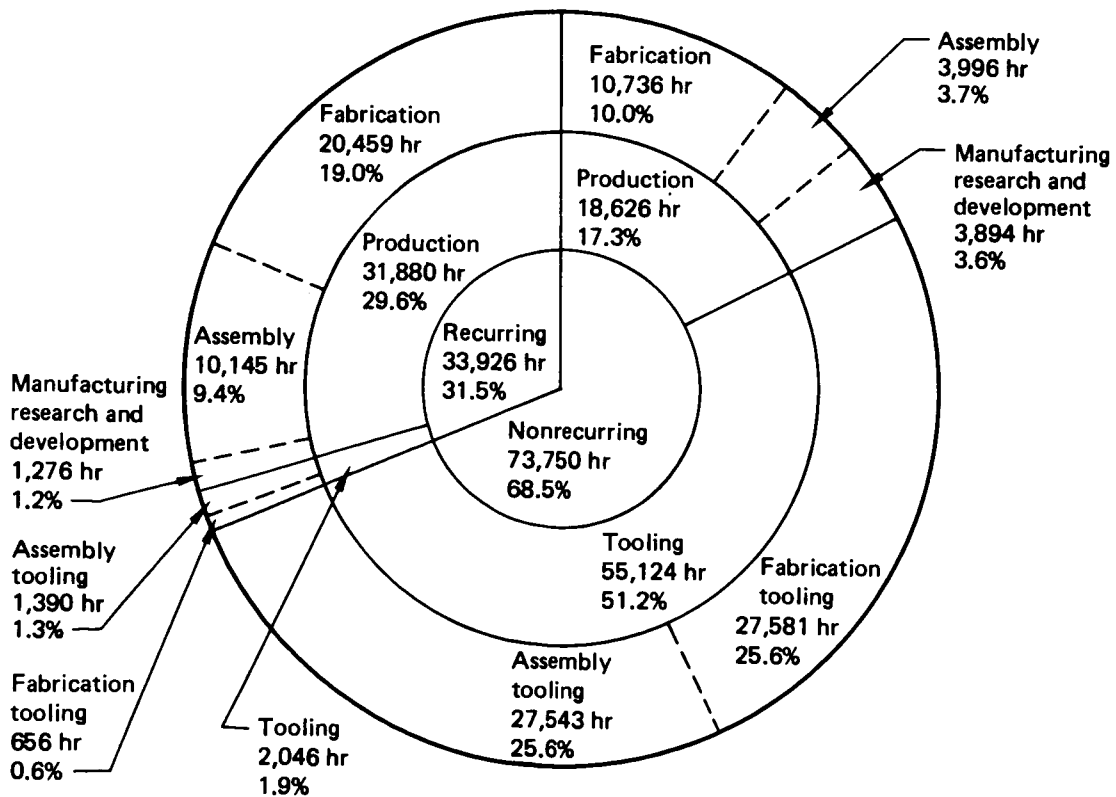


Figure 60. Total Recurring and Nonrecurring Production Labor by Major Element (5 1/2 Shipsets)

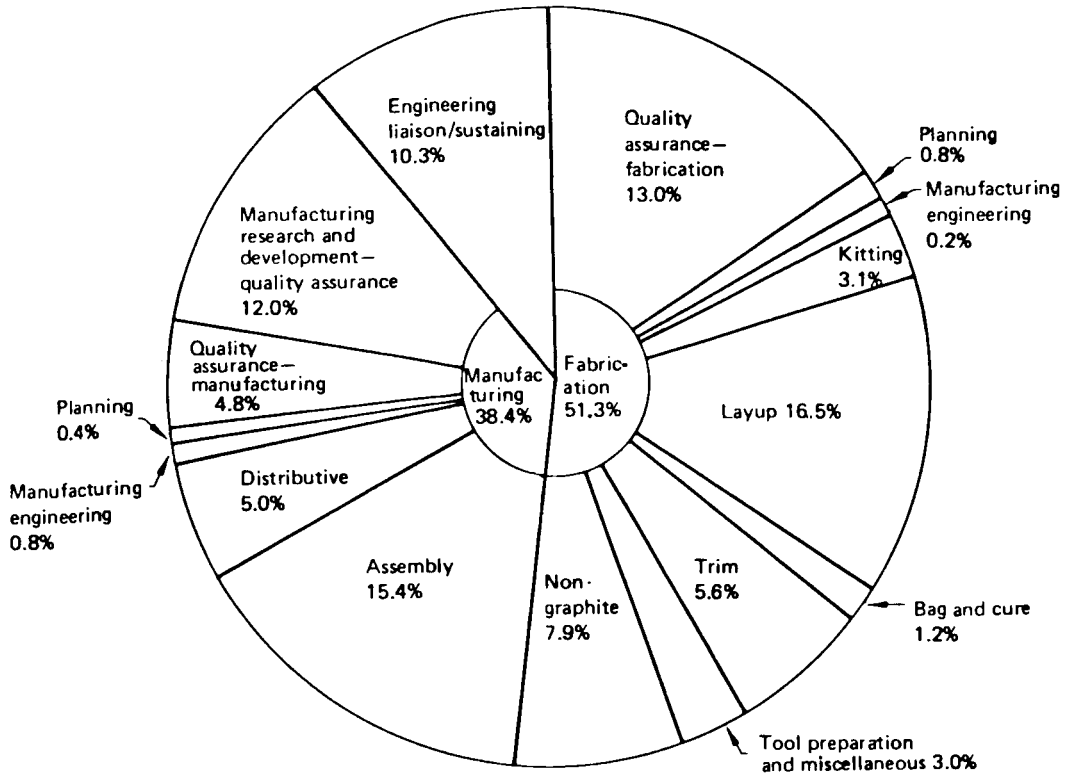


Figure 61. Fabrication and Assembly Recurring Costs, Percentage of Labor Hours (5 1/2 Shipsets)

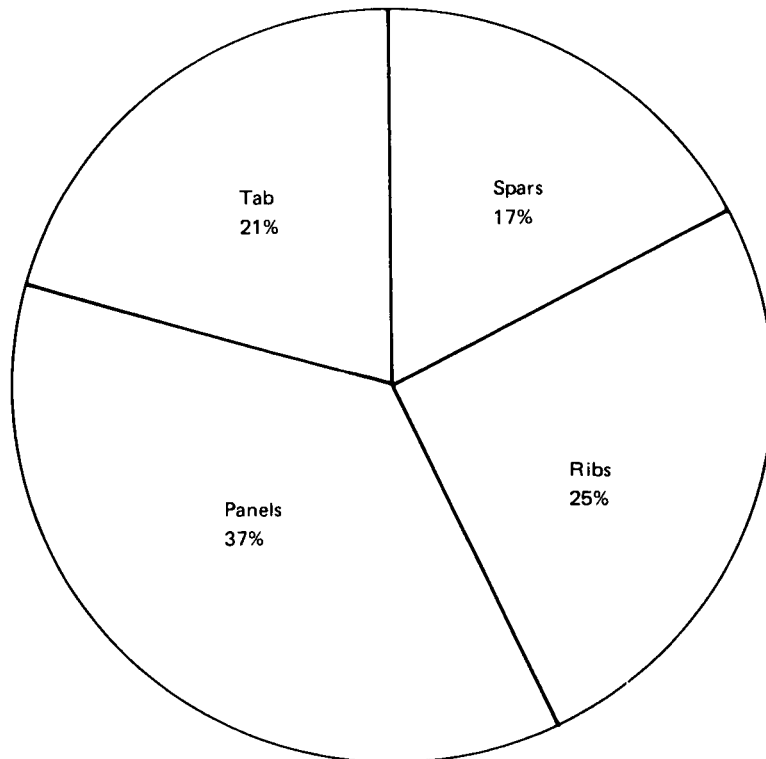


Figure 62. 727 Composite Elevator-Graphite Components Recurring Costs (5 1/2 Shipsets)

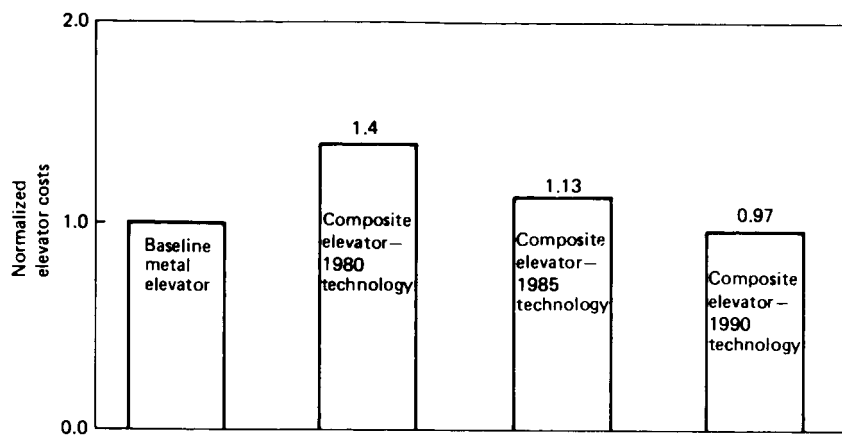



Figure 63. Relative Elevator Cost Comparison (for Initial 200 Shipsets)

Table 1. Concept Comparison








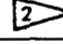
Concept	Rib ratio	Fastener ratio	Weight ratio	Recurring cost ratio	Remarks
1. Minimum-rib honeycomb panel design Concept 1	1.0	1.0	1.0	1.0	Simple panel tools CHOSEN CONCEPT
2. Multirib unstiffened panel design Concept 2	8.25	2.5	1.3-1.5	2.6	8 times the number of rib tools
3. Multirib bead-stiffened panel design Concept 3	3.5	1.5	1.1-1.3	1.7	3.5 times the number of rib tools More complex panel tools Difficult to cocure panels
4. Multirib blade-stiffened panel design Concept 4	3.5	1.5	1.2-1.4	1.6	3.5 times the number of rib tools More complex panel tools

Table 2. Design Ultimate Loads

Load case	Description	Altitude, m (ft)	Mach no.	Ultimate load factor 
1. Load case 120R	Positive maneuver at V_D	4145 (13,600)	0.90	3.75
2. Load case 122R	Negative maneuver at V_D	0	0.59	0
3. Load case 124	Check maneuver maximum negative loads	0	0.59	-3.44
4. Load case 125	Instantaneous elevator balanced maneuver	0	0.39	0.12
5. Load case 128	Positive maneuver at V_D	0	0.70	3.75

 At horizontal tail cg

Table 3. Major Structural Items (Ultimate Design Value Strains)

Structural Item		Strain	Critical Environmental Condition 	Ultimate Design Value Strain x 10 ⁻⁶ mm/mm (in/in)
Honeycomb skin panel	Spanwise bending	Tension	82°C (180°F) Wet	4040
		Compression	82°C (180°F) Wet	-4040
	Chordwise bending	Tension	82°C (180°F) Wet	3260
		Compression	82°C (180°F) Wet	-3260
In-plane shear	Shear	-59°C (-75°F) Wet	6420	
Front spar chord	 W/D = 5.5	Tension	-59°C (-75°F) Wet	3100
	 W/D = 5.5	Compression	82°C (180°F) Wet	-3600
Front spar web		Shear	RT Dry	4030
Rear spar chord	 W/D = 6.7	Tension	-59°C (-75°F) Wet	3350
	 W/D = 6.7	Compression	82°C (180°F) Wet	-3900
Actuator rib chord	 W/D = 5.5	Tension	-59°C (-75°F) Wet	3100
	 W/D = 5.5	Compression	82°C (180°F) Wet	-3600

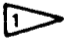
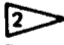

-  Wet condition is 1.1% moisture content by weight; dry refers to ambient conditions
-  W = 2 x fastener edge margin; D = fastener diameter
-  Includes effect of stiffener fasteners

Table 4. Comparison of Ground Vibration Test and Analysis Natural Frequencies

Vibration mode		Frequency, Hz	
		Analysis	Test
First stabilizer bending	Symmetrical	6.64	6.72
	Asymmetrical	6.96	7.12
Second stabilizer bending	Symmetrical	18.3	18.2
	Asymmetrical	23.4	23.5
Torsion	Symmetrical	27.1	26.6
	Asymmetrical	28.4	28.8
Elevator rotation		13.4	13.4
Elevator torsion		28.7	27.7
Column-tab		28.3	28.4
Tab rotation		34.3	40.0

Table 5. Material Form and Finishing Cost Study

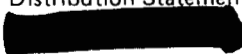

Material form	Relative Cost	
	Without finishing	With finishing
Woven fabric	1.00	1.00
2-ply preplied tape	1.25	1.21
4-ply preplied tape	1.10	1.05
30.5-cm (12-in) wide unidirectional tape	1.39	1.35

Table 6. Weight Comparison [kg (lb)/airplane]

Item	Baseline aluminum elevator, kg (lb)/airplane	Predicted advanced composites elevator kg (lb)/airplane	Weight difference, kg (lb)/airplane	Percent weight difference
Front and rear spars	35.2 (77.7)	28.4 (62.7)	-6.8 (-15.0)	-19
Ribs—inspar	12.0 (26.6)	4.4 (9.6)	-7.6 (-17.0)	-64
Skin panels	52.8 (116.3)	45.4 (100.2)	-7.4 (-16.1)	-14
Control tab	11.1 (24.4)	6.8 (15.0)	-4.3 (-9.4)	-39
Horn rib fairings	6.0 (13.2)	3.8 (8.4)	-2.6 (-4.8)	-36
Corrosion protection	0 (0)	0.6 (1.3)	+0.6 (+1.3)	—
	0 (0)	0 (0)	0 (0)	—
Replace structure	117.1 (258.2)	89.4 (197.2)	-27.7 (-61.0)	-24
Balance panel weights	32.0 (70.6)	0 (0)	-32.0 (-70.6)	-100
Balance panel hinges	54.6 (120.3)	38.3 (84.4)	-16.3 (-35.9)	-30
Horn balance weight	18.8 (41.5)	23.6 (52.1)	+ 4.8 (+10.6)	+26
Elevator adjust weight	0 (0)	1.8 (4.0)	+ 1.8 (+4.0)	—
Nose ribs and skins	18.9 (41.6)	20.1 (44.4)	+ 1.2 (+2.8)	+7
Balance panel structure	16.0 (35.2)	16.2 (35.7)	+ 0.2 (+0.5)	+1
Revised structure	140.3 (309.2)	100.0 (220.6)	-40.3 (-88.6)	-29
Total elevator system, kg (lb) airplane	257.4 (567.4)	189.4 (417.8)	-68.0 (-149.6)	-26.4

Table 7. Metal Elevator Versus Composite Elevator Cost Comparison Assumptions

	1980 technology	1985 technology	1990 technology
Metal elevator	<ul style="list-style-type: none"> ● Current production 	<ul style="list-style-type: none"> ● Aluminum material escalation of 152% in 5 years based on producers' price index ● Labor rate escalation of 147% in 5 years 	<ul style="list-style-type: none"> ● Aluminum material escalation of 224% in 5 years based on producers' price index ● Labor escalation of 216% in 5 years
Composite elevator	<ul style="list-style-type: none"> ● Hand layup and cutting ● High material usage ● High material cost 	<ul style="list-style-type: none"> ● Automatic tape layup and cutting ● Material waste cut by 72% ● Material price per lb cut 20% due to increased industry usage ● Labor rate escalation of 147% in 5 years 	<ul style="list-style-type: none"> ● Advanced manufacturing technology ● Material waste cut by 72% ● Material price per lb cut 20% due to increased industry usage ● Labor rate escalation of 216% in 5 years

1. Report No. NASA CR-3290		2. Government Accession No.		3. Recipient's Catalog No.	
4. Title and Subtitle ADVANCED COMPOSITE ELEVATOR FOR BOEING 727 AIRCRAFT VOLUME I - TECHNICAL SUMMARY				5. Report Date November 1981	
				6. Performing Organization Code	
7. Author(s) D. V. Chovil S. T. Harvey J. E. McCarty O. E. Desper E. S. Jamison H. Syder				8. Performing Organization Report No.	
				10. Work Unit No.	
9. Performing Organization Name and Address Boeing Commercial Airplane Company P.O. Box 3707 Seattle, Washington 98124				11. Contract or Grant No. NAS1-14952	
				13. Type of Report and Period Covered Contractor Report 5/77 through 12/79	
12. Sponsoring Agency Name and Address National Aeronautics and Space Administration Washington, D. C. 20546				14. Sponsoring Agency Code	
15. Supplementary Notes Langley Technical Monitor: Herbert A. Leybold Topical Report					
16. Abstract This report is a summary of the design, development, analysis, and testing activities and results that were required to produce five and one-half shipsets of advanced composite elevators for Boeing 727 aircraft. During the preliminary design period, alternative concepts were developed. After selection of the best design, detail design and basic configuration improvements were evaluated. Five and one-half shipsets were manufactured. We accomplished all program goals (except competitive cost demonstration) when our design met or exceeded all requirements, criteria, and objectives.					
17. Key Words (Suggested by Author(s)) advanced composite Energy Efficient Transport Program long-term durability structural integrity weight savings			18. Distribution Statement  		
19. Security Classif. (of this report) Unclassified	20. Security Classif. (of this page) Unclassified	21. No. of Pages 93	22. Price		

